**THE EUROPEAN
PHYSICAL JOURNAL C**

CrossMark

Regular Article - Theoretical Physics

Search for heavy resonances decaying into WW in the $e\nu\mu\nu$ final state in pp collisions at $\sqrt{s} = 13$ TeV with the ATLAS detector

ATLAS Collaboration⋆

CERN, 1211 Geneva 23, Switzerland

Abstract A search for neutral heavy resonances is performed in the $WW \rightarrow e\nu\mu\nu$ decay channel using pp collision data corresponding to an integrated luminosity of 36.1 fb^{-1}, collected at a centre-of-mass energy of 13 TeV by the ATLAS detector at the Large Hadron Collider. No evidence of such heavy resonances is found. In the search for production via the quark–antiquark annihilation or gluon–gluon fusion process, upper limits on $\sigma_X \times B(X \rightarrow WW)$ as a function of the resonance mass are obtained in the mass range between 200 GeV and up to 5 TeV for various benchmark models: a Higgs-like scalar in different width scenarios, a two-Higgs-doublet model, a heavy vector triplet model, and a warped extra dimensions model. In the vector-boson fusion process, constraints are also obtained on these resonances, as well as on a Higgs boson in the Georgi–Machacek model and a heavy tensor particle coupling only to gauge bosons.

1 Introduction

The measured properties [1–4] of the Higgs boson discovered in 2012 by the ATLAS [5] and CMS [6] collaborations at the Large Hadron Collider (LHC) are, within experimental uncertainties, consistent with those predicted for the Standard Model (SM) Higgs boson, h. Nevertheless, the SM is thought to be an incomplete theory and many scenarios beyond the SM (BSM) predict an extended Higgs sector [7,8]. Diboson vector and tensor resonances are also predicted in several other extensions to the SM, such as in composite Higgs models [9,10] and models with warped extra dimensions [11–14].

This article reports on the results of a search for heavy neutral resonances decaying into two W bosons, which then decay into the $e\nu\mu\nu$ final state, either directly or via leptonic tau decays with additional neutrinos. The analysis is based on the full pp collision dataset collected by the ATLAS detector in 2015 and 2016 at the centre-of-mass energy of

$\sqrt{s} = 13$ TeV, corresponding to an integrated luminosity of 36.1 fb^{-1}.

The results are interpreted in terms of different benchmark models. For the case of a scalar resonance produced by gluon–gluon fusion (ggF) or vector-boson fusion (VBF), two scenarios with different intrinsic widths are considered. Constraints on the heavy neutral scalar in two-Higgs-doublet models (2HDM) are also obtained. The neutral member of the fiveplet in the Georgi–Machacek (GM) model [15,16] also serves as a reference model in the VBF production mode. The parameterisation of heavy vector triplet (HVT) Lagrangians [17,18] permits the interpretation of searches for spin-1 resonances in a generic way. The bulk Randall–Sundrum (RS) model [11,19] features a spin-2 Kaluza–Klein (KK) graviton excitation (G_{KK}) decaying into WW, while a tensor resonance signal in the VBF production mode is based on an effective Lagrangian model (ELM) [20].

A previous search for a heavy Higgs boson in the $e\nu\mu\nu$ final state was performed by ATLAS [21] based on a data sample with an integrated luminosity of 20.3 fb^{-1} at $\sqrt{s} = 8$ TeV. The CMS Collaboration also published a search for a high-mass scalar decaying into two W bosons in the fully leptonic final state [22], using datasets at $\sqrt{s} = 7$ and 8 TeV with integrated luminosities of 5.1 and 19.5 fb^{-1}, respectively. A search for heavy resonances in the RS models in the leptonic decays of the WW channel, using a dataset of 4.7 fb^{-1} at 7 TeV [23], was reported by the ATLAS Collaboration. The ATLAS and CMS collaborations have obtained constraints on the HVT and bulk RS models, based on other decay modes of the VV channels, with V being either a W or a Z boson [24–36]. The search in the $e\nu\mu\nu$ decay mode is complementary to searches performed in other decay modes. In particular, the sensitivity to low mass resonances is higher in the fully leptonic final state than in final states that include jets due to background from jet production.

The article is organised as follows. Section 2 presents the various models used in this analysis. Section 3 describes the ATLAS detector. The data and simulated event samples are discussed in Sect. 4. The event reconstruction and selection

⋆ e-mail: atlas.publications@cern.ch

🌱 Springer

are described in Sects. 5 and 6, respectively, followed by the background estimation techniques in Sect. 7. Systematic uncertainties are discussed in Sect. 8 and the results are presented in Sect. 9. Finally, the conclusions are given in Sect. 10.

2 Theoretical models

The different signal models studied are presented in Table 1. One scenario for the heavy scalar assumes that the scalar has a width much smaller than the detector resolution. This is referred to as the narrow-width approximation (NWA). Larger widths (large-width assumption, LWA) of 5, 10 and 15% of the heavy Higgs boson mass, are also considered. The choice of the width range for the heavy Higgs boson is motivated by the fact that, for several of the most relevant BSM models, widths above 15% are already excluded by indirect limits [37].

The 2HDM comes in different types [38], defined by assumptions about the couplings of each of the Higgs doublets and the discrete symmetries imposed. This analysis considers Type I, where one Higgs doublet couples to vector bosons while the other couples to fermions, and Type II of the minimal supersymmetric (SUSY)-like model in which one Higgs doublet couples to up-type quarks and the other one to down-type quarks and charged leptons. This analysis uses a generic charge-conjugation- and parity-conserving (CP-conserving) 2HDM with a softly broken Z_2 symmetry [38] which has several free parameters: (i) four masses m_h, m_H, m_A and $m_{H^\pm}$ for the two CP-even neutral states, the pseudo-scalar and the charged Higgs boson pair, respectively, (ii) a mixing angle α between the CP-even neutral Higgs fields, and (iii) the ratio of the vacuum expectation values of the two Higgs doublets $\tan \beta = \upsilon_2/\upsilon_1$. The bench-

Table 1 Summary of the different signal models and resonances considered in the analysis. The resonance spin and production mode are also specified with ggF for gluon–gluon fusion, qqA for quark–antiquark annihilation and VBF for vector-boson fusion

Model	Resonance spin	Production mode		
		ggF	qqA	VBF
NWA	Spin-0	x		x
2HDM		x		x
LWA		x		x
GM				x
HVT	Spin-1		x	x
Bulk RS	Spin-2	x		
ELM				x

mark is defined by setting $m_h = 125\,\text{GeV}$ and the masses of the supersymmetric particles heavy enough so that Higgs boson decays into SUSY particles are kinematically forbidden. The cross sections and branching fractions are calculated with SusHi and 2HDMC [39,40].

The GM model extends the Higgs sector with the addition of a real and a complex triplet of $SU(2)_L$ in a way which preserves the SM value of $\rho = M_W^2/(M_Z^2 \cos^2\theta_W) = 1$ at tree level, with m_W, m_Z and θ_W being the W and Z boson mass and the weak mixing angle, respectively. The physical states include a fermiophobic fiveplet, H_5^0, $H_5^\pm$, and $H_5^{\pm\pm}$, of custodial SU(2) symmetry which couples preferentially to vector bosons [41]. For that reason, the GM model is less constrained [42], when produced by the VBF process, than other standard benchmark models of a triplet Higgs field, such as the little Higgs model [43] or the left–right symmetric model [44]. The model has many parameters [45,46], but, if the other new Higgs bosons are heavier than those of the H_5 multiplet, the only production mode is via the VBF process. The cross section and decay width into VV are then proportional to a single parameter, $\sin^2\theta_H$, which characterises the fraction of the gauge boson masses generated by the triplet Higgs fields.

The HVT Lagrangian [18] parameterises the couplings of the new spin-1 heavy bosons to SM particles in a generic manner and allows their mixing with SM gauge bosons. The s-channel production mechanism of the heavy gauge bosons is primarily via $q\bar{q}$ annihilation (qqA). The HVT bosons couple to the Higgs boson and SM gauge bosons with coupling strength $c_h g_V$ and to the fermions with coupling strength $g^2 c_F/g_V$, where g is the SM $SU(2)_L$ gauge coupling, c_h and c_F are multiplicative factors that modify the couplings to the Higgs boson and to the fermions, and g_V represents its coupling strength to the W and Z bosons. For the case of vector-boson fusion, it is assumed that there is no coupling to fermions so that non-VBF production processes are suppressed.

The spin-2 G_{KK} is the first Kaluza–Klein excitation of the graviton in the RS model with a warped extra dimension [11, 19], where the SM fields are localised in the bulk [12–14]. This model is characterised by the dimensionless coupling constant $k/\bar{M}_{Pl} \sim \mathcal{O}(1)$ where k determines the curvature of the space, and where $\bar{M}_{Pl} = M_{Pl}/\sqrt{8\pi}$ is the reduced Planck scale.

For the VBF production mode, the spin-2 signal is based on an effective Lagrangian approach with Λ as a characteristic energy scale of the underlying new physics [20],

$$\mathcal{L} = \frac{1}{\Lambda} T_{\mu\nu} \left(f_1 B^{\alpha\nu} B_\alpha^\mu + f_2 W_i^{\alpha\nu} W_\alpha^{i,\mu} + 2f_5 (D^\mu \Phi)^\dagger (D^\nu \Phi) \right).$$

Here, f_i are variable coupling parameters, $T_{\mu\nu}$ is the spin-2 singlet field, $B^{\alpha\nu}$ and $W_i^{\alpha\nu}$ are the electroweak field strength

tensors, and Φ is the scalar Higgs field. The covariant derivative D^μ is $D^\mu = \partial^\mu - igW_i^\mu \sigma^i/2 - ig'YB^\mu$, where σ^i are the Pauli matrices, Y the weak hypercharge, and g and g' the corresponding gauge coupling constants. The model differs from the RS model in that the couplings to fermions or gluons are not included in the Lagrangian. Also, the BSM amplitude is multiplied by a form factor which is a function of a cut-off scale Λ_{ff} and a suppression power n_{ff} in order to preserve unitarity at high energies:

$$f(p_1^2, p_2^2, k_{sp2}^2)$$
$$= \left(\frac{\Lambda_{ff}^2}{|p_1^2| + \Lambda_{ff}^2} \cdot \frac{\Lambda_{ff}^2}{|p_2^2| + \Lambda_{ff}^2} \cdot \frac{\Lambda_{ff}^2}{|k_{sp2}^2| + \Lambda_{ff}^2} \right)^{n_{ff}},$$

where p_1^2 and p_2^2 are the squared invariant masses of the incoming electroweak bosons and k_{sp2}^2 is the squared invariant mass of the sum of the initial boson momenta, equivalent to that of an s-channel spin-2 particle. The specific parameter settings for the signal models used are given in Sect. 4.

3 ATLAS detector

The ATLAS detector [47,48] is a general-purpose particle detector used to investigate a broad range of physics processes. It includes an inner tracking detector (ID) surrounded by a thin superconducting solenoid, electromagnetic and hadronic calorimeters and a muon spectrometer (MS) incorporating three large superconducting toroidal magnets with eight coils each. The ID consists of fine-granularity silicon pixel and microstrip detectors, and a straw-tube tracker. It is immersed in a 2 T axial magnetic field produced by the solenoid and provides precision tracking for charged particles in the range $|\eta| < 2.5$, where η is the pseudorapidity of the particle.[1] The straw-tube detector also provides transition radiation measurements for electron identification. The calorimeter system covers the pseudorapidity range $|\eta| < 4.9$. It is composed of sampling calorimeters with either liquid argon (LAr) or scintillator tiles as the active medium, and lead, steel, copper, or tungsten as the absorber material. The MS provides muon identification and momentum measurements for $|\eta| < 2.7$. The ATLAS detector has a two-level trigger system [49] to select events for further analysis.

---

[1] ATLAS uses a right-handed coordinate system with its origin at the nominal interaction point (IP) in the centre of the detector and the z-axis along the beam pipe. The x-axis points from the IP to the centre of the LHC ring, and the y-axis points upwards. Cylindrical coordinates (r, ϕ) are used in the transverse plane, ϕ being the azimuthal angle around the beam pipe. The pseudorapidity is defined in terms of the polar angle θ as $\eta = -\ln \tan(\theta/2)$. Angular distance is measured in units of $\Delta R \equiv \sqrt{(\Delta\eta)^2 + (\Delta\phi)^2}$.

4 Data and simulation samples

The data used in this analysis were collected with a single-electron or single-muon trigger. These triggers have a transverse energy or momentum threshold, E_T or p_T, that depends on the data-taking period, with the lowest threshold varying between 20 and 26 GeV. The trigger efficiency for WW events passing the offline event selection (Sect. 6) is greater than 99%. Data quality criteria are applied to ensure that events are recorded with stable beam conditions and with all relevant subdetector systems operational.

Samples of simulated signal and background events are used to optimise the event selection and to estimate the signal acceptance and the background yields from various SM processes.

The sample for the NWA heavy Higgs boson signal was produced with POWHEG-BOX 2.0 [50–52] which calculates separately the ggF [53] and VBF [54] production mechanisms with matrix elements up to next-to-leading order (NLO) in quantum chromodynamics (QCD). It uses the CT10 NLO parton distribution function (PDF) set [55] and is interfaced with PYTHIA 8.186 [56] for the $H \to WW$ decays, for parton showering and hadronisation. A set of tuned parameters called the AZNLO tune [57] is used to describe the underlying event. The NWA Higgs boson is generated with a width of 4 MeV. This event sample is also used to constrain the 2HDM. The LWA heavy Higgs boson signal was simulated at NLO using the MADGRAPH5_AMC@NLO 2.3.2 event generator [58] with the NNPDF23LO PDF set [59]. The generated particles at matrix element level are showered by PYTHIA 8.186 with the A14 tune [60] for the underlying event. The mass of the heavy Higgs boson signals considered in this analysis spans the range between 200 GeV and 4 (3) TeV for the ggF-induced (VBF-induced) signals. Both NWA and LWA samples were generated in steps of 100 GeV up to 1 TeV, and in steps of 200 GeV thereafter.

The POWHEG-BOX samples describe the production of a ggF-induced heavy Higgs boson in association with one jet at leading-order (LO) precision, while further jets are emulated by the parton shower generator, PYTHIA. A more precise calculation of higher jet multiplicities is provided by using MADGRAPH5_AMC@NLO 2.3.2 to simulate $gg \to H$ events in association with up to two jets at NLO precision. Here, the overlap between identical final states generated at the matrix element (ME) and the parton shower (PS) stage is removed using FxFx merging [61]. The fraction of ggF events passing the event selection requirements of the $N_{jet} = 1$ and $N_{jet} \geq 2$ VBF categories (defined later in Sect. 6) predicted by the POWHEG-BOX event generator is reweighted to match that of the MADGRAPH5_AMC@NLO FxFx samples. The corresponding scale factors are calculated for several hypothetical heavy Higgs boson masses. It is the largest, 1.14, for the 200 GeV mass point, and decreases with increasing res-

onance mass to a value of 0.85 for the 4 TeV mass point, for the $N_{\text{jet}} = 1$ VBF category. The corresponding numbers are 0.91 and 0.73 for the $N_{\text{jet}} \geq 2$ VBF category.

Benchmark samples for the GM, HVT and bulk RS models were generated at LO using MADGRAPH5_AMC@NLO interfaced to PYTHIA 8.186 with the NNPDF23LO PDF set. A value of $\sin\theta_H = 0.4$ is chosen for the GM benchmark model. For the HVT interpretation in the $q\bar{q}$ annihilation mode, samples were generated according to the extended gauge symmetry model A [18] with $g_V = 1$. In the VBF mode, samples were generated using the same g_V value but setting the couplings to the fermions to zero so that the new vector boson couples only to the SM vector and Higgs bosons. For the bulk RS model, a curvature scale parameter $k/\bar{M}_{\text{Pl}}$ of either 0.5 or 1 is considered. The ELM VBF spin-2 signals were generated at LO with VBFNLO 3.0.0 beta 2 [62] with the NNPDF30LO PDF set [63] and using the following parameter setting [20]: $\Lambda_{ff} = 3$ TeV, $n_{ff} = 4$, $\Lambda = 1.5$ TeV and $f_1 = f_2 = f_5 = 1$. The mass range considered is between 200 GeV and 5 TeV for the KK graviton signal, between 250 GeV and 5 TeV for the HVT qqA signal, between 200 GeV and 1 TeV for the GM and ELM VBF signals, and between 300 GeV and 1 TeV for the HVT VBF signal.

The main sources of SM background include events from the production of single top quarks, $t\bar{t}$, dibosons (WW, WZ and ZZ), Z/γ^*+jets and W+jets. Single-top-quark simulated events were generated with POWHEG-BOX 2.0 [64,65] using the CT10 NLO PDF set interfaced to PYTHIA 6.428 [66] for parton showering and hadronisation, with the PERUGIA2012 tune [67] and CTEQ6L1 PDF [68] to describe the underlying event. The $t\bar{t}$ events were generated with POWHEG-BOX 2.0 [69] using the NNPDF30NLO PDF set [63] interfaced to PYTHIA 8.186 for parton showering and hadronisation, with the A14 tune and CTEQ6L1 PDF to describe the underlying event. The sample was generated by setting the resummation damping parameter h_{damp} to 1.5 times the top-quark mass, m_{top}, which was set to 172.5 GeV. The h_{damp} parameter controls the ME/PS matching and effectively regulates the high-p_T radiation. The EVT-GEN 1.2.0 [70] package was used to model the properties of the bottom and charm hadron decays. Diboson samples were generated with SHERPA 2.1.1 [71–75] for the gg production processes and SHERPA 2.2.1 for the $q\bar{q}$ production processes, using the CT10 NLO and NNPDF30NNLO PDF sets, respectively. The SHERPA event generator for the latter processes produces up to one additional parton at NLO and up to three additional partons at LO. Production of W and Z bosons in association with jets was also simulated using SHERPA 2.1.1 with the CT10 NLO PDF set, where b- and c-quarks are treated as massive particles. The $gg \rightarrow WW$ production also includes the contribution of the SM Higgs boson at 125 GeV and the interference effects between the

continuum and Higgs resonance processes. The VBF part of SM Higgs boson production was generated with POWHEG-BOX [54] interfaced to PYTHIA 8.186 for parton showering and hadronisation.

The effect of multiple pp interactions in the same and neighbouring bunch crossings (pile-up) was included by overlaying minimum-bias collisions, simulated with PYTHIA 8.186, on each generated signal and background event. The number of overlaid collisions is such that the distribution of the average number of interactions per pp bunch crossing in the simulation matches the pile-up conditions observed in the data, which is about 25 interactions per bunch crossing on average. The generated samples were processed through a GEANT4-based detector simulation [76,77], followed by the standard ATLAS reconstruction software used for collision data.

5 Event reconstruction

Events used in this analysis are required to have at least one primary vertex with a minimum of two associated tracks, each with transverse momentum $p_T > 400$ MeV. If there is more than one vertex reconstructed in an event that meets these conditions, the one with the highest sum of track p_T^2 is chosen as the primary vertex.

Electrons are reconstructed from clusters of energy deposits in the electromagnetic calorimeter that match a track reconstructed in the ID. They are identified using the likelihood identification criteria described in Ref. [78]. The electrons used in this analysis are required to pass the "MediumLH" selection for $p_T > 25$ GeV[2] or the "TightLH" selection for $p_T < 25$ GeV and be within $|\eta| < 2.47$, excluding the transition region between the barrel and endcaps in the LAr calorimeter $(1.37 < |\eta| < 1.52)$. These "MediumLH" and "TightLH" selection categories have identification efficiencies of 84 and 74%, respectively, for electrons with p_T of 25 GeV. The corresponding probabilities to misidentify hadrons as electrons are approximately 0.5 and 0.3%, respectively.

Muons are reconstructed by combining ID and MS tracks that have consistent trajectories and curvatures [79]. The muon candidates used in this analysis are required to have $|\eta| < 2.5$ and pass the "Medium" selection for $p_T > 25$ GeV or the "Tight" selection for $p_T < 25$ GeV, defined on the basis of the quality of the reconstruction and identification. These selections have a reconstruction efficiency of approximately 96 and 92%, respectively, for muons originating from the decay of W bosons [80]. The corresponding

---

[2] For electrons, p_T is defined as the magnitude of the transverse component of the electron momentum as measured using the electromagnetic calorimeter.

probabilities to misidentify hadrons as muons are approximately 0.2 and 0.1%, respectively.

To ensure that leptons originate from the interaction point, a requirement of $|d_0|/\sigma_{d_0} < 5$ (3) is imposed on the electrons (muons) and $|z_0 \sin\theta| < 0.5$ mm is applied to both lepton types. Here d_0 and z_0 are the transverse and longitudinal impact parameters of the lepton with respect to the primary vertex, respectively, and σ_{d_0} is the uncertainty in the measured value of d_0. In addition, electrons and muons are required to be isolated from other tracks and calorimetric activities by applying p_T- and η-dependent isolation criteria. For muons, the calorimeter isolation is based on energy deposits in the calorimeter within a cone ΔR of 0.2 around the muons. The muon track isolation uses a variable cone size starting at $\Delta R = 0.3$ and shrinking with increasing p_T of the muon [81]. The same calorimeter isolation is used for electrons, and the electron track isolation uses a variable cone size starting at $\Delta R = 0.2$. The efficiency of these isolation requirements is 90% for both lepton types with p_T of 25 GeV, increasing to 99% at 60 GeV.

Jets are reconstructed from three-dimensional clusters of energy deposits in the calorimeters using the anti-k_t algorithm [82] with a radius parameter of $R = 0.4$ implemented in the FastJet package [83]. The four-momenta of the jets are calculated as the sum of the four-momenta of their constituents, which are assumed to be massless. Jets are corrected for energy from pile-up using the pile-up subtraction based on jet areas [84]. The jet energy scale is estimated in Ref. [85]. Jets are required to have $p_T > 30$ GeV and $|\eta| < 4.5$.

For jets with $p_T < 60$ GeV and $|\eta| < 2.5$, the multivariate "jet vertex tagger" algorithm [86] is used to suppress jets from pile-up interactions. To avoid double counting, jets of any transverse momentum are discarded if they are within a cone of size $\Delta R = 0.2$ around an electron candidate or if they have fewer than three associated tracks and are within a cone of size $\Delta R = 0.2$ around a muon candidate. However, if a jet with three or more associated tracks is within a cone of size $\Delta R < 0.4$ of a muon candidate, or the separation between an electron and any jet is within $0.2 < \Delta R < 0.4$, the corresponding muon or electron candidate is rejected.

To estimate the number of b-tags in the event, jets with $p_T > 20$ GeV and within $|\eta| < 2.5$ are considered to contain a b-hadron if they yield a b-tagging algorithm discriminant value exceeding a reference value. The MV2c10 algorithm [87,88] is chosen at the 85% b-tagging efficiency benchmark point, estimated from b-jets in simulated $t\bar{t}$ events. The misidentification rate for jets which originate from a light quark or gluon is less than 1%, while it is approximately 17% for c-jets.

The missing transverse momentum, with magnitude E_T^{miss}, is calculated as the negative vectorial sum of the transverse momenta of calibrated electrons, muons, and jets originating from the primary vertex, as well as tracks with $p_T >$ 500 MeV compatible with the primary vertex and not associated with any of these [89].

6 Event selection

As a first step, WW candidate events are selected by requiring two oppositely charged, different-flavour leptons (e or μ). Both leptons must satisfy the minimal quality criteria discussed in Sect. 5. When ordered in p_T, these leptons are called the leading and subleading ones, $p_T^{\ell,(sub)lead}$. In order to suppress the background from diboson processes, a veto is imposed on events with an additional lepton with $p_T^{\ell,other} > 15$ GeV.

Table 2 summaries the selections and the definition of signal regions (SRs). The variables used in the selections are the most discriminating ones chosen by a boosted decision tree (BDT) [90], based on the NWA signal samples. These are $p_T^{\ell,lead}$, the invariant mass of the leading and subleading leptons, $m_{\ell\ell}$, and the pseudorapidity difference between the two leptons, $\Delta\eta_{\ell\ell}$. The first two variables provide good separation between a heavy resonance signal and the WW and top-quark background. The separation of signal from background based on the $\Delta\eta_{\ell\ell}$ distribution is found to have a reasonable efficiency and allows, at the same time, a control region to be defined for the WW background (Sect. 7.2). For each selected variable, the selection criterion is set by maximising the signal significance in the presence of background. The optimised selection is checked to be applicable to the LWA signals.

In order to further suppress the top-quark background, events with at least one b-tagged jet ($N_{b\text{-tag}} \geq 1$) are rejected

Table 2 Selection conditions and phase space definitions used in the ggF and VBF signal regions

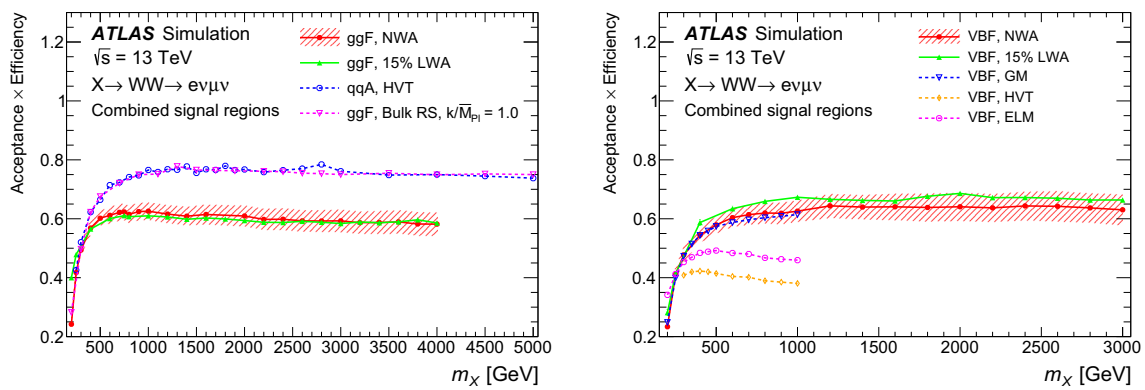| SR$_{ggF}$	SR$_{VBF1J}$	SR$_{VBF2J}$
	Common selections	
	$N_{b\text{-tag}} = 0$	
	$|\Delta\eta_{\ell\ell}| < 1.8$	
	$m_{\ell\ell} > 55$ GeV	
	$p_T^{\ell,lead} > 45$ GeV	
	$p_T^{\ell,sublead} > 30$ GeV	
	veto if $p_T^{\ell,other} > 15$ GeV	
	$\max(m_T^W) > 50$ GeV	
ggF phase space	VBF1J phase space	VBF2J phase space
Inclusive in N_{jet} but excluding VBF1J and VBF2J phase space	$N_{jet} = 1$ and $|\eta_j| > 2.4$, $\min(|\Delta\eta_{j\ell}|) > 1.75$	$N_{jet} \geq 2$ and $m_{jj} > 500$ GeV, $|\Delta y_{jj}| > 4$

Fig. 1 Acceptance times efficiency as a function of signal mass for the ggF or qqA (left) and VBF (right) productions. All three signal event categories are combined. The hatched band around the NWA signal curve shows the typical size of the total statistical and systematic uncertainties

from the signal regions. To reduce the Z+jets and W+jets contributions, two other variables are used: $p_T^{\ell,\text{sublead}}$ and the maximum value of the transverse mass calculated with either of the two leptons and the missing transverse momentum, m_T^W. The latter variable is defined as:

$$m_T^W = \sqrt{2 p_T^\ell E_T^{\text{miss}} \left(1 - \cos(\phi^\ell - \phi^{E_T^{\text{miss}}})\right)},$$

where p_T^ℓ and ϕ^ℓ are the transverse momentum and azimuthal angle of a given lepton and $\phi^{E_T^{\text{miss}}}$ is the azimuthal angle of the missing transverse momentum vector.

Three event categories are defined: two disjoint categories optimised for the VBF production, VBF $N_{\text{jet}} = 1$ and VBF $N_{\text{jet}} \geq 2$ (SR$_{\text{VBF1J}}$ and SR$_{\text{VBF2J}}$), and one quasi-inclusive category (excluding the VBF phase space) dedicated to the ggF or qqA signal (SR$_{\text{ggF}}$). For the VBF $N_{\text{jet}} = 1$ category, two discriminating variables are used to minimise the contribution of the ggF signal: the pseudorapidity of the jet, η_j, and the minimum value of the pseudorapidity difference between the jet and either of the leptons, $\min(|\Delta\eta_{j\ell}|)$. For the VBF $N_{\text{jet}} \geq 2$ category, the invariant mass, m_{jj}, and the rapidity difference, Δy_{jj}, of the two leading jets are used to select the VBF signal.

The NWA and LWA signal acceptance times the efficiency, after all selection requirements for a 700 GeV ggF signal, is approximately 50% in the quasi-inclusive ggF category and 5% or less in the VBF $N_{\text{jet}} = 1$ and $N_{\text{jet}} \geq 2$ categories. For a 700 GeV VBF signal, it is between 15 and 25% for the three event categories. The acceptance times efficiency for the three event categories combined, as a function of resonance mass, is shown in Fig. 1 for the different signals. For the spin-1 and spin-2 signals, the range up to 1 TeV is considered in the case of VBF model processes. For samples with lower resonance masses, the acceptance times efficiency is lower because the leptons are softer. This is also the reason why the search is limited to signal mass values greater than

about 200 GeV. The same selection is applied to all models and the different selection efficiencies between the models are mainly due to different $\Delta\eta_{\ell\ell}$ distributions for the different spin states.

The discriminating variable used for the statistical analysis (Sect. 9) in this search is the transverse mass defined as

$$m_T = \sqrt{\left(E_T^{\ell\ell} + E_T^{\text{miss}}\right)^2 - \left|\text{p}_T^{\ell\ell} + E_T^{\text{miss}}\right|^2},$$

where

$$E_T^{\ell\ell} = \sqrt{\left|\text{p}_T^{\ell\ell}\right|^2 + m_{\ell\ell}^2},$$

and $\text{p}_T^{\ell\ell}$ is the transverse momentum vector of the leading and subleading leptons.

7 Background estimation

The dominant background for the $e\nu\mu\nu$ final state is due to events with top quarks and due to SM WW events. Additional contributions to the background arise from V+jets and the diboson processes VZ, $V\gamma$ and $V\gamma^*$. Since the discriminating variable used for this search is the transverse mass, m_T, both the normalisation and the shape of the background m_T distribution must be estimated. The shape of the background is modelled using simulated events while the top-quark and WW background normalisations are determined by a simultaneous fit (Sect. 9) to the data in m_T-binned distributions in the signal regions and the total event yields in control regions. The normalisation factors of the fit, named "post-fit" normalisation factors[3] hereafter, provide the best overall matching

---

[3] The post-fit normalisation factors are checked to be consistent within the quoted uncertainties with the pre-fit ones obtained using the control regions only.

Table 3 Summary of all the selections used in the ggF and VBF WW and top-quark control regions. The common selection "veto if $p_T^{\ell,\text{other}} > 15\,\text{GeV}$" applied to all the regions is not explicitly shown

WW CR$_{\text{ggF}}$	Top CR$_{\text{ggF}}$	WW CR$_{\text{VBF1J}}$	Top CR$_{\text{VBF}}$
$N_{b\text{-tag}} = 0$	$N_{b\text{-tag}} = 1$	$N_{b\text{-tag}} = 0$	$N_{b\text{-tag}} \geq 1$
$|\Delta\eta_{\ell\ell}| > 1.8$	$|\Delta\eta_{\ell\ell}| < 1.8$	$(|\Delta\eta_{\ell\ell}| > 1.8$ or	–
	$m_{\ell\ell} > 55\,\text{GeV}$	$10\,\text{GeV} < m_{\ell\ell} < 55\,\text{GeV})$	$m_{\ell\ell} > 10\,\text{GeV}$
	$p_T^{\ell,\text{lead}} > 45\,\text{GeV}$		$p_T^{\ell,\text{lead}} > 25\,\text{GeV}$
	$p_T^{\ell,\text{sublead}} > 30\,\text{GeV}$		$p_T^{\ell,\text{sublead}} > 25\,\text{GeV}$
	$\max(m_T^W) > 50\,\text{GeV}$		–
	Excluding VBF1J and	VBF1J	VBF1J and VBF2J
	VBF2J phase space	phase space	phase space

between the number of observed data events and the corresponding SM background expectations in all the signal and control regions. The control regions are defined by criteria similar to those used for the signal regions, but with some requirements loosened or reversed to obtain signal-depleted samples, enriched in the relevant background. These criteria are summarised in Table 3.

The following subsections describe the methods used to estimate the most important background processes, namely top quark, WW, and W+jets. The Z/γ^*+jets and non-WW diboson background contributions are small. The Z/γ^*+jets Monte Carlo (MC) samples are normalised using NNLO cross sections [91] and the non-WW ones with NLO cross sections from the SHERPA event generator. The small background from the $m_h \simeq 125\,\text{GeV}$ Higgs boson resonance and its off-shell component is included and its interference with the continuum WW background is taken into account.

7.1 Top-quark background

Events containing top quarks can be produced as a $t\bar{t}$ pair or as a single top quark in association with either a W boson or a quark of another flavour. In this analysis, contributions from $t\bar{t}$ and single-top-quark events are estimated together, with their relative contributions determined by their predicted cross sections and by their relative acceptances obtained from MC simulation. The single-top-quark contribution varies from about 10 to 30% depending on the signal event category.

The normalisation of the top-quark background for the quasi-inclusive ggF category is determined in a control region (Top CR$_{\text{ggF}}$) where one jet is required to be b-tagged in addition to the signal region selection. The purity of the top-quark background in this CR is high (97%) and thus allows the modelling of the MC simulation to be validated. The distribution of the simulated leading lepton p_T in the Top CR$_{\text{ggF}}$ is found to disagree with the data and the ratio between the data and the simulation decreases with increasing $p_T^{\ell,\text{lead}}$. The simulated distribution is corrected in the SR$_{\text{ggF}}$ and corresponding CRs with factors obtained by fitting the ratio with a linear

function. The correction varies between $+4$ and -10% as $p_T^{\ell,\text{lead}}$ increases from 50 to 200 GeV.

The top-quark background control regions for the VBF categories (Top CR$_{\text{VBF}}$) have a small number of data events and are therefore merged. At least one jet is required to be b-tagged. In addition, the selection thresholds imposed on $m_{\ell\ell}$ and $p_T^{\ell,\text{(sub)lead}}$ are relaxed to 10 and 25 GeV, respectively, and the selection on $|\Delta\eta_{\ell\ell}|$ and $\max(m_T^W)$ is removed. The threshold value on $m_{\ell\ell}$ of 10 GeV is used to suppress background contributions from low-mass resonances decaying into different-flavour final states via $\tau^+\tau^-$. In this control region, the purity of the top-quark background is 96%, and no mis-modelling of the $p_T^{\ell,\text{lead}}$ distribution is observed.

The post-fit normalisation factors from the simultaneous fit are 0.96 ± 0.05 and $1.12^{+0.13}_{-0.12}$ in the ggF and the VBF control regions, respectively, where the uncertainty quoted corresponds to the combined statistical and systematic uncertainties.

Figure 2 shows the m_T distributions in the ggF and VBF top-quark CRs. The different background components are scaled according to the event yields obtained from the simultaneous fit. In the control regions the fit uses only the integrated event yields. The shape of the distributions is compared between data and MC predictions and found to be in good agreement after the application of the $p_T^{\ell,\text{lead}}$ correction described above for the ggF top-quark CR. The shapes of the m_T distribution for 700 GeV and 2 TeV NWA Higgs boson signals are also shown, normalised to the expected limits on $\sigma_H \times B(H \to WW)$ from this analysis. The ggF contribution from the SM Higgs boson is included in the WW component. The SM Higgs boson VBF contribution is negligibly small and is not shown in this and following figures.

7.2 WW background

The WW CR for the quasi-inclusive ggF category (WW CR$_{\text{ggF}}$) uses the same selection as for the SR except for $|\Delta\eta_{\ell\ell}|$ which is reversed so that the CR and SR are orthogonal. The selection conditions are shown in Table 3. The m_T distributions of the $q\bar{q} \to WW$ SHERPA MC sample in the
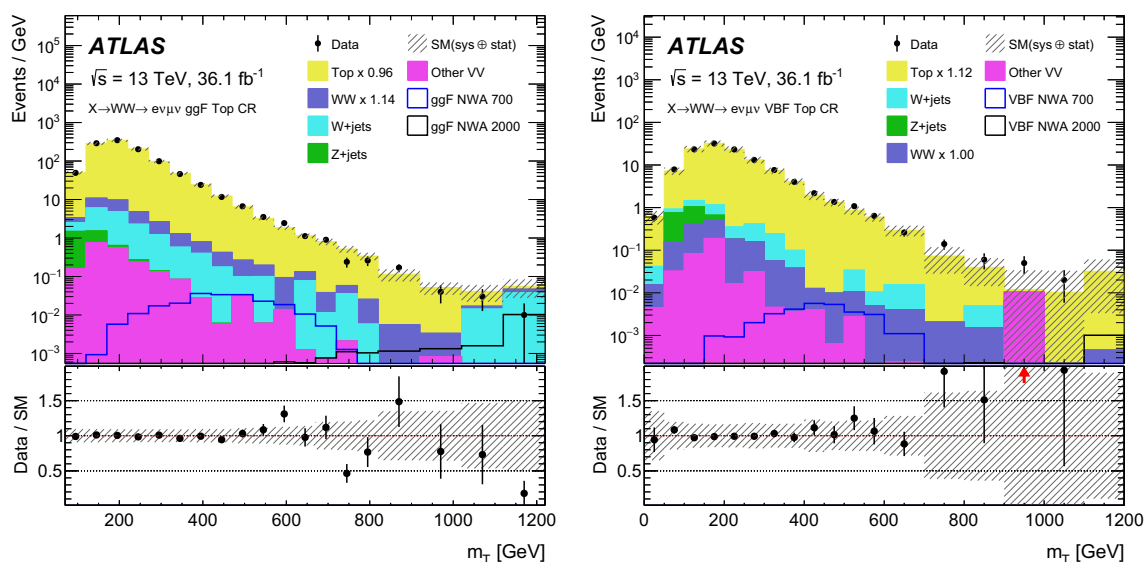
Fig. 2 Transverse mass distribution in the ggF (left) and VBF (right) top-quark control regions. In each plot, the last bin contains the overflow. The hatched band in the upper and lower panels shows the combined statistical, experimental and theoretical uncertainties in the predictions. The arrow in the lower right panel indicates that an entry is outside of the vertical scale. The top-quark and WW background event yields are scaled using the indicated normalisation factors obtained from the simultaneous fit to all signal and control regions. The heavy Higgs boson signal event yield, normalised to the expected limits on $\sigma_H \times B(H \to WW)$, is shown for masses of 700 GeV and 2 TeV in the NWA scenario

SR_{ggF} and WW CR_{ggF} are compared at MC generator level with corresponding predictions combining NNLO QCD calculations [92] with NLO electroweak (EW) corrections [93]. While the integrated yields of the distributions agree within 3% in both the SR_{ggF} and the WW CR_{ggF}, a small m_T shape difference is observed, particularly in the SR. The m_T distributions of the SHERPA samples are thus reweighted to the combined NNLO QCD and NLO EW predictions. The postfit normalisation factor obtained from the simultaneous fit for the WW contributions in the quasi-inclusive ggF categories is 1.14 ± 0.09, where the uncertainty quoted corresponds to the combined statistical and systematic uncertainties. The postfit purity of the WW background in the control region is 51%.

In order to select more data events, the WW CR for the $N_{jet} = 1$ VBF category (WW CR_{VBF1J}) uses a slightly different selection (shown in Table 3) from the one in the SR, but still disjoint from the SR. The normalisation factor obtained from the same simultaneous fit for the WW contribution in the WW CR_{VBF1J} is 1.0 ± 0.2, where the uncertainty quoted corresponds to the combined statistical and systematic uncertainties. The post-fit purity of the WW background in the control region is 44%.

The WW contribution in the $N_{jet} \geq 2$ VBF category is about 20%, and its prediction is taken from simulation because it is difficult to isolate a kinematic region with a sufficient number of WW events and with a small contamination from the top-quark background.

Figure 3 shows the m_T distributions in the WW CR_{ggF} and CR_{VBF1J}. The different background contributions are scaled

according to the event yields obtained from the simultaneous fit. For the WW control regions only integrated event yields are used in the fit, like in the fits of the top control regions.

7.3 W+jets background

Events with W bosons produced in association with jets may enter the SR when a jet is misidentified as a lepton. Due to the difficulties in accurately modelling the misidentification process in the simulation, the W+jets background contribution is estimated using the data-driven method developed for the SM $h \to WW$ analysis [94]. A sample of events is used which satisfies all event selection criteria, except that one of the two lepton candidates fails to meet the quality criteria for being an identified lepton but satisfies a less restrictive selection, referred to as "anti-identified". Anti-identified muons (electrons) have loosened isolation and impact parameter (likelihood identification) selection criteria as compared to the identified selection. From this data sample the non-W+jets contribution, dominated by top-quark and WW background processes, is subtracted on the basis of MC predictions. The W+jets purity of the samples is 46, 59 and 22% for the quasi-inclusive ggF, $N_{jet} = 1$ and $N_{jet} \geq 2$ VBF categories, respectively.

The W+jets contamination in the signal region is then determined by scaling the number of events in the background-subtracted data sample by an extrapolation factor, which is the ratio of the number of identified leptons to the number of anti-identified leptons in a data sample
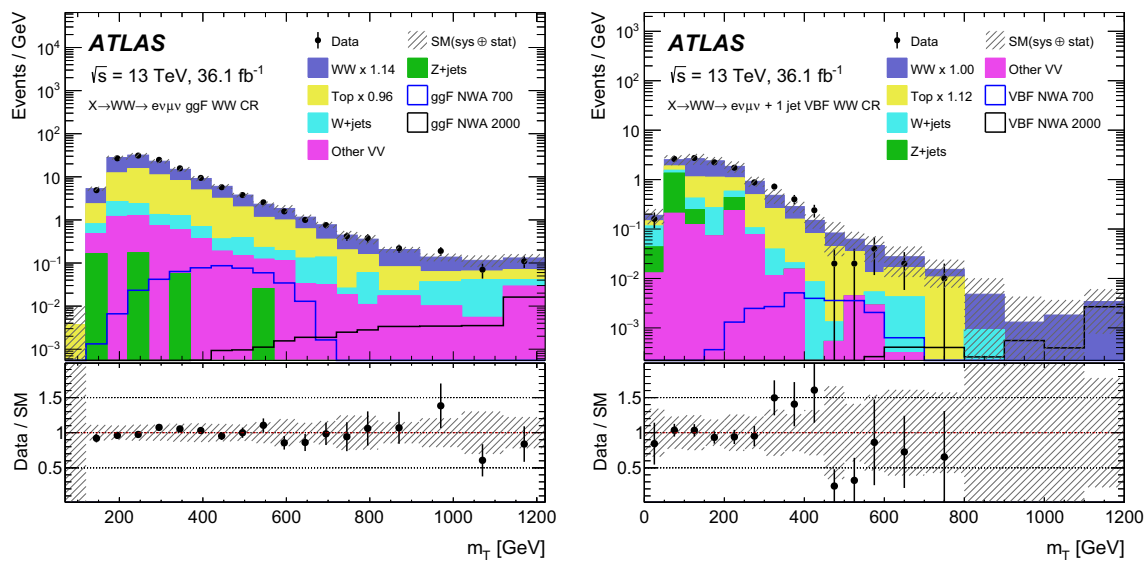
Fig. 3 Transverse mass distribution in the quasi-inclusive ggF (left) and $N_{jet} = 1$ VBF WW (right) control regions. In each plot, the last bin contains the overflow. The hatched band in the upper and lower panels shows the combined statistical, experimental and theoretical uncertainties in the predictions. The top-quark and WW background events are scaled using the indicated normalisation factors obtained from the simultaneous fit to all signal and control regions. The heavy Higgs boson signal event yield, normalised to the expected limits on $\sigma_H \times B(H \to WW)$, is shown for masses of 700 GeV and 2 TeV in the NWA scenario

of dijet events in bins of lepton p_T and η. The dijet sample is collected using prescaled low-p_T single-lepton triggers with thresholds of 12 GeV for electrons and 14 GeV for muons. Events are selected with exactly one candidate lepton, back-to-back with the leading jet. Electroweak processes in the dijet event sample, dominated by W+jets and Z/γ^* background contributions, are subtracted. The dominant systematic uncertainty in the estimation of the W+jets background is due to the differences between dijet and W+jets sample characteristics. All systematic uncertainties associated with this background estimate are listed in Sect. 8.1.

8 Systematic uncertainties

In this section, experimental and theoretical uncertainties in the normalisation and shape of the m_T distributions of the background and the signal are described. Except for those explicitly mentioned here, the shape uncertainties are small and thus neglected. Overall, the systematic uncertainty dominates, except in the tails of the m_T distributions where the statistical uncertainty is larger.

8.1 Experimental uncertainties

The dominant sources of experimental uncertainty in the signal and background yields are the jet energy scale and resolution (Jet) [85], the b-tagging efficiency (b-tag) [87], and the

pile-up modelling [86]. Other systematic uncertainties such as those associated with trigger efficiencies, lepton reconstruction and identification efficiencies, lepton momentum scales and resolutions [78,80], missing transverse momentum reconstruction [89] and the jet vertex tagger [86] are also considered when evaluating systematic effects on the shape and normalisation of the background, or the shape and efficiency of the signal yield. The uncertainty associated with the pile-up modelling is assessed by performing a variation of ±9% in the number of simulated pile-up interactions to cover the uncertainty in the ratio of the predicted and measured cross sections of non-diffractive inelastic events producing a hadronic system of mass $m_{X,had} > 13$ GeV [95].

For the main background from top-quark and WW processes, the impact of the most important experimental systematic uncertainties is summarised in Tables 4 and 5 together with dominant theoretical uncertainties. The maximum changes in yield for the up and down variations are shown in the various signal and control regions. The correlation between the SRs and CRs is taken into account in the simultaneous fit.

Systematic effects due to lepton identification efficiencies, momentum and scale resolutions, are found to be approximately 1%. They are not shown in the tables. The last column in the tables shows the total uncertainty, including these small uncertainty sources.

The data-driven W+jets background estimate is subject to several sources of systematic uncertainty. The subtraction of the subdominant electroweak processes (Sect. 7.3) has a

Table 4 Relative impact (in %) of dominant experimental and theoretical uncertainties in the event yields for the top-quark background processes in the three signal regions (SR$_{ggF}$, SR$_{VBF1J}$ and SR$_{VBF2J}$) and the top-quark and WW control regions (Top CR$_{ggF/VBF}$ and the WW CR$_{ggF/VBF1J}$). Jet and b-tag sources dominate the experimental uncertainty while ME+PS, Scale, Single top and PDF are the dominant theoretical uncertainties. The last column shows the total uncertainty including those not listed here

Source	Jet	b-tag	ME+PS	Scale	Single top	PDF	Total
SR$_{ggF}$	5.2	17	1.3	3.0	4.2	2.5	19
SR$_{VBF1J}$	9.6	7.8	1.0	1.6	5.9	2.6	15
SR$_{VBF2J}$	9.7	14	9.5	5.0	2.1	3.4	21
Top CR$_{ggF}$	2.2	4.8	0.34	0.21	2.6	3.0	6.6
WW CR$_{ggF}$	5.3	18	1.1	6.3	4.0	3.2	20
Top CR$_{VBF}$	8.2	3.5	10	1.5	1.3	3.7	14
WW CR$_{VBF1J}$	9.9	8.3	9.4	3.9	5.3	2.7	18

Table 5 Relative impact (in %) of dominant experimental and theoretical uncertainties in the event yields for the WW background processes in the three signal regions (SR$_{ggF}$, SR$_{VBF1J}$ and SR$_{VBF2J}$) and the WW control regions (WW CR$_{ggF/VBF1J}$). Jet and Pile-up sources dominate the experimental uncertainty while ME+PS, μ_R, Resummation and PDF are the dominant theoretical uncertainties. The last column shows the total uncertainty including those not listed here

Source	Jet	Pile-up	ME+PS	μ_R	Resummation	PDF	Total
SR$_{ggF}$	1.2	1.8	2.4	1.7	3.1	2.7	5.5
SR$_{VBF1J}$	17	2.8	11	7.3	5.0	2.3	23
SR$_{VBF2J}$	18	3.1	38	18	1.4	2.1	47
WW CR$_{ggF}$	1.1	1.8	2.6	0.95	2.9	3.6	5.9
WW CR$_{VBF1J}$	16	4.5	12	11	2.3	2.8	23

significant impact on the extrapolation factor calculation at high lepton p_T. The subtraction is varied, as described in Ref. [94], and the variation of the event yield in the signal region is taken as the uncertainty. The method assumes that the extrapolation factors of the dijet and W+jets samples are equal. Differences in the jet flavour composition between dijet and W+jets events introduce an additional systematic uncertainty. This is evaluated as the sum in quadrature of two contributions: differences between the extrapolation factors calculated with dijet samples and Z+jets samples in data, and differences between the extrapolation factors evaluated with W+jets and Z+jets MC samples. Finally, the statistical uncertainties of the different data and MC samples used to evaluate the extrapolation factors are taken as an additional source of systematic uncertainty. The overall relative systematic uncertainty of the W+jets background is found to be approximately 35% for each of the three signal event categories, with the dominant uncertainty being associated with the jet flavour composition.

The uncertainty in the total 2015 and 2016 integrated luminosity is 2.1%. It is derived, following a methodology similar to that detailed in Ref. [96], from van der Meer scans performed in August 2015 and May 2016, calibrated at high luminosity by various luminosity detectors.

8.2 Theoretical uncertainties of the background

For background sources which are normalised using control regions, theoretical uncertainties are evaluated for the extrapolation from the control region to the signal region.

For the top-quark and WW background, theoretical uncertainties in the extrapolation are evaluated according to the prescription from the LHC Higgs Cross Section Working Group [97]. The uncertainties include the impact of missing higher-order corrections, PDF variations and other MC modelling. The dominant theoretical uncertainties are shown in Tables 4 and 5.

For the top-quark background, the uncertainty from the event generator and parton shower modelling (ME+PS) is estimated by comparing the nominal POWHEG-BOX+PYTHIA8 generated samples with those from an alternative event generator, SHERPA 2.2.1. The uncertainty named "Scale" corresponds to variations of the renormalisation μ_R and factorisation μ_F scales as well as h_{damp}. The variations for μ_R and μ_F are between 0.5 and 2 from their nominal scale of $\sqrt{m_{top}^2 + p_T^2}$, with p_T being the top-quark transverse momentum. The parameter h_{damp} is varied between m_{top} and $2 \cdot m_{top}$ from its nominal scale $h_{damp} = 1.5 \cdot m_{top}$. In the analysis the single-top-quark and $t\bar{t}$ processes are studied together. An uncertainty of 20% [98,99] is assigned to the relative contribution of the single-top-quark processes, corresponding to the source "Single top" in Table 4. The PDF uncertainty is obtained by taking the envelope of the uncertainty of the NNPDF30NLO PDF set and its differences in central value with the CT14 [100] and MMHT 2014 [101] PDF sets, following the recommendations of Ref. [55]. The PDF uncertainties are m_T dependent and increase from 2 to 10% with m_T. This m_T dependence is taken into account in the signal regions. In the ggF quasi-inclusive category, two additional shape systematic uncertainties associated with the scale variations and the p_T reweighting for the leading lepton in the top-quark background are applied, the latter corresponding to $\pm 50\%$ of the reweighting correction. These two uncertainties are comparable and vary from a few percent at low m_T to about 10% at $m_T \simeq 1$ TeV, without affecting the integrated event yield of the top-quark background in the category.

For the WW background, the ME+PS modelling uncertainty is obtained by comparing the nominal SHERPA 2.2.1 sample with an alternative sample generated with POWHEG-BOX+PYTHIA8. The renormalisation, factorisation, and resummation scales are varied separately by factors of 0.5

and 2. The uncertainty corresponding to the factorisation scale variation is smaller than the other uncertainties and is not shown. The PDF uncertainty for the WW background is obtained and treated in the same way as for the top-quark background. In the ggF quasi-inclusive category, an additional shape uncertainty from ME+PS is applied. It varies from a few percent at low m_T to about 20% at $m_T \simeq 1$ TeV. There are no significant shape uncertainties in the m_T distributions in the VBF categories.

In addition to the scale uncertainties described above, a relative uncertainty of $\pm 50\%$ is assigned to the reweighting corrections of the $q\bar{q} \rightarrow WW$ SHERPA sample to the combined NNLO QCD and NLO EW predictions in the ggF SR and WW CR.

The $gg \rightarrow (h^*) \rightarrow WW$ process, where the SM 125 GeV Higgs boson is off-shell, is modelled at leading order with the SHERPA event generator with a K-factor of 1.7 that is used to account for higher-order cross-section corrections with an uncertainty of 60%, following the studies in Refs. [102–105].

Other small background processes, such as WZ, ZZ, Z/γ^*+jets and WW in the $N_{\text{jet}} \geq 2$ VBF category, do not have their own control regions. They are normalised to the theoretical predictions. The uncertainties in their yields due to the uncertainties in the predictions are evaluated with the same prescription as described above. The impact of these uncertainties is small (see Tables 6, 7 in Sect. 9).

8.3 Theoretical uncertainties in the signal predictions

Theoretical uncertainties in the signal acceptance include effects due to the choice of QCD renormalisation and factorisation scales, the PDF set as well as the underlying-event modelling, the parton shower model and the parton shower tune. These uncertainties are evaluated separately in each of

Table 6 Event yields in the signal and control regions for the quasi-inclusive ggF category. The predicted background yields and uncertainties are calculated after the simultaneous fit to the data in all the SRs and the CRs including those from Table 7. The statistical and systematic uncertainties are combined. The notation "VV" represents non-WW diboson background

	SR_{ggF}	Top CR_{ggF}	WW CR_{ggF}
WW	$11{,}500 \pm 800$	820 ± 120	3360 ± 220
Top quark	$11{,}800 \pm 600$	$52{,}550 \pm 330$	2610 ± 180
Z/γ^*	1420 ± 110	111 ± 20	20.9 ± 2.0
W+jets	1180 ± 320	710 ± 190	280 ± 70
VV	866 ± 34	101 ± 12	250 ± 11
Background	$26{,}740 \pm 170$	$54{,}290 \pm 250$	6510 ± 80
Data	$26{,}739$	$54{,}295$	6515

Table 7 Event yields in the signal and control regions for the $N_{\text{jet}} = 1$ and ≥ 2 VBF categories. The predicted background yields and uncertainties are calculated after the same simultaneous fit to the data in all the event categories as in Table 6. The statistical and systematic uncertainties are combined. The notation "VV" represents non-WW diboson background

	SR_{VBF1J}	SR_{VBF2J}	Top CR_{VBF}	WW CR_{VBF1J}
WW	390 ± 50	120 ± 26	61 ± 11	265 ± 32
Top quark	450 ± 50	391 ± 24	5650 ± 90	167 ± 18
Z/γ^*	45 ± 11	24 ± 6	68 ± 19	74 ± 12
W+jets	52 ± 13	8.9 ± 2.5	91 ± 24	43 ± 11
VV	32 ± 7	16.6 ± 1.9	20 ± 9	38 ± 4
Background	972 ± 29	563 ± 22	5890 ± 80	596 ± 22
Data	978	560	5889	594

the three event categories as a function of the resonance mass and independently for ggF- and VBF-induced resonances.

The effect of missing higher-order corrections in QCD on the signal acceptance is estimated by varying the renormalisation and factorisation scales independently by factors of 0.5 and 2 from the nominal scale of $\sqrt{m_H^2 + p_{T,H}^2}$, with m_H and $p_{T,H}$ being the mass and the transverse momentum of the heavy Higgs boson, respectively. The acceptance values obtained with these modified MC samples are compared to the signal acceptance of the nominal sample. For resonances produced via ggF, these uncertainties are found to be negligible in the quasi-inclusive ggF and $N_{\text{jet}} = 1$ VBF categories, while in the $N_{\text{jet}} \geq 2$ VBF category they range between 2.5 and 0.2% for a resonance mass varying from 200 GeV to 4 TeV (unless stated otherwise, the following uncertainties are quoted for the same mass range). For resonances produced via vector-boson fusion, these uncertainties range from 0.9 to 2.8% in the quasi-inclusive ggF category, from 1.9 to 3.6% in the $N_{\text{jet}} = 1$ VBF category and from 1.0 to 7.3% in the $N_{\text{jet}} \geq 2$ VBF category.

The PDF-induced uncertainties in the signal acceptance are determined in the same way as for the top-quark and WW background processes. For the ggF-induced (VBF-induced) signal, these uncertainties reach 0.4% (1.7%), 1.5% (1.2%) and 1.6% (1.5%) for the quasi-inclusive ggF, $N_{\text{jet}} = 1$ and $N_{\text{jet}} \geq 2$ VBF event categories, respectively.

The uncertainties corresponding to the parton shower tune and the underlying event are derived by moving independently, up or down, the PYTHIA internal parameters that are associated with final-state radiation or the multiple parton interactions to study separately their influence on the signal acceptance of the various signal mass points. These uncertainties are compared for each event category and mass point to the uncertainties from the choice of parton shower model, which are estimated by comparing the results obtained for the nominal parton shower generator to those obtained using
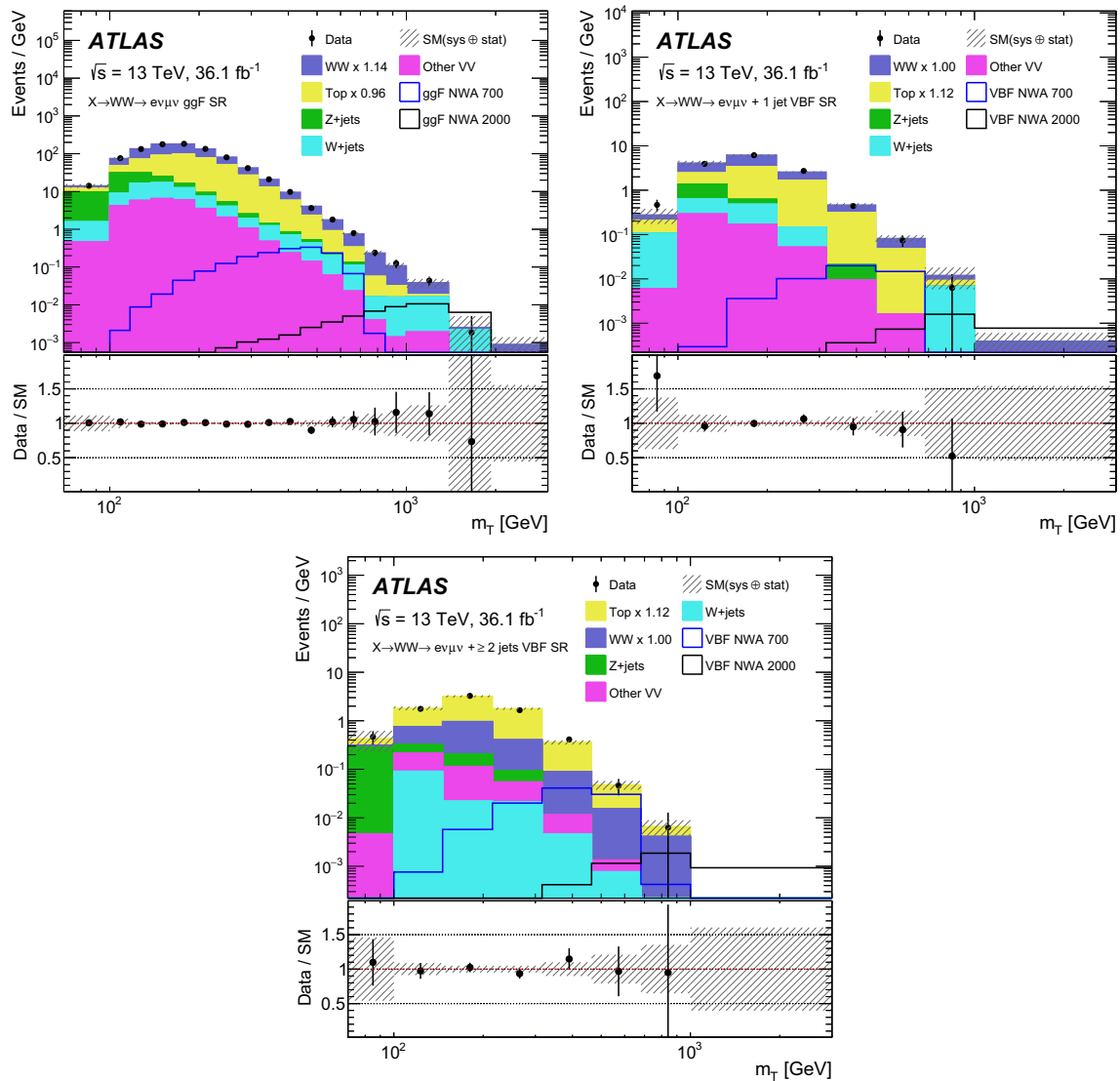
Fig. 4 Post-fit distributions of the transverse mass m_T in the SR_{ggF} (top left), SR_{VBF1J} (top right) and SR_{VBF2J} (bottom) categories. In each plot, the last bin contains the overflow. The hatched band in the upper and lower panels shows the total uncertainty of the fit. The top-quark and WW background event yields are scaled using the indicated nor- malisation factors obtained from the simultaneous fit to all signal and control regions. The heavy Higgs boson signal event yield is normalised to the expected limits on $\sigma_H \times B(H \rightarrow WW)$ and is shown for masses of 700 GeV and 2 TeV in the NWA scenario

HERWIG++ [106,107]. The tune uncertainties are found to be smaller than the shower uncertainties for all mass points. Thus only the latter uncertainties are considered in the final results. The corresponding uncertainties for ggF-induced signals increase from 1.3 to 3.1%, from 13 to 28%, and from 2.3 to 15% for increasing resonance masses in the quasi-inclusive ggF, $N_{jet} = 1$ and $N_{jet} \geq 2$ VBF categories, respectively. The uncertainties for VBF-induced signals increase from 4.3 to 19%, from 5.1 to 9.0%, and from 3.3 to 8.0% in the three categories.

In addition, uncertainties due to missing higher-order corrections in QCD are evaluated for ggF-induced processes for each event category, considering also event migration effects between different event categories. This follows the method proposed by Stewart and Tackmann [108]. The corresponding uncertainties range from 3 to 10% for the quasi-inclusive ggF category and from 4 to 30% (30–60) for the $N_{jet} = 1$ ($N_{jet} \geq 2$) VBF event categories.

9 Results

The statistical method used to interpret the results of the search is described in Ref. [109]. A likelihood function $\mathcal{L}$
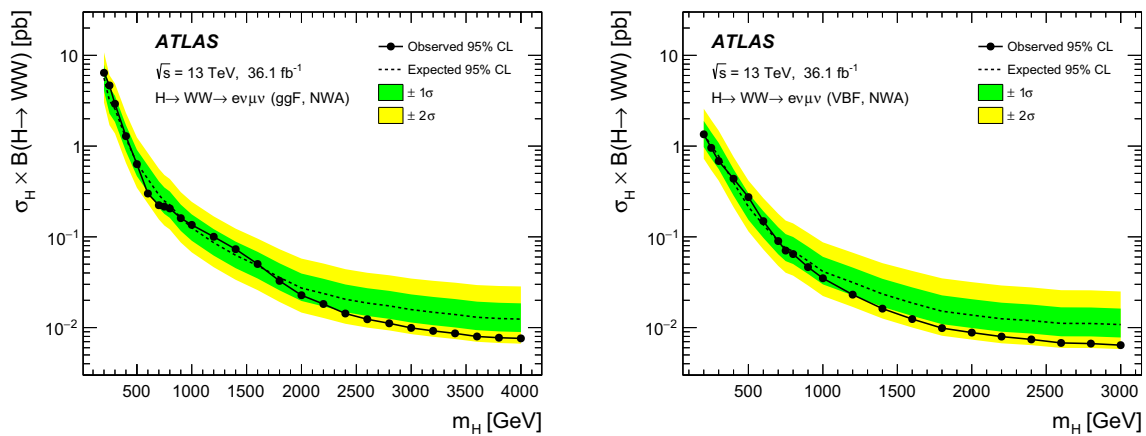
Fig. 5 Upper limits at 95% CL on the Higgs boson production cross section times branching fraction $\sigma_H \times B(H \to WW)$ in the $e\nu\mu\nu$ channel, for ggF (left) and VBF (right) signals with narrow-width lineshape as a function of the signal mass. The inner and outer bands show the $\pm 1\sigma$ and $\pm 2\sigma$ ranges around the expected limit
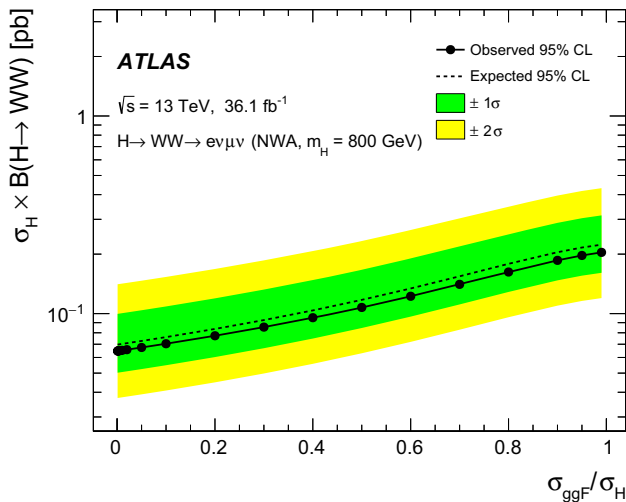

Fig. 6 Upper limits at 95% CL on the total ggF and VBF Higgs boson production cross section times branching fraction $\sigma_H \times B(H \to WW)$ in the $e\nu\mu\nu$ channel, for a signal at 800 GeV as a function of the ggF cross section divided by the combined ggF and VBF production cross section. The inner and outer bands show the $\pm 1\sigma$ and $\pm 2\sigma$ ranges around the expected limit

is defined as the product of Poisson probabilities associated with the number of events in bins of the m_T distributions in the signal regions and of the total yields in the control regions. Each source of systematic uncertainty is parameterised by a corresponding nuisance parameter θ constrained by a Gaussian function.

The m_T distributions in the signal regions are divided into 18 (8) bins for the ggF quasi-inclusive ($N_{jet} = 1$ and ≥ 2 VBF) categories. The bins are of variable size to reflect the increasing width of the m_T distribution of the expected signal with increasing mass, while keeping the statistical precision of the background contributions in each bin sufficiently high.

The numbers of events predicted and observed in the signal and control regions are shown for the quasi-inclusive ggF categories in Table 6 and for the VBF $N_{jet} = 1$ and ≥ 2 categories in Table 7. These yields are obtained from a simultaneous fit to the data in all the SRs and the CRs. The fitted signal event yield is consistent with zero. The background compositions depend strongly on the event categories: the top-quark and WW processes are comparable in SR$_{ggF}$ and SR$_{VBF1J}$ while the top-quark events dominate in SR$_{VBF2J}$. The large reduction of the total background uncertainty is due to strong anti-correlations between some of the uncertainty sources of the top-quark and WW background. The m_T distributions in SR$_{ggF}$, SR$_{VBF1J}$ and SR$_{VBF2J}$ are shown in Fig. 4. As no excess over the background prediction is observed, upper limits at 95% confidence level (CL) are set on the production cross section times the branching fraction, $\sigma_X \times B(X \to WW)$, for signals in each benchmark model.

The 95% CL upper limits are computed using the modified frequentist method known as CL$_s$ [110], using the asymptotic approximation of the distribution of a test statistic [111], q_μ, a function of the signal strength μ, defined as the ratio of the measured $\sigma_X \times B(X \to WW)$ to that of the prediction:

$$q_\mu = -2 \ln \left(\frac{\mathcal{L}(\mu; \hat{\boldsymbol{\theta}}_\mu)}{\mathcal{L}(\hat{\mu}; \hat{\boldsymbol{\theta}})} \right).$$

The quantities $\hat{\mu}$ and $\hat{\boldsymbol{\theta}}$ are those values of μ and $\boldsymbol{\theta}$, respectively, that unconditionally maximise $\mathcal{L}$. The numerator depends on the values $\hat{\boldsymbol{\theta}}_\mu$ that maximise $\mathcal{L}$ for a given value of μ.

Limits are obtained separately for ggF and VBF production for the NWA and LWA signal hypotheses. To derive the expected limits on the ggF (VBF) production modes, the VBF (ggF) production cross section is set to zero so that the

Fig. 7 Exclusion contours at 95% CL in the plane of $\tan \beta$ and $\cos(\beta - \alpha)$ for Type I (left) and Type II (right) 2HDM signals with three mass values of 200 GeV (top), 300 GeV (middle) and 500 GeV (bottom). The inner and outer bands show the $\pm 1\sigma$ and $\pm 2\sigma$ ranges around the expected limit and the hatched regions are excluded
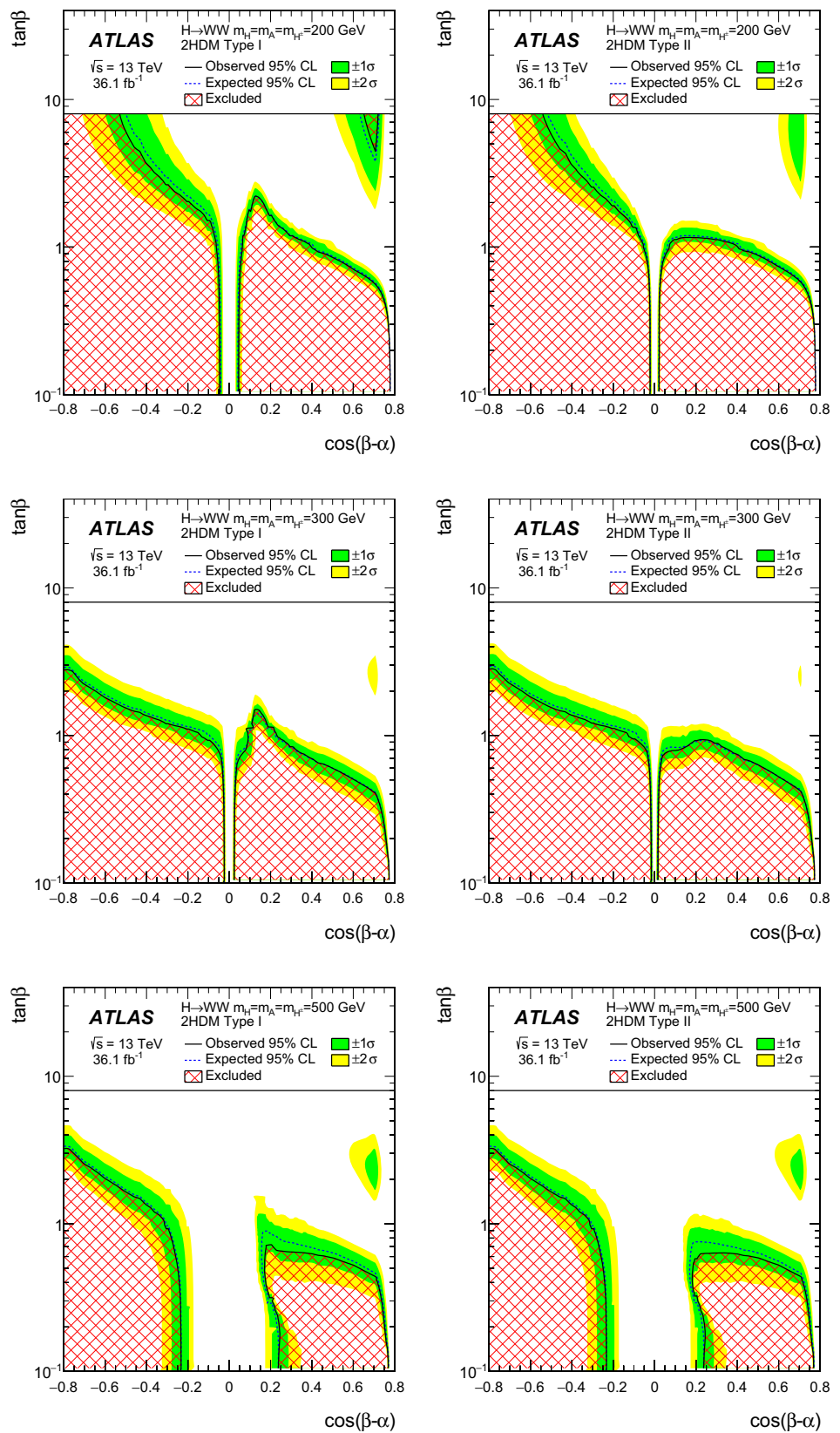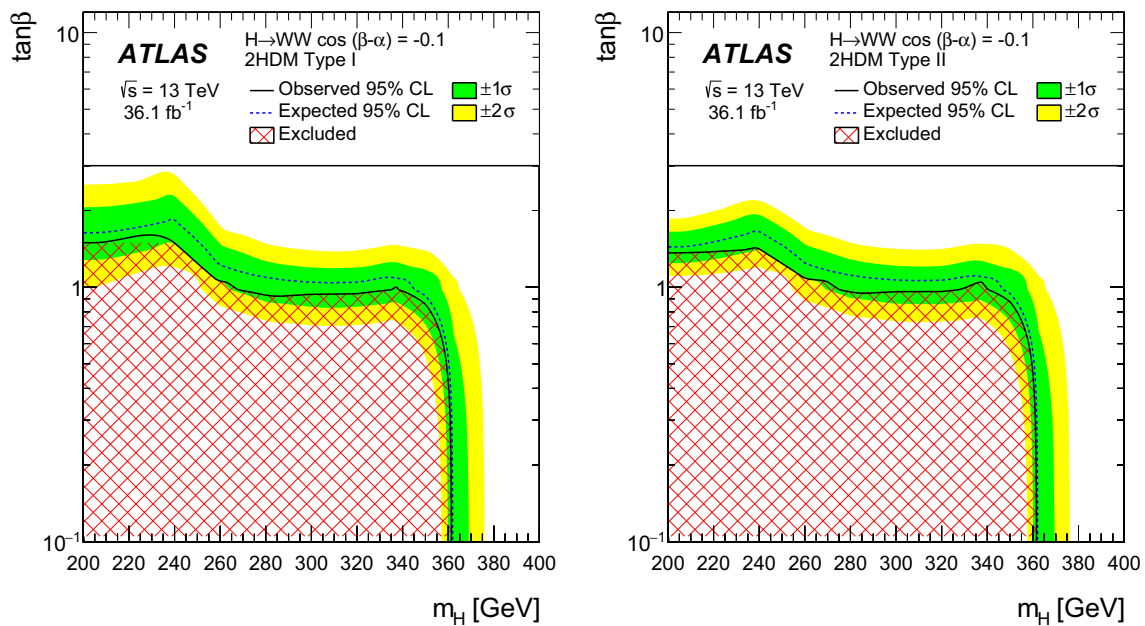
Fig. 8 Exclusion contours at 95% CL in the plane of $\tan\beta$ and m_H for Type I (left) and Type II (right) 2HDM signals with $\cos(\beta-\alpha) = -0.1$. The inner and outer bands show the $\pm 1\sigma$ and $\pm 2\sigma$ ranges around the expected limit and the hatched regions are excluded. The other heavy Higgs boson states A and $H^{\pm}$ are assumed to have the same mass as H

expected limits correspond to the background-only hypothesis. To derive the observed limits on the ggF (VBF) production mode, the VBF (ggF) production cross section is treated as a nuisance parameter in the fit and profiled, in the same way as dealing with the normalisation factors of the different background processes. This approach avoids making any assumption about the presence or absence of the signal in any of these production modes.

Figure 5 shows the 95% CL upper limits on $\sigma_H \times B(H \to WW)$ as a function of m_H for a Higgs boson in the NWA scenario in the mass range $200\,\text{GeV} \leq m_H \leq 4(3)\,\text{TeV}$ for the ggF (VBF) production. Values above 6.4 pb (1.3 pb) at $m_H = 200\,\text{GeV}$ and above 0.008 pb (0.006 pb) at 4 (3) TeV are excluded at 95% CL by the quasi-inclusive ggF (VBF) NWA analysis. The main systematic uncertainties affecting the limits are the p_T correction for the leading lepton in the top-quark background, scale variations for the top-quark background, the parton shower modelling of the WW MC generator, and the jet energy scale and resolution uncertainties. Limits are consistent with those expected in the absence of a signal over the investigated mass range. The fact that the observed limits are more stringent than the expected ones for mass values beyond 2 TeV is explained by the deficit in data at the high m_T tail in Fig. 4. These limits are extracted using the asymptotic approximation and their accuracy is verified to be consistent within about 5% at 800 GeV and better than 20% at 2 TeV and beyond using pseudo-experiments.

The analysis can be extended to a more general case where the relative fraction of the ggF production cross section varies over the total ggF and VBF production cross section. The corresponding 95% CL upper exclusion limits for a signal at 800 GeV are shown in Fig. 6. The dependence of the limits on the ggF fraction for other masses is similar but becomes slightly stronger (weaker) for lower (higher) mass values. The limit values for a ggF fraction of 0 and 1 are comparable with the VBF and ggF limits shown in Fig. 5 at the same mass value. The VBF limits are tighter than the ggF limits since the VBF $N_{\text{jet}} \geq 2$ signal region has the smallest background contribution and thus is the most sensitive.

The NWA exclusion limit shown above can be further translated to exclusion contours in the 2HDM for the phase space where the narrow-width approximation is valid. The 95% CL exclusion contours for Type I and Type II in the plane of $\tan\beta$ and $\cos(\beta-\alpha)$ for three mass values of 200, 300 and 500 GeV are shown in Fig. 7. For a fixed value of $\cos(\beta-\alpha) = -0.1$, 95% CL exclusion limits on $\tan\beta$ as a function of the heavy Higgs boson mass are shown in Fig. 8. The coupling of the heaviest CP-even Higgs boson to vector bosons is proportional to $\cos(\beta-\alpha)$ and in the decoupling limit $\cos(\beta-\alpha) \to 0$, the light CP-even Higgs boson is indistinguishable from a SM Higgs boson with the same mass. The range of $\cos(\beta-\alpha)$ and $\tan\beta$ explored is limited to the region where the assumption of a heavy narrow-width Higgs boson with negligible interference is valid. When calculating the limits at a given choice of $\cos(\beta-\alpha)$ and $\tan\beta$,
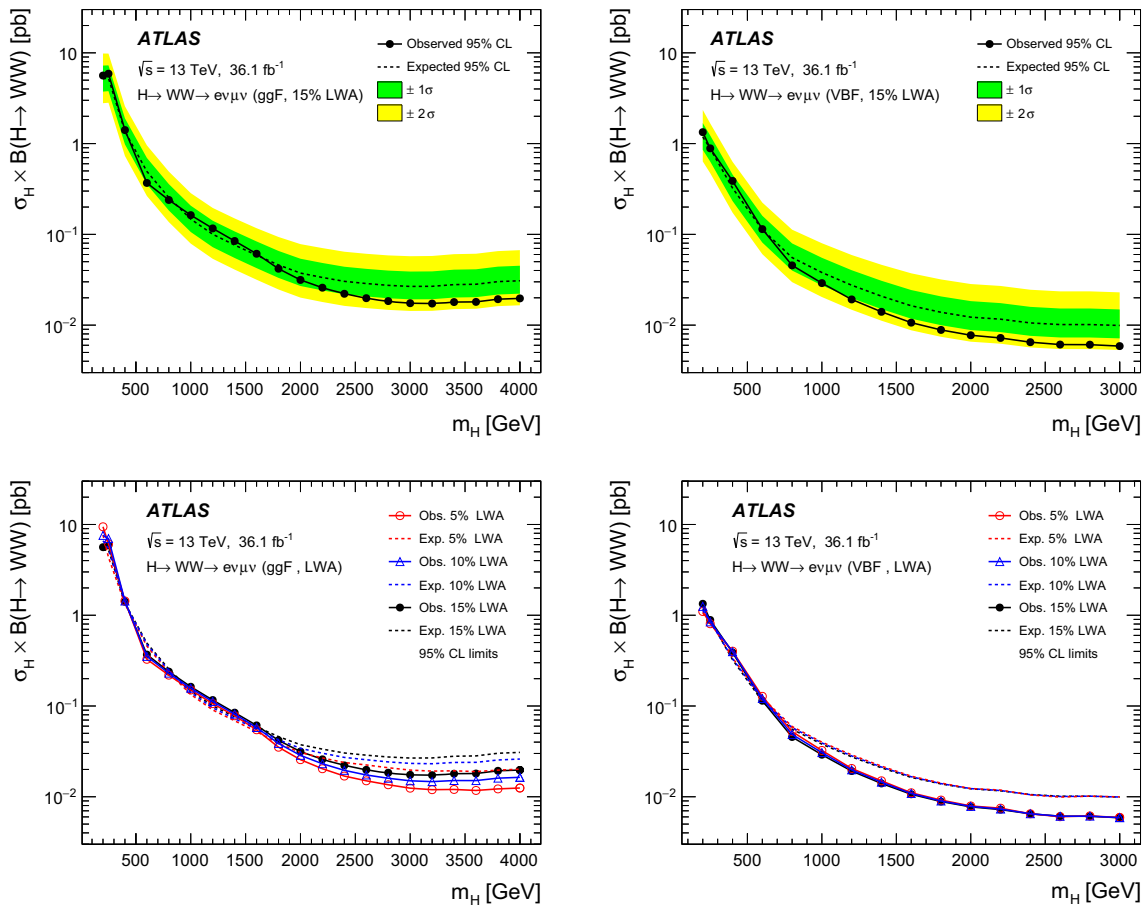
Fig. 9 Upper limits at 95% CL on the Higgs boson production cross section times branching fraction $\sigma_H \times B(H \to WW)$ in the $e\nu\mu\nu$ channel, for a signal with a width of 15% of the mass (top) and the comparison of three different widths (bottom) for the ggF (left) and VBF (right) production. The inner and outer bands show the $\pm 1\sigma$ and $\pm 2\sigma$ ranges around the expected limit
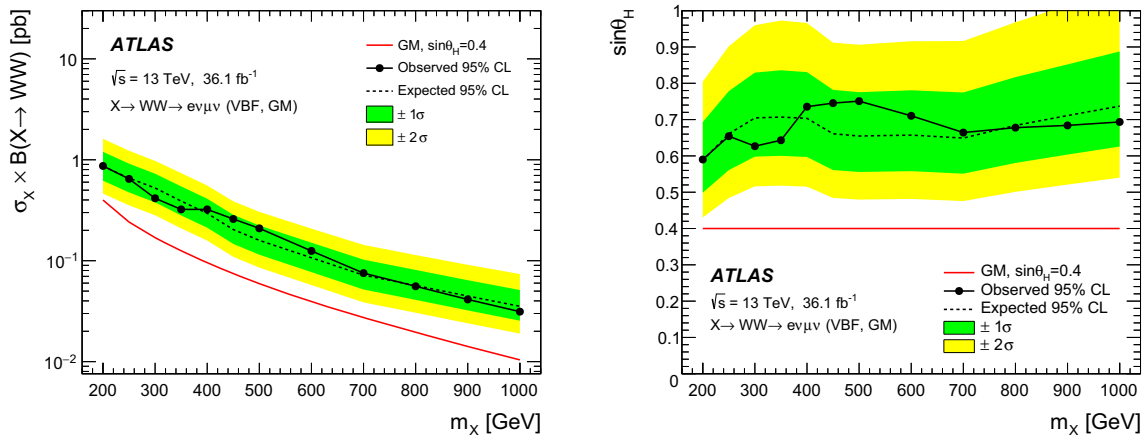

Fig. 10 Upper limits at 95% CL on the resonance production cross section times branching fraction $\sigma_X \times B(X \to WW)$ (left) and on $\sin\theta_H$ (right) in the $e\nu\mu\nu$ channel, for a GM signal. The inner and outer bands show the $\pm 1\sigma$ and $\pm 2\sigma$ ranges around the expected limit. The full curves without dots correspond to the predicted theoretical cross section and the model parameter used in the benchmark model, respectively
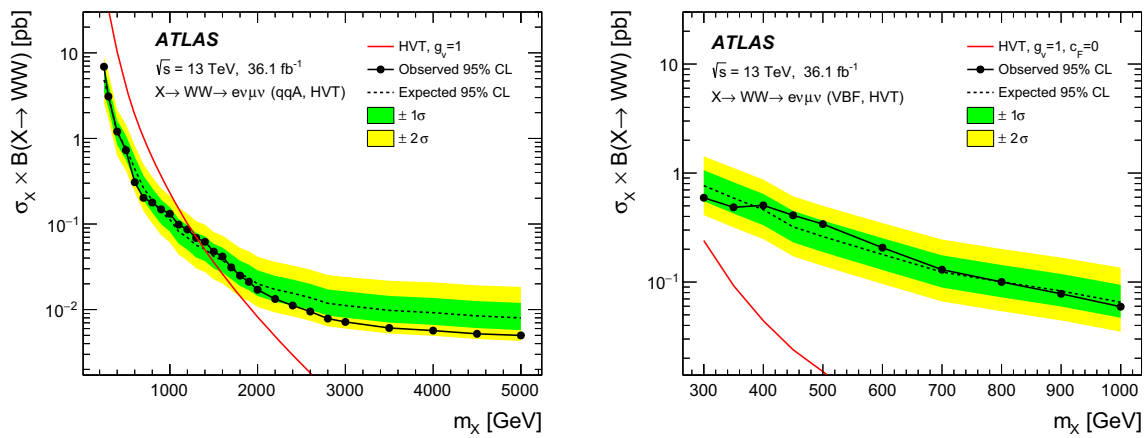
Fig. 11 Upper limits at 95% CL on the resonance production cross section times branching faction $\sigma_X \times B(X \to WW)$ in the $e\nu\mu\nu$ channel, for HVT qqA (left) and VBF (right) signals. The inner and outer bands show the $\pm 1\sigma$ and $\pm 2\sigma$ ranges around the expected limit. The full curves without dots correspond to the predicted theoretical cross sections

Fig. 12 Upper limits at 95% CL on the resonance production cross section times branching fraction $\sigma_X \times B(X \to WW)$ in the $e\nu\mu\nu$ channel, for a graviton signal with two different couplings of $k/\bar{M}_{Pl} = 1$ (left) and $k/\bar{M}_{Pl} = 0.5$ (right), and for an ELM spin-2 VBF signal (bottom). The inner and outer bands show the $\pm 1\sigma$ and $\pm 2\sigma$ ranges around the expected limit. The full curves without dots correspond to the predicted theoretical cross sections
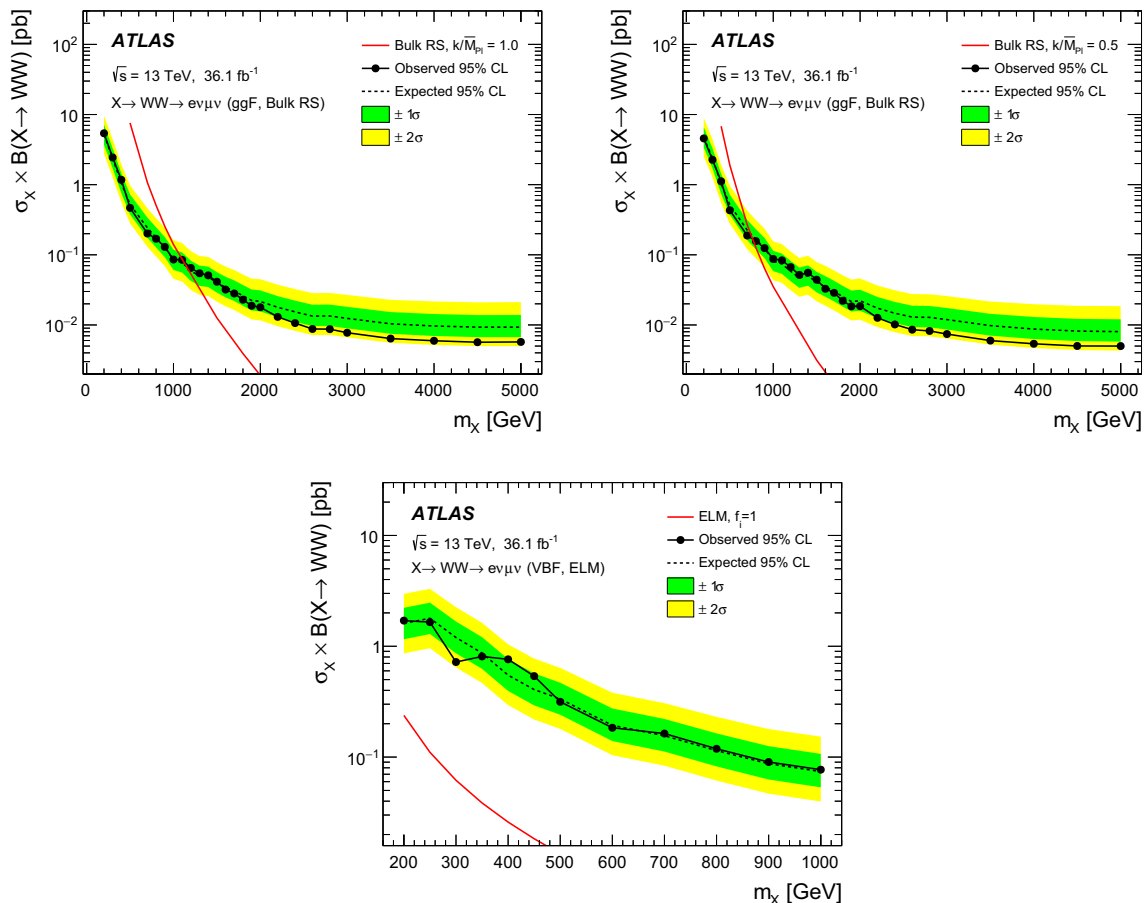
the relative rate of ggF and VBF production in the fit is set to the prediction of the 2HDM for that parameter choice. The white regions in the exclusion plots indicate regions of parameter space which are not excluded by the present analysis.

For the LWA scenario, the interference effects among the heavy boson, the light Higgs boson at 125 GeV and the SM WW continuum background were studied and found to have negligible impact on the exclusion limits. The 95% CL upper limits are shown in Fig. 9. The limits for signal widths of 5, 10 and 15% are comparable with those from the NWA scenario for the VBF signals while for the ggF signals, the limits weaken slightly at high masses as the width increases. For the LWA 15% case, the upper exclusion limit ranges between 5.2 pb (1.3 pb) at $m_H = 200$ GeV and 0.02 pb (0.006 pb) at 4 (3) TeV for the ggF (VBF) signals.

Figure 10 shows the limits on the resonance production cross section times branching fraction $\sigma_X \times B(X \to WW)$ and $\sin \theta_H$ for a scalar GM signal with masses between 200 GeV and 1 TeV. At the observed limit, the width is narrower than the experimental resolution [46]. The current sensitivity is not sufficient to exclude the benchmark model with $\sin \theta_H = 0.4$.

Limits are derived in the mass range from 250 GeV to 5 TeV and from 300 GeV to 1 TeV for a qqA and VBF HVT signal, respectively, as shown in Fig. 11. For the qqA production, signals below about 1.3 TeV are excluded at 95% CL. No limit can be set for the VBF production in the benchmark model that assumes a coupling strength to gauge bosons $g_V = 1$ and a coupling to fermions $c_F = 0$. The model has an intrinsic width much narrower than the detector resolution.

Figure 12 shows the limits on a $G_{KK} \to WW$ signal for two different couplings: $k/\bar{M}_{Pl} = 1$ and $k/\bar{M}_{Pl} = 0.5$, for masses between 200 GeV and 5 TeV, and for an ELM spin-2 VBF signal for masses between 200 GeV and 1 TeV. The observed limits exclude a KK graviton signal lighter than 1.1 TeV (750 GeV) with the higher (lower) coupling, while the current sensitivity is not sufficient to exclude the ELM spin-2 VBF signal.

10 Conclusion

A search for heavy neutral resonances decaying into a WW boson pair in the $e\nu\mu\nu$ channel performed by the ATLAS Collaboration at the LHC is presented. The search uses proton–proton collision data collected at a centre-of-mass energy of 13 TeV corresponding to an integrated luminosity of 36.1 fb^{-1}. No significant excess of events beyond the Standard Model background prediction is found in the mass range between 200 GeV and up to 5 TeV. Upper lim-

its are set on the product of the production cross section and the $X \to WW$ branching fraction in several scenarios: a high-mass Higgs boson with a narrow width or with intermediate widths (of 5, 10 and 15% of the heavy Higgs boson mass), as well as other spin-0, spin-1, and spin-2 signals. For the narrow-width heavy Higgs boson signals, values above 6.4 pb at $m_H = 200$ GeV and above 0.008 pb at 4 TeV are excluded at 95% confidence level for the gluon–gluon fusion production mode. The corresponding values for the vector-boson fusion production modes are 1.3 pb and 0.006 pb at 200 GeV and 3 TeV, respectively. For the signals of the heavy vector triplet model A produced by quark–antiquark annihilation and of the Randall–Sundrom graviton model with $k/\bar{M}_{Pl} = 1$ and 0.5, mass values below 1.3, 1.1 TeV and 750 GeV are excluded, respectively.

References

1. ATLAS Collaboration, Measurements of the Higgs boson production and decay rates and coupling strengths using pp collision data at $\sqrt{s}$ = 7 and 8 TeV in the ATLAS experiment. Eur. Phys. J. C **76**, 6 (2016). arXiv:1507.04548 [hep-ex]
2. ATLAS Collaboration, Study of the spin and parity of the Higgs boson in diboson decays with the ATLAS detector. Eur. Phys. J. C **75**, 476 (2015). arXiv:1506.05669 [hep-ex]
3. CMS Collaboration, Precise determination of the mass of the Higgs boson and tests of compatibility of its couplings with the standard model predictions using proton collisions at 7 and 8 TeV. Eur. Phys. J. C **75**, 212 (2015). arXiv:1412.8662 [hep-ex]
4. ATLAS and CMS Collaborations, Measurements of the Higgs boson production and decay rates and constraints on its couplings from a combined ATLAS and CMS analysis of the LHC pp collision data at $\sqrt{s}$ = 7 and 8 TeV. JHEP **08**, 045 (2016). arXiv:1606.02266 [hep-ex]
5. ATLAS Collaboration, Observation of a new particle in the search for the Standard Model Higgs boson with the ATLAS detector at the LHC. Phys. Lett. B **716**, 1 (2012). arXiv:1207.7214 [hep-ex]
6. CMS Collaboration, Observation of a new boson at a mass of 125 GeV with the CMS experiment at the LHC. Phys. Lett. B **716**, 30 (2012). arXiv:1207.7235 [hep-ex]
7. D. de Florian et al., Handbook of LHC Higgs cross sections: 4. Deciphering the nature of the Higgs sector (2016). arXiv:1610.07922 [hep-ph]
8. I.P. Ivanov, Building and testing models with extended Higgs sectors. Prog. Part. Nucl. Phys. **95**, 160 (2017). arXiv:1702.03776 [hep-ph]
9. K. Agashe, R. Contino, A. Pomarol, The minimal composite Higgs model. Nucl. Phys. B **719**, 165 (2005). arXiv:hep-ph/0412089
10. G. Giudice et al., The strongly-interacting light Higgs. JHEP **06**, 045 (2007). arXiv:hep-ph/0703164
11. L. Randall, R. Sundrum, A large mass hierarchy from a small extra dimension. Phys. Rev. Lett. **83**, 3370 (1999). arXiv:hep-ph/9905221
12. K. Agashe et al., Warped gravitons at the LHC and beyond. Phys. Rev. D **76**, 036006 (2007). arXiv:hep-ph/0701186
13. O. Antipin, D. Atwood, A. Soni, Search for RS gravitons via $W_L W_L$ decays. Phys. Lett. B **666**, 155 (2008). arXiv:0711.3175 [hep-ph]
14. O. Antipin, A. Soni, Towards establishing the spin of warped gravitons. JHEP **10**, 018 (2008). arXiv:0806.3427 [hep-ph]
15. H. Georgi, M. Machacek, Doubly charged Higgs bosons. Nucl. Phys. B **262**, 463 (1985)
16. M.S. Chanowitz, M. Golden, Higgs boson triplets with $M_W = M_Z \cos\theta_W$. Phys. Lett. B **165**, 105 (1985)
17. J. de Blas, J.M. Lizana, M. Perez-Victoria, Combining searches of Z' and W' bosons. JHEP **01**, 166 (2013). arXiv:1211.2229 [hep-ph]
18. D. Pappadopulo et al., Heavy vector triplets: bridging theory and data. JHEP **09**, 060 (2014). arXiv:1402.4431 [hep-ph]
19. T. Han, J.D. Lykken, R.-J. Zhang, On Kaluza–Klein states from large extra dimensions. Phys. Rev. D **59**, 105006 (1999). arXiv:hep-ph/9811350
20. J. Frank, M. Rauch, D. Zeppenfeld, Spin-2 resonances in vector-boson-fusion processes at next-to-leading order QCD. Phys. Rev. D **87**, 055020 (2013). arXiv:1211.3658 [hep-ph]
21. ATLAS Collaboration, Search for a high-mass Higgs boson decaying to a W boson pair in pp collisions at $\sqrt{s}$ = 8 TeV with the ATLAS detector. JHEP **01**, 032 (2016). arXiv:1509.00389 [hep-ex]

22. CMS Collaboration, Search for a Higgs boson in the mass range from 145 to 1000 GeV decaying to a pair of W or Z bosons. JHEP **10**, 144 (2015). arXiv:1504.00936 [hep-ex]
23. ATLAS Collaboration, Search for new phenomena in the $WW \to \ell\nu\ell'\nu'$ final state in pp collisions at $\sqrt{s}$ = 7 TeV with the ATLAS detector. Phys. Lett. B **718**, 860 (2013). arXiv:1208.2880 [hep-ex]
24. CMS Collaboration, Search for massive resonances in dijet systems containing jets tagged as W or Z boson decays in pp collisions at $\sqrt{s}$ = 8 TeV. JHEP **08**, 173 (2014). arXiv:1405.1994 [hep-ex]
25. CMS Collaboration, Search for massive resonances decaying into pairs of boosted bosons in semi-leptonic final states at $\sqrt{s}$ = 8 TeV. JHEP **08**, 174 (2014). arXiv:1405.3447 [hep-ex]
26. ATLAS Collaboration, Search for WZ resonances in the fully leptonic channel using pp collisions at $\sqrt{s}$ = 8 TeV with the ATLAS detector. Phys. Lett. B **737**, 223 (2014). arXiv:1406.4456 [hep-ex]
27. CMS Collaboration, Search for new resonances decaying via WZ to leptons in proton-proton collisions at $\sqrt{s}$ = 8 TeV. Phys. Lett. B **740**, 83 (2015). arXiv:1407.3476 [hep-ex]
28. ATLAS Collaboration, Search for production of WW/WZ resonances decaying to a lepton, neutrino and jets in pp collisions at $\sqrt{s}$ = 8 TeV with the ATLAS detector. Eur. Phys. J. C **75**, 209 (2015). Erratum: Eur. Phys. J. C **75**, 370 (2015). arXiv:1503.04677 [hep-ex]
29. ATLAS Collaboration, Search for high-mass diboson resonances with boson-tagged jets in proton-proton collisions at $\sqrt{s}$ = 8 TeV with the ATLAS detector. JHEP **12**, 055 (2015). arXiv:1506.00962 [hep-ex]
30. ATLAS Collaboration, Combination of searches for WW, WZ, and ZZ resonances in pp collisions at $\sqrt{s}$ = 8 TeV with the ATLAS detector. Phys. Lett. B **755**, 285 (2016). arXiv:1512.05099 [hep-ex]
31. ATLAS Collaboration, Searches for heavy diboson resonances in pp collisions at $\sqrt{s}$ = 13 TeV with the ATLAS detector. JHEP **09**, 173 (2016). arXiv:1606.04833 [hep-ex]
32. CMS Collaboration, Search for massive resonances decaying into WW, WZ or ZZ bosons in proton-proton collisions at $\sqrt{s}$ = 13 TeV. JHEP **03**, 162 (2017). arXiv:1612.09159 [hep-ex]
33. CMS Collaboration, Combination of searches for heavy resonances decaying to WW, WZ, ZZ, WH, and ZH boson pairs in proton-proton collisions at $\sqrt{s}$ = 8 and 13 TeV. Phys. Lett. B **774**, 533 (2017). arXiv:1705.09171 [hep-ex]
34. ATLAS Collaboration, Search for diboson resonances with boson-tagged jets in pp collisions at $\sqrt{s}$ = 13 TeV with the ATLAS detector (2017). arXiv:1708.04445 [hep-ex]
35. CMS Collaboration, Search for massive resonances decaying into WW, WZ, ZZ, qW, and qZ with dijet final states at $\sqrt{s}$ = 13 TeV (2017). arXiv:1708.05379 [hep-ex]
36. ATLAS Collaboration, Searches for heavy ZZ and ZW resonances in the $\ell\ell qq$ and $\nu\nu qq$ final states in pp collisions at $\sqrt{s}$ = 13 TeV with the ATLAS detector (2017). arXiv:1708.09638 [hep-ex]
37. ATLAS Collaboration, Constraints on new phenomena via Higgs boson couplings and invisible decays with the ATLAS detector. JHEP **11**, 206 (2015). arXiv:1509.00672 [hep-ex]
38. G. Branco et al., Theory and phenomenology of two-Higgs-doublet models. Phys. Rep. **516**, 1 (2012). arXiv:1106.0034 [hep-ph]
39. R.V. Harlander, S. Liebler, H. Mantler, SusHi: a program for the calculation of Higgs production in gluon fusion and bottom-quark annihilation in the Standard Model and the MSSM. Comput. Phys. Commun. **184**, 1605 (2013). arXiv:1212.3249 [hep-ph]
40. D. Eriksson, J. Rathsman, O. Stal, 2HDMC: two-Higgs-doublet model calculator. Erratum: Comput. Phys. Commun. **181**, 985 (2010). arXiv:0902.0851 [hep-ph]

41. C. Degrande et al., Automatic predictions in the Georgi–Machacek model at next-to-leading order accuracy. Phys. Rev. D **93**, 035004 (2016). arXiv:1512.01243 [hep-ph]
42. S. Godfrey, K. Moats, Exploring Higgs triplet models via vector boson scattering at the LHC. Phys. Rev. D **81**, 075026 (2010). arXiv:1003.3033 [hep-ph]
43. N. Arkani-Hamed et al., The littlest Higgs. JHEP **07**, 034 (2002). arXiv:hep-ph/0206021
44. J.F. Gunion et al., Higgs bosons in left-right symmetric models. Phys. Rev. D **40**, 1546 (1989)
45. K. Hartling, K. Kumar, H. E. Logan, GMCALC: a calculator for the Georgi-Machacek model (2014). arXiv:1412.7387 [hep-ph]
46. M. Zaro, H. Logan, Recommendations for the interpretation of LHC searches for H_5^0, $H_5^\pm$, and $H_5^{\pm\pm}$ in vector boson fusion with decays to vector boson pairs, LHC Higgs Cross Section Working Group. LHCHXSWG-2015-001. https://cds.cern.ch/record/2002500
47. ATLAS Collaboration, The ATLAS experiment at the CERN large hadron collider. JINST **3**, S08003 (2008)
48. ATLAS Collaboration, ATLAS insertable B-layer technical design report, ATLAS-TDR-19 (2010). https://cds.cern.ch/record/1291633. ATLAS insertable B-layer technical design report addendum, ATLAS-TDR-19-ADD-1 (2012). https://cds.cern.ch/record/1451888
49. ATLAS Collaboration, Performance of the ATLAS trigger system in 2015. Eur. Phys. J. C **77**, 317 (2017). arXiv:1611.09661 [hep-ex]
50. P. Nason, A new method for combining NLO QCD with shower Monte Carlo algorithms. JHEP **11**, 040 (2004). arXiv:hep-ph/0409146
51. S. Frixione, P. Nason, C. Oleari, Matching NLO QCD computations with parton shower simulations: the POWHEG method. JHEP **11**, 070 (2007). arXiv:0709.2092 [hep-ph]
52. S. Alioli et al., A general framework for implementing NLO calculations in shower Monte Carlo programs: the POWHEG BOX. JHEP **06**, 043 (2010). arXiv:1002.2581 [hep-ph]
53. S. Alioli et al., NLO Higgs boson production via gluon fusion matched with shower in POWHEG. JHEP **04**, 002 (2009). arXiv:0812.0578 [hep-ph]
54. P. Nason, C. Oleari, NLO Higgs boson production via vector-boson fusion matched with shower in POWHEG. JHEP **02**, 037 (2010). arXiv:0911.5299 [hep-ph]
55. H.-L. Lai et al., New parton distributions for collider physics. Phys. Rev. D **82**, 074024 (2010). arXiv:1007.2241 [hep-ph]
56. T. Sjöstrand, S. Mrenna, P.Z. Skands, A brief Introduction to PYTHIA 8.1. Comput. Phys. Commun. **178**, 852 (2008). arXiv:0710.3820 [hep-ph]
57. ATLAS Collaboration, Measurement of the Z/γ^* boson transverse momentum distribution in pp collisions at $\sqrt{s} = 7$ TeV with the ATLAS detector. JHEP **09**, 145 (2014). arXiv:1406.3660 [hep-ex]
58. J. Alwall et al., The automated computation of tree-level and next-to-leading order differential cross sections, and their matching to parton shower simulations. JHEP **07**, 079 (2014). arXiv:1405.0301 [hep-ph]
59. S. Carrazza, S. Forte, J. Rojo, Parton distributions and event generators (2013). arXiv:1311.5887 [hep-ph]
60. ATLAS Collaboration, ATLAS PYTHIA 8 tunes to 7 TeV data, ATL-PHYS-PUB-2014-021 (2014). https://cds.cern.ch/record/1966419
61. R. Frederix, S. Frixione, Merging meets matching in MC@NLO. JHEP **12**, 061 (2012). arXiv:1209.6215 [hep-ph]
62. J. Baglio et al., Release note—VBFNLO 2.7.0 (2014). arXiv:1404.3940 [hep-ph]
63. R.D. Ball et al., Parton distributions for the LHC Run II. JHEP **04**, 040 (2015). arXiv:1410.8849 [hep-ph]
64. S. Alioli et al., NLO single-top production matched with shower in POWHEG: s- and t-channel contributions. JHEP **09**, 111 (2009). Erratum: JHEP **02**, 011 (2010). arXiv:0907.4076 [hep-ph]
65. E. Re, Single-top Wt-channel production matched with parton showers using the POWHEG method. Eur. Phys. J. C **71**, 1547 (2011). arXiv:1009.2450 [hep-ph]
66. T. Sjöstrand, S. Mrenna, P.Z. Skands, PYTHIA 6.4 physics and manual. JHEP **05**, 026 (2006). arXiv:hep-ph/0603175
67. P.Z. Skands, Tuning Monte Carlo generators: the Perugia tunes. Phys. Rev. D **82**, 074018 (2010). arXiv:1005.3457 [hep-ph]
68. J. Pumplin et al., New generation of parton distributions with uncertainties from global QCD analysis. JHEP **07**, 012 (2002). arXiv:hep-ph/0201195
69. S. Alioli, S.-O. Moch, P. Uwer, Hadronic top-quark pair-production with one jet and parton showering. JHEP **01**, 137 (2012). arXiv:1110.5251 [hep-ph]
70. D.J. Lange, The EvtGen particle decay simulation package. Nucl. Instrum. Methods A **462**, 152 (2001)
71. T. Gleisberg et al., Event generation with SHERPA 1.1. JHEP **02**, 007 (2009). arXiv:0811.4622 [hep-ph]
72. T. Gleisberg, S. Höche, Comix, a new matrix element generator. JHEP **12**, 039 (2008). arXiv:0808.3674 [hep-ph]
73. F. Cascioli, P. Maierhofer, S. Pozzorini, Scattering amplitudes with open loops. Phys. Rev. Lett. **108**, 111601 (2012). arXiv:1111.5206 [hep-ph]
74. S. Schumann, F. Krauss, A Parton shower algorithm based on Catani–Seymour dipole factorisation. JHEP **03**, 038 (2008). arXiv:0709.1027 [hep-ph]
75. S. Höche et al., QCD matrix elements + parton showers: the NLO case. JHEP **04**, 027 (2013). arXiv:1207.5030 [hep-ph]
76. S. Agostinelli et al., GEANT4: a simulation toolkit. Nucl. Instrum. Methods A **506**, 250 (2003)
77. ATLAS Collaboration, The ATLAS simulation infrastructure. Eur. Phys. J. C **70**, 823 (2010). arXiv:1005.4568 [physics.ins-det]
78. ATLAS Collaboration, Electron efficiency measurements with the ATLAS detector using the 2015 LHC proton–proton collision data, ATLAS-CONF-2016-024 (2016). https://cds.cern.ch/record/2157687
79. ATLAS Collaboration, Measurement of the muon reconstruction performance of the ATLAS detector using 2011 and 2012 LHC proton-proton collision data. Eur. Phys. J. C **74**, 3130 (2014). arXiv:1407.3935 [hep-ex]
80. ATLAS Collaboration, Muon reconstruction performance of the ATLAS detector in proton-proton collision data at $\sqrt{s} = 13$ TeV. Eur. Phys. J. C **76**, 292 (2016). arXiv:1603.05598 [hep-ex]
81. K. Rehermann, B. Tweedie, Efficient identification of boosted semileptonic top quarks at the LHC. JHEP **03**, 059 (2011). arXiv:1007.2221 [hep-ph]
82. M. Cacciari, G.P. Salam, G. Soyez, The anti-k_t jet clustering algorithm. JHEP **04**, 063 (2008). arXiv:0802.1189 [hep-ph]
83. M. Cacciari, G.P. Salam, G. Soyez, FastJet user manual. Eur. Phys. J. C **72**, 1896 (2012). arXiv:1111.6097 [hep-ph]
84. M. Cacciari, G.P. Salam, Pileup subtraction using jet areas. Phys. Lett. B **659**, 119 (2008)
85. ATLAS Collaboration, Jet energy scale measurements and their systematic uncertainties in proton-proton collisions at $\sqrt{s} = 13$ TeV with the ATLAS detector. Phys. Rev. D **96**, 072002 (2017). arXiv:1703.09665 [hep-ex]
86. ATLAS Collaboration, Tagging and suppression of pileup jets with the ATLAS detector, ATLAS-CONF-2014-018 (2014). https://cds.cern.ch/record/1700870
87. ATLAS Collaboration, Performance of b-jet identification in the ATLAS experiment. JINST **11**, P04008 (2016). arXiv:1512.01094 [hep-ex]

99. ATLAS Collaboration, Measurement of the cross-section for producing a W boson in association with a single top quark in pp collisions at $\sqrt{s} = 13$ TeV with ATLAS (2016). arXiv:1612.07231 [hep-ex]

100. S. Dulat et al., New parton distribution functions from a global analysis of quantum chromodynamics. Phys. Rev. D **93**, 033006 (2016). arXiv:1506.07443 [hep-ph]

101. L.A. Harland-Lang et al., Parton distributions in the LHC era: MMHT 2014 PDFs. Eur. Phys. J. C **75**, 204 (2015). arXiv:1412.3989 [hep-ph]

102. K. Melnikov, M. Dowling, Production of two Z-bosons in gluon fusion in the heavy top quark approximation. Phys. Lett. B **744**, 43 (2015). arXiv:1503.01274 [hep-ph]

103. F. Caola et al., QCD corrections to W^+W^- production through gluon fusion. Phys. Lett. B **754**, 275 (2016). arXiv:1511.08617 [hep-ph]

104. M. Bonvini et al., Signal-background interference effects for $gg \to H \to W^+W^-$ beyond leading order. Phys. Rev. D **88**, 034032 (2013). arXiv:1304.3053 [hep-ph]

105. C.S. Li et al., Soft gluon resummation in the signal-background interference process of $gg(\to h^*) \to ZZ$. JHEP **08**, 065 (2015). arXiv:1504.02388 [hep-ph]

106. M. Bahr et al., HERWIG++ physics and manual. Eur. Phys. J. C **58**, 639 (2008). arXiv:0803.0883 [hep-ph]

107. J. Bellm et al., HERWIG++ 2.7 release note (2013). arXiv:1310.6877 [hep-ph]

108. I. Stewart, F. Tackmann, Theory uncertainties for Higgs mass and other searches using jet bins. Phys. Rev. D **85**, 034011 (2012). arXiv:1107.2117 [hep-ph]

109. ATLAS Collaboration, Combined search for the Standard Model Higgs boson in pp collisions at $\sqrt{s} = 7$ TeV with the ATLAS detector. Phys. Rev. D **86**, 032003 (2012). arXiv:1207.0319 [hep-ex]

110. A.L. Read, Presentation of search results: the CL$_s$ technique. J. Phys. G **28**, 2693 (2002)

111. G. Cowan et al., Asymptotic formulae for likelihood-based tests of new physics. Eur. Phys. J. C **71**, 1554 (2011). Erratum: Eur. Phys. J. C **73**, 2501 (2013). arXiv:1007.1727 [physics.data-an]

112. ATLAS Collaboration, ATLAS computing acknowledgements 2016–2017, ATL-GEN-PUB-2016-002. https://cds.cern.ch/record/2202407

ATLAS Collaboration

M. Aaboud[137d], G. Aad[88], B. Abbott[115], O. Abdinov[12,*], B. Abeloos[119], S. H. Abidi[161], O. S. AbouZeid[139], N. L. Abraham[151], H. Abramowicz[155], H. Abreu[154], R. Abreu[118], Y. Abulaiti[148a,148b], B. S. Acharya[167a,167b,a], S. Adachi[157], L. Adamczyk[41a], J. Adelman[110], M. Adersberger[102], T. Adye[133], A. A. Affolder[139], Y. Afik[154], C. Agheorghiesei[28c], J. A. Aguilar-Saavedra[128a,128f], S. P. Ahlen[24], F. Ahmadov[68,b], G. Aielli[135a,135b], S. Akatsuka[71], H. Akerstedt[148a,148b], T. P. A. Åkesson[84], E. Akilli[52], A. V. Akimov[98], G. L. Alberghi[22a,22b], J. Albert[172], P. Albicocco[50], M. J. Alconada Verzini[74], S. C. Alderweireldt[108], M. Aleksa[32], I. N. Aleksandrov[68], C. Alexa[28b], G. Alexander[155], T. Alexopoulos[10], M. Alhroob[115], B. Ali[130], M. Aliev[76a,76b], G. Alimonti[94a], J. Alison[33], S. P. Alkire[38], B. M. M. Allbrooke[151], B. W. Allen[118], P. P. Allport[19], A. Aloisio[106a,106b], A. Alonso[39], F. Alonso[74], C. Alpigiani[140], A. A. Alshehri[56], M. I. Alstaty[88], B. Alvarez Gonzalez[32], D. Álvarez Piqueras[170], M. G. Alviggi[106a,106b], B. T. Amadio[16], Y. Amaral Coutinho[26a], C. Amelung[25], D. Amidei[92], S. P. Amor Dos Santos[128a,128c], S. Amoroso[32], C. Anastopoulos[141], L. S. Ancu[52], N. Andari[19], T. Andeen[11], C. F. Anders[60b], J. K. Anders[77], K. J. Anderson[33], A. Andreazza[94a,94b], V. Andrei[60a], S. Angelidakis[37], I. Angelozzi[109], A. Angerami[38], A. V. Anisenkov[111,c], N. Anjos[13], A. Annovi[126a], C. Antel[60a], M. Antonelli[50], A. Antonov[100,*], D. J. Antrim[166], F. Anulli[134a], M. Aoki[69], L. Aperio Bella[32], G. Arabidze[93], Y. Arai[69], J. P. Araque[128a], V. Araujo Ferraz[26a], A. T. H. Arce[48], R. E. Ardell[80], F. A. Arduh[74], J-F. Arguin[97], S. Argyropoulos[66], M. Arik[20a], A. J. Armbruster[32], L. J. Armitage[79], O. Arnaez[161], H. Arnold[51], M. Arratia[30], O. Arslan[23], A. Artamonov[99,*], G. Artoni[122], S. Artz[86], S. Asai[157], N. Asbah[45], A. Ashkenazi[155], L. Asquith[151], K. Assamagan[27], R. Astalos[146a], M. Atkinson[169], N. B. Atlay[143], K. Augsten[130], G. Avolio[32], B. Axen[16], M. K. Ayoub[35a], G. Azuelos[97,d], A. E. Baas[60a], M. J. Baca[19], H. Bachacou[138], K. Bachas[76a,76b], M. Backes[122], P. Bagnaia[134a,134b], M. Bahmani[42], H. Bahrasemani[144], J. T. Baines[133], M. Bajic[39], O. K. Baker[179], P. J. Bakker[109], E. M. Baldin[111,c], P. Balek[175], F. Balli[138], W. K. Balunas[124], E. Banas[42], A. Bandyopadhyay[23], Sw. Banerjee[176,e], A. A. E. Bannoura[178], L. Barak[155], E. L. Barberio[91], D. Barberis[53a,53b], M. Barbero[88], T. Barillari[103], M-S Barisits[65], J. T. Barkeloo[118], T. Barklow[145], N. Barlow[30], S. L. Barnes[36c], B. M. Barnett[133], R. M. Barnett[16], Z. Barnovska-Blenessy[36a], A. Baroncelli[136a], G. Barone[25], A. J. Barr[122], L. Barranco Navarro[170], F. Barreiro[85], J. Barreiro Guimarães da Costa[35a], R. Bartoldus[145], A. E. Barton[75], P. Bartos[146a], A. Basalaev[125], A. Bassalat[119,f], R. L. Bates[56], S. J. Batista[161], J. R. Batley[30], M. Battaglia[139], M. Bauce[134a,134b], F. Bauer[138], K. T. Bauer[166], H. S. Bawa[145,g], J. B. Beacham[113], M. D. Beattie[75], T. Beau[83], P. H. Beauchemin[165], P. Bechtle[23], H. P. Beck[18,h], H. C. Beck[57], K. Becker[122], M. Becker[86], C. Becot[112], A. J. Beddall[20d], A. Beddall[20b], V. A. Bednyakov[68], M. Bedognetti[109], C. P. Bee[150], T. A. Beermann[32], M. Begalli[26a], M. Begel[27], J. K. Behr[45], A. S. Bell[81], G. Bella[155], L. Bellagamba[22a], A. Bellerive[31], M. Bellomo[154], K. Belotskiy[100], O. Beltramello[32], N. L. Belyaev[100], O. Benary[155,*], D. Benchekroun[137a], M. Bender[102], N. Benekos[10], Y. Benhammou[155], E. Benhar Noccioli[179], J. Benitez[66], D. P. Benjamin[48], M. Benoit[52], J. R. Bensinger[25], S. Bentvelsen[109], L. Beresford[122], M. Beretta[50], D. Berge[109], E. Bergeaas Kuutmann[168], N. Berger[5], L. J. Bergsten[25], J. Beringer[16],

S. Berlendis[58], N. R. Bernard[89], G. Bernardi[83], C. Bernius[145], F. U. Bernlochner[23], T. Berry[80], P. Berta[86], C. Bertella[35a], G. Bertoli[148a,148b], I. A. Bertram[75], C. Bertsche[45], G. J. Besjes[39], O. Bessidskaia Bylund[148a,148b], M. Bessner[45], N. Besson[138], A. Bethani[87], S. Bethke[103], A. Betti[23], A. J. Bevan[79], J. Beyer[103], R. M. Bianchi[127], O. Biebel[102], D. Biedermann[17], R. Bielski[87], K. Bierwagen[86], N. V. Biesuz[126a,126b], M. Biglietti[136a], T. R. V. Billoud[97], H. Bilokon[50], M. Bindi[57], A. Bingul[20b], C. Bini[134a,134b], S. Biondi[22a,22b], T. Bisanz[57], C. Bittrich[47], D. M. Bjergaard[48], J. E. Black[145], K. M. Black[24], R. E. Blair[6], T. Blazek[146a], I. Bloch[45], C. Blocker[25], A. Blue[56], U. Blumenschein[79], Dr. Blunier[34a], G. J. Bobbink[109], V. S. Bobrovnikov[111,c], S. S. Bocchetta[84], A. Bocci[48], C. Bock[102], M. Boehler[51], D. Boerner[178], D. Bogavac[102], A. G. Bogdanchikov[111], C. Bohm[148a], V. Boisvert[80], P. Bokan[168,i], T. Bold[41a], A. S. Boldyrev[101], A. E. Bolz[60b], M. Bomben[83], M. Bona[79], M. Boonekamp[138], A. Borisov[132], G. Borissov[75], J. Bortfeldt[32], D. Bortoletto[122], V. Bortolotto[62a], D. Boscherini[22a], M. Bosman[13], J. D. Bossio Sola[29], J. Boudreau[127], E. V. Bouhova-Thacker[75], D. Boumediene[37], C. Bourdarios[119], S. K. Boutle[56], A. Boveia[113], J. Boyd[32], I. R. Boyko[68], A. J. Bozson[80], J. Bracinik[19], A. Brandt[8], G. Brandt[57], O. Brandt[60a], F. Braren[45], U. Bratzler[158], B. Brau[89], J. E. Brau[118], W. D. Breaden Madden[56], K. Brendlinger[45], A. J. Brennan[91], L. Brenner[109], R. Brenner[168], S. Bressler[175], D. L. Briglin[19], T. M. Bristow[49], D. Britton[56], D. Britzger[45], F. M. Brochu[30], I. Brock[23], R. Brock[93], G. Brooijmans[38], T. Brooks[80], W. K. Brooks[34b], E. Brost[110], J. H Broughton[19], P. A. Bruckman de Renstrom[42], D. Bruncko[146b], A. Bruni[22a], G. Bruni[22a], L. S. Bruni[109], S. Bruno[135a,135b], BH Brunt[30], M. Bruschi[22a], N. Bruscino[127], P. Bryant[33], L. Bryngemark[45], T. Buanes[15], Q. Buat[144], P. Buchholz[143], A. G. Buckley[56], I. A. Budagov[68], F. Buehrer[51], M. K. Bugge[121], O. Bulekov[100], D. Bullock[8], T. J. Burch[110], S. Burdin[77], C. D. Burgard[109], A. M. Burger[5], B. Burghgrave[110], K. Burka[42], S. Burke[133], I. Burmeister[46], J. T. P. Burr[122], D. Büscher[51], V. Büscher[86], P. Bussey[56], J. M. Butler[24], C. M. Buttar[56], J. M. Butterworth[81], P. Butti[32], W. Buttinger[27], A. Buzatu[153], A. R. Buzykaev[111,c], S. Cabrera Urbán[170], D. Caforio[130], H. Cai[169], V. M. Cairo[40a,40b], O. Cakir[4a], N. Calace[52], P. Calafiura[16], A. Calandri[88], G. Calderini[83], P. Calfayan[64], G. Callea[40a,40b], L. P. Caloba[26a], S. Calvente Lopez[85], D. Calvet[37], S. Calvet[37], T. P. Calvet[88], R. Camacho Toro[33], S. Camarda[32], P. Camarri[135a,135b], D. Cameron[121], R. Caminal Armadans[169], C. Camincher[58], S. Campana[32], M. Campanelli[81], A. Camplani[94a,94b], A. Campoverde[143], V. Canale[106a,106b], M. Cano Bret[36c], J. Cantero[116], T. Cao[155], M. D. M. Capeans Garrido[32], I. Caprini[28b], M. Caprini[28b], M. Capua[40a,40b], R. M. Carbone[38], R. Cardarelli[135a], F. Cardillo[51], I. Carli[131], T. Carli[32], G. Carlino[106a], B. T. Carlson[127], L. Carminati[94a,94b], R. M. D. Carney[148a,148b], S. Caron[108], E. Carquin[34b], S. Carrá[94a,94b], G. D. Carrillo-Montoya[32], D. Casadei[19], M. P. Casado[13,j], A.F. Casha[161], M. Casolino[13], D. W. Casper[166], R. Castelijn[109], V. Castillo Gimenez[170], N. F. Castro[128a,k], A. Catinaccio[32], J. R. Catmore[121], A. Cattai[32], J. Caudron[23], V. Cavaliere[169], E. Cavallaro[13], D. Cavalli[94a], M. Cavalli-Sforza[13], V. Cavasinni[126a,126b], E. Celebi[20c], F. Ceradini[136a,136b], L. Cerda Alberich[170], A. S. Cerqueira[26b], A. Cerri[151], L. Cerrito[135a,135b], F. Cerutti[16], A. Cervelli[22a,22b], S. A. Cetin[20c], A. Chafaq[137a], D. Chakraborty[110], S. K. Chan[59], W. S. Chan[109], Y. L. Chan[62a], P. Chang[169], J. D. Chapman[30], D. G. Charlton[19], C. C. Chau[31], C. A. Chavez Barajas[151], S. Che[113], S. Cheatham[167a,167c], A. Chegwidden[93], S. Chekanov[6], S. V. Chekulaev[163a], G. A. Chelkov[68,l], M. A. Chelstowska[32], C. Chen[36a], C. Chen[67], H. Chen[27], J. Chen[36a], S. Chen[35b], S. Chen[157], X. Chen[35c,m], Y. Chen[70], H. C. Cheng[92], H. J. Cheng[35a,35d], A. Cheplakov[68], E. Cheremushkina[132], R. Cherkaoui El Moursli[137e], E. Cheu[7], K. Cheung[63], L. Chevalier[138], V. Chiarella[50], G. Chiarelli[126a], G. Chiodini[76a], A. S. Chisholm[32], A. Chitan[28b], Y. H. Chiu[172], M. V. Chizhov[68], K. Choi[64], A. R. Chomont[37], S. Chouridou[156], Y. S. Chow[62a], V. Christodoulou[81], M. C. Chu[62a], J. Chudoba[129], A. J. Chuinard[90], J. J. Chwastowski[42], L. Chytka[117], A. K. Ciftci[4a], D. Cinca[46], V. Cindro[78], I. A. Cioara[23], A. Ciocio[16], F. Cirotto[106a,106b], Z. H. Citron[175], M. Citterio[94a], M. Ciubancan[28b], A. Clark[52], M. R. Clark[38], P. J. Clark[49], R. N. Clarke[16], C. Clement[148a,148b], Y. Coadou[88], M. Cobal[167a,167c], A. Coccaro[52], J. Cochran[67], L. Colasurdo[108], B. Cole[38], A. P. Colijn[109], J. Collot[58], T. Colombo[166], P. Conde Muiño[128a,128b], E. Coniavitis[51], S. H. Connell[147b], I. A. Connelly[87], S. Constantinescu[28b], G. Conti[32], F. Conventi[106a,n], M. Cooke[16], A. M. Cooper-Sarkar[122], F. Cormier[171], K. J. R. Cormier[161], M. Corradi[134a,134b], E. E. Corrigan[84], F. Corriveau[90,o], A. Cortes-Gonzalez[32], G. Costa[94a], M. J. Costa[170], D. Costanzo[141], G. Cottin[30], G. Cowan[80], B. E. Cox[87], K. Cranmer[112], S. J. Crawley[56], R. A. Creager[124], G. Cree[31], S. Crépé-Renaudin[58], F. Crescioli[83], W. A. Cribbs[148a,148b], M. Cristinziani[23], V. Croft[112], G. Crosetti[40a,40b], A. Cueto[85], T. Cuhadar Donszelmann[141], A. R. Cukierman[145], J. Cummings[179], M. Curatolo[50], J. Cúth[86], S. Czekierda[42], P. Czodrowski[32], G. D'amen[22a,22b], S. D'Auria[56], L. D'eramo[83], M. D'Onofrio[77], M. J. Da Cunha Sargedas De Sousa[128a,128b], C. Da Via[87], W. Dabrowski[41a], T. Dado[146a], T. Dai[92], O. Dale[15], F. Dallaire[97], C. Dallapiccola[89], M. Dam[39], J. R. Dandoy[124], M. F. Daneri[29], N. P. Dang[176], A. C. Daniells[19], N. S. Dann[87], M. Danninger[171], M. Dano Hoffmann[138], V. Dao[150], G. Darbo[53a], S. Darmora[8], J. Dassoulas[3], A. Dattagupta[118], T. Daubney[45], W. Davey[23], C. David[45], T. Davidek[131], D. R. Davis[48], P. Davison[81], E. Dawe[91], I. Dawson[141], K. De[8], R. de Asmundis[106a], A. De Benedetti[115], S. De Castro[22a,22b], S. De Cecco[83], N. De Groot[108], P. de Jong[109], H. De la Torre[93], F. De Lorenzi[67], A. De Maria[57], D. De Pedis[134a], A. De Salvo[134a], U. De Sanctis[135a,135b], A. De Santo[151], K. De Vasconcelos Corga[88], J. B. De Vivie De Regie[119], R. Debbe[27],

C. Debenedetti[139], D. V. Dedovich[68], N. Dehghanian[3], I. Deigaard[109], M. Del Gaudio[40a,40b], J. Del Peso[85], D. Delgove[119], F. Deliot[138], C. M. Delitzsch[7], A. Dell'Acqua[32], L. Dell'Asta[24], M. Dell'Orso[126a,126b], M. Della Pietra[106a,106b], D. della Volpe[52], M. Delmastro[5], C. Delporte[119], P. A. Delsart[58], D. A. DeMarco[161], S. Demers[179], M. Demichev[68], A. Demilly[83], S. P. Denisov[132], D. Denysiuk[138], D. Derendarz[42], J. E. Derkaoui[137d], F. Derue[83], P. Dervan[77], K. Desch[23], C. Deterre[45], K. Dette[161], M. R. Devesa[29], P. O. Deviveiros[32], A. Dewhurst[133], S. Dhaliwal[25], F. A. Di Bello[52], A. Di Ciaccio[135a,135b], L. Di Ciaccio[5], W. K. Di Clemente[124], C. Di Donato[106a,106b], A. Di Girolamo[32], B. Di Girolamo[32], B. Di Micco[136a,136b], R. Di Nardo[32], K. F. Di Petrillo[59], A. Di Simone[51], R. Di Sipio[161], D. Di Valentino[31], C. Diaconu[88], M. Diamond[161], F. A. Dias[39], M. A. Diaz[34a], J. Dickinson[16], E. B. Diehl[92], J. Dietrich[17], S. Díez Cornell[45], A. Dimitrievska[14], J. Dingfelder[23], P. Dita[28b], S. Dita[28b], F. Dittus[32], F. Djama[88], T. Djobava[54b], J. I. Djuvsland[60a], M. A. B. do Vale[26c], M. Dobre[28b], D. Dodsworth[25], C. Doglioni[84], J. Dolejsi[131], Z. Dolezal[131], M. Donadelli[26d], S. Donati[126a,126b], J. Donini[37], J. Dopke[133], A. Doria[106a], M. T. Dova[74], A. T. Doyle[56], E. Drechsler[57], M. Dris[10], Y. Du[36b], J. Duarte-Campderros[155], F. Dubinin[98], A. Dubreuil[52], E. Duchovni[175], G. Duckeck[102], A. Ducourthial[83], O. A. Ducu[97,p], D. Duda[109], A. Dudarev[32], A. Chr. Dudder[86], E. M. Duffield[16], L. Duflot[119], M. Dührssen[32], C. Dulsen[178], M. Dumancic[175], A. E. Dumitriu[28b], A. K. Duncan[56], M. Dunford[60a], A. Duperrin[88], H. Duran Yildiz[4a], M. Düren[55], A. Durglishvili[54b], D. Duschinger[47], B. Dutta[45], D. Duvnjak[1], M. Dyndal[45], B. S. Dziedzic[42], C. Eckardt[45], K. M. Ecker[103], R. C. Edgar[92], T. Eifert[32], G. Eigen[15], K. Einsweiler[16], T. Ekelof[168], M. El Kacimi[137c], R. El Kosseifi[88], V. Ellajosyula[88], M. Ellert[168], S. Elles[5], F. Ellinghaus[178], A. A. Elliot[172], N. Ellis[32], J. Elmsheuser[27], M. Elsing[32], D. Emeliyanov[133], Y. Enari[157], J. S. Ennis[173], M. B. Epland[48], J. Erdmann[46], A. Ereditato[18], M. Ernst[27], S. Errede[169], M. Escalier[119], C. Escobar[170], B. Esposito[50], O. Estrada Pastor[170], A. I. Etienvre[138], E. Etzion[155], H. Evans[64], A. Ezhilov[125], M. Ezzi[137e], F. Fabbri[22a,22b], L. Fabbri[22a,22b], V. Fabiani[108], G. Facini[81], R. M. Fakhrutdinov[132], S. Falciano[134a], R. J. Falla[81], J. Faltova[32], Y. Fang[35a], M. Fanti[94a,94b], A. Farbin[8], A. Farilla[136a], E. M. Farina[123a,123b], T. Farooque[93], S. Farrell[16], S. M. Farrington[173], P. Farthouat[32], F. Fassi[137e], P. Fassnacht[32], D. Fassouliotis[9], M. Faucci Giannelli[49], A. Favareto[53a,53b], W. J. Fawcett[122], L. Fayard[119], O. L. Fedin[125,q], W. Fedorko[171], S. Feigl[121], L. Feligioni[88], C. Feng[36b], E. J. Feng[32], M. Feng[48], M. J. Fenton[56], A. B. Fenyuk[132], L. Feremenga[8], P. Fernandez Martinez[170], J. Ferrando[45], A. Ferrari[168], P. Ferrari[109], R. Ferrari[123a], D. E. Ferreira de Lima[60b], A. Ferrer[170], D. Ferrere[52], C. Ferretti[92], F. Fiedler[86], A. Filipčič[78], M. Filipuzzi[45], F. Filthaut[108], M. Fincke-Keeler[172], K. D. Finelli[24], M. C. N. Fiolhais[128a,128c,r], L. Fiorini[170], A. Fischer[2], C. Fischer[13], J. Fischer[178], W. C. Fisher[93], N. Flaschel[45], I. Fleck[143], P. Fleischmann[92], R. R. M. Fletcher[124], T. Flick[178], B. M. Flierl[102], L. R. Flores Castillo[62a], M. J. Flowerdew[103], G. T. Forcolin[87], A. Formica[138], F. A. Förster[13], A. Forti[87], A. G. Foster[19], D. Fournier[119], H. Fox[75], S. Fracchia[141], P. Francavilla[126a,126b], M. Franchini[22a,22b], S. Franchino[60a], D. Francis[32], L. Franconi[121], M. Franklin[59], M. Frate[166], M. Fraternali[123a,123b], D. Freeborn[81], S. M. Fressard-Batraneanu[32], B. Freund[97], W. S. Freund[26a], D. Froidevaux[32], J. A. Frost[122], C. Fukunaga[158], T. Fusayasu[104], J. Fuster[170], O. Gabizon[154], A. Gabrielli[22a,22b], A. Gabrielli[16], G. P. Gach[41a], S. Gadatsch[32], S. Gadomski[80], G. Gagliardi[53a,53b], L. G. Gagnon[97], C. Galea[108], B. Galhardo[128a,128c], E. J. Gallas[122], B. J. Gallop[133], P. Gallus[130], G. Galster[39], K. K. Gan[113], S. Ganguly[37], Y. Gao[77], Y. S. Gao[145,g], F. M. Garay Walls[34a], C. García[170], J. E. García Navarro[170], J. A. García Pascual[35a], M. Garcia-Sciveres[16], R. W. Gardner[33], N. Garelli[145], V. Garonne[121], A. Gascon Bravo[45], K. Gasnikova[45], C. Gatti[50], A. Gaudiello[53a,53b], G. Gaudio[123a], I. L. Gavrilenko[98], C. Gay[171], G. Gaycken[23], E. N. Gazis[10], C. N. P. Gee[133], J. Geisen[57], M. Geisen[86], M. P. Geisler[60a], K. Gellerstedt[148a,148b], C. Gemme[53a], M. H. Genest[58], C. Geng[92], S. Gentile[134a,134b], C. Gentsos[156], S. George[80], D. Gerbaudo[13], G. Geßner[46], S. Ghasemi[143], M. Ghneimat[23], B. Giacobbe[22a], S. Giagu[134a,134b], N. Giangiacomi[22a,22b], P. Giannetti[126a,126b], S. M. Gibson[80], M. Gignac[171], M. Gilchriese[16], D. Gillberg[31], G. Gilles[178], D. M. Gingrich[3,d], M. P. Giordani[167a,167c], F. M. Giorgi[22a], P. F. Giraud[138], P. Giromini[59], G. Giugliarelli[167a,167c], D. Giugni[94a], F. Giuli[122], C. Giuliani[103], M. Giulini[60b], B. K. Gjelsten[121], S. Gkaitatzis[156], I. Gkialas[9,s], E. L. Gkougkousis[13], P. Gkountoumis[10], L. K. Gladilin[101], C. Glasman[85], J. Glatzer[13], P. C. F. Glaysher[45], A. Glazov[45], M. Goblirsch-Kolb[25], J. Godlewski[42], S. Goldfarb[91], T. Golling[52], D. Golubkov[132], A. Gomes[128a,128b,128d], R. Gonçalo[128a], R. Goncalves Gama[26a], J. Goncalves Pinto Firmino Da Costa[138], G. Gonella[51], L. Gonella[19], A. Gongadze[68], F. Gonnella[19], J. L. Gonski[59], S. González de la Hoz[170], S. Gonzalez-Sevilla[52], L. Goossens[32], P. A. Gorbounov[99], H. A. Gordon[27], B. Gorini[32], E. Gorini[76a,76b], A. Gorišek[78], A. T. Goshaw[48], C. Gössling[46], M. I. Gostkin[68], C. A. Gottardo[23], C. R. Goudet[119], D. Goujdami[137c], A. G. Goussiou[140], N. Govender[147b,t], C. Goy[5], E. Gozani[154], I. Grabowska-Bold[41a], P. O. J. Gradin[168], E. C. Graham[77], J. Gramling[166], E. Gramstad[121], S. Grancagnolo[17], V. Gratchev[125], P. M. Gravila[28f], C. Gray[56], H. M. Gray[16], Z. D. Greenwood[82,u], C. Grefe[23], K. Gregersen[81], I. M. Gregor[45], P. Grenier[145], K. Grevtsov[5], J. Griffiths[8], A. A. Grillo[139], K. Grimm[75], S. Grinstein[13,v], Ph. Gris[37], J.-F. Grivaz[119], S. Groh[86], E. Gross[175], J. Grosse-Knetter[57], G. C. Grossi[82], Z. J. Grout[81], A. Grummer[107], L. Guan[92], W. Guan[176], J. Guenther[32], F. Guescini[163a], D. Guest[166], O. Gueta[155], B. Gui[113], E. Guido[53a,53b], T. Guillemin[5], S. Guindon[32], U. Gul[56], C. Gumpert[32], J. Guo[36c], W. Guo[92], Y. Guo[36a,w], R. Gupta[43], S. Gurbuz[20a],

G. Gustavino[115], B. J. Gutelman[154], P. Gutierrez[115], N. G. Gutierrez Ortiz[81], C. Gutschow[81], C. Guyot[138], M. P. Guzik[41a], C. Gwenlan[122], C. B. Gwilliam[77], A. Haas[112], C. Haber[16], H. K. Hadavand[8], N. Haddad[137e], A. Hadef[88], S. Hageböck[23], M. Hagihara[164], H. Hakobyan[180,*], M. Haleem[45], J. Haley[116], G. Halladjian[93], G. D. Hallewell[88], K. Hamacher[178], P. Hamal[117], K. Hamano[172], A. Hamilton[147a], G. N. Hamity[141], P. G. Hamnett[45], K. Han[36a,x], L. Han[36a], S. Han[35a,35d], K. Hanagaki[69,y], K. Hanawa[157], M. Hance[139], D. M. Handl[102], B. Haney[124], P. Hanke[60a], J. B. Hansen[39], J. D. Hansen[39], M. C. Hansen[23], P. H. Hansen[39], K. Hara[164], A. S. Hard[176], T. Harenberg[178], F. Hariri[119], S. Harkusha[95], P. F. Harrison[173], N. M. Hartmann[102], Y. Hasegawa[142], A. Hasib[49], S. Hassani[138], S. Haug[18], R. Hauser[93], L. Hauswald[47], L. B. Havener[38], M. Havranek[130], C. M. Hawkes[19], R. J. Hawkings[32], D. Hayden[93], C. P. Hays[122], J. M. Hays[79], H. S. Hayward[77], S. J. Haywood[133], T. Heck[86], V. Hedberg[84], L. Heelan[8], S. Heer[23], K. K. Heidegger[51], S. Heim[45], T. Heim[16], B. Heinemann[45,z], J. J. Heinrich[102], L. Heinrich[112], C. Heinz[55], J. Hejbal[129], L. Helary[32], A. Held[171], S. Hellman[148a,148b], C. Helsens[32], R. C. W. Henderson[75], Y. Heng[176], S. Henkelmann[171], A. M. Henriques Correia[32], S. Henrot-Versille[119], G. H. Herbert[17], H. Herde[25], V. Herget[177], Y. Hernández Jiménez[147c], H. Herr[86], G. Herten[51], R. Hertenberger[102], L. Hervas[32], T. C. Herwig[124], G. G. Hesketh[81], N. P. Hessey[163a], J. W. Hetherly[43], S. Higashino[69], E. Higón-Rodriguez[170], K. Hildebrand[33], E. Hill[172], J. C. Hill[30], K. H. Hiller[45], S. J. Hillier[19], M. Hils[47], I. Hinchliffe[16], M. Hirose[51], D. Hirschbuehl[178], B. Hiti[78], O. Hladik[129], D. R. Hlaluku[147c], X. Hoad[49], J. Hobbs[150], N. Hod[163a], M. C. Hodgkinson[141], P. Hodgson[141], A. Hoecker[32], M. R. Hoeferkamp[107], F. Hoenig[102], D. Hohn[23], T. R. Holmes[33], M. Holzbock[102], M. Homann[46], S. Honda[164], T. Honda[69], T. M. Hong[127], B. H. Hooberman[169], W. H. Hopkins[118], Y. Horii[105], A. J. Horton[144], J-Y. Hostachy[58], A. Hostiuc[140], S. Hou[153], A. Hoummada[137a], J. Howarth[87], J. Hoya[74], M. Hrabovsky[117], J. Hrdinka[32], I. Hristova[17], J. Hrivnac[119], T. Hryn'ova[5], A. Hrynevich[96], P. J. Hsu[63], S.-C. Hsu[140], Q. Hu[27], S. Hu[36c], Y. Huang[35a], Z. Hubacek[130], F. Hubaut[88], F. Huegging[23], T. B. Huffman[122], E. W. Hughes[38], M. Huhtinen[32], R. F. H. Hunter[31], P. Huo[150], N. Huseynov[68,b], J. Huston[93], J. Huth[59], R. Hyneman[92], G. Iacobucci[52], G. Iakovidis[27], I. Ibragimov[143], L. Iconomidou-Fayard[119], Z. Idrissi[137e], P. Iengo[32], O. Igonkina[109,aa], T. Iizawa[174], Y. Ikegami[69], M. Ikeno[69], Y. Ilchenko[11,ab], D. Iliadis[156], N. Ilic[145], F. Iltzsche[47], G. Introzzi[123a,123b], P. Ioannou[9,*], M. Iodice[136a], K. Iordanidou[38], V. Ippolito[59], M. F. Isacson[168], N. Ishijima[120], M. Ishino[157], M. Ishitsuka[159], C. Issever[122], S. Istin[20a], F. Ito[164], J. M. Iturbe Ponce[62a], R. Iuppa[162a,162b], H. Iwasaki[69], J. M. Izen[44], V. Izzo[106a], S. Jabbar[3], P. Jackson[1], R. M. Jacobs[23], V. Jain[2], K. B. Jakobi[86], K. Jakobs[51], S. Jakobsen[65], T. Jakoubek[129], D. O. Jamin[116], D. K. Jana[82], R. Jansky[52], J. Janssen[23], M. Janus[57], P. A. Janus[41a], G. Jarlskog[84], N. Javadov[68,b], T. Javůrek[51], M. Javurkova[51], F. Jeanneau[138], L. Jeanty[16], J. Jejelava[54a,ac], A. Jelinskas[173], P. Jenni[51,ad], C. Jeske[173], S. Jézéquel[5], H. Ji[176], J. Jia[150], H. Jiang[67], Y. Jiang[36a], Z. Jiang[145], S. Jiggins[81], J. Jimenez Pena[170], S. Jin[35b], A. Jinaru[28b], O. Jinnouchi[159], H. Jivan[147c], P. Johansson[141], K. A. Johns[7], C. A. Johnson[64], W. J. Johnson[140], K. Jon-And[148a,148b], R. W. L. Jones[75], S. D. Jones[151], S. Jones[7], T. J. Jones[77], J. Jongmanns[60a], P. M. Jorge[128a,128b], J. Jovicevic[163a], X. Ju[176], A. Juste Rozas[13,v], M. K. Köhler[175], A. Kaczmarska[42], M. Kado[119], H. Kagan[113], M. Kagan[145], S. J. Kahn[88], T. Kaji[174], E. Kajomovitz[154], C. W. Kalderon[84], A. Kaluza[86], S. Kama[43], A. Kamenshchikov[132], N. Kanaya[157], L. Kanjir[78], V. A. Kantserov[100], J. Kanzaki[69], B. Kaplan[112], L. S. Kaplan[176], D. Kar[147c], K. Karakostas[10], N. Karastathis[10], M. J. Kareem[163b], E. Karentzos[10], S. N. Karpov[68], Z. M. Karpova[68], V. Kartvelishvili[75], A. N. Karyukhin[132], K. Kasahara[164], L. Kashif[176], R. D. Kass[113], A. Kastanas[149], Y. Kataoka[157], C. Kato[157], A. Katre[52], J. Katzy[45], K. Kawade[70], K. Kawagoe[73], T. Kawamoto[157], G. Kawamura[57], E. F. Kay[77], V. F. Kazanin[111,c], R. Keeler[172], R. Kehoe[43], J. S. Keller[31], E. Kellermann[84], J. J. Kempster[80], J Kendrick[19], H. Keoshkerian[161], O. Kepka[129], B. P. Kerševan[78], S. Kersten[178], R. A. Keyes[90], M. Khader[169], F. Khalil-zada[12], A. Khanov[116], A. G. Kharlamov[111,c], T. Kharlamova[111,c], A. Khodinov[160], T. J. Khoo[52], V. Khovanskiy[99,*], E. Khramov[68], J. Khubua[54b,ae], S. Kido[70], C. R. Kilby[80], H. Y. Kim[8], S. H. Kim[164], Y. K. Kim[33], N. Kimura[167a,167c], O. M. Kind[17], B. T. King[77], D. Kirchmeier[47], J. Kirk[133], A. E. Kiryunin[103], T. Kishimoto[157], D. Kisielewska[41a], V. Kitali[45], O. Kivernyk[5], E. Kladiva[146b], T. Klapdor-Kleingrothaus[51], M. H. Klein[92], M. Klein[77], U. Klein[77], K. Kleinknecht[86], P. Klimek[110], A. Klimentov[27], R. Klingenberg[46,*], T. Klingl[23], T. Klioutchnikova[32], F. F. Klitzner[102], E.-E. Kluge[60a], P. Kluit[109], S. Kluth[103], E. Kneringer[65], E. B. F. G. Knoops[88], A. Knue[103], A. Kobayashi[157], D. Kobayashi[73], T. Kobayashi[157], M. Kobel[47], M. Kocian[145], P. Kodys[131], T. Koffas[31], E. Koffeman[109], N. M. Köhler[103], T. Koi[145], M. Kolb[60b], I. Koletsou[5], T. Kondo[69], N. Kondrashova[36c], K. Köneke[51], A. C. König[108], T. Kono[69,af], R. Konoplich[112,ag], N. Konstantinidis[81], B. Konya[84], R. Kopeliansky[64], S. Koperny[41a], K. Korcyl[42], K. Kordas[156], A. Korn[81], I. Korolkov[13], E. V. Korolkova[141], O. Kortner[103], S. Kortner[103], T. Kosek[131], V. V. Kostyukhin[23], A. Kotwal[48], A. Koulouris[10], A. Kourkoumeli-Charalampidi[123a,123b], C. Kourkoumelis[9], E. Kourlitis[141], V. Kouskoura[27], A. B. Kowalewska[42], R. Kowalewski[172], T. Z. Kowalski[41a], C. Kozakai[157], W. Kozanecki[138], A. S. Kozhin[132], V. A. Kramarenko[101], G. Kramberger[78], D. Krasnopevtsev[100], M. W. Krasny[83], A. Krasznahorkay[32], D. Krauss[103], J. A. Kremer[41a], J. Kretzschmar[77], K. Kreutzfeldt[55], P. Krieger[161], K. Krizka[16], K. Kroeninger[46], H. Kroha[103], J. Kroll[129], J. Kroll[124], J. Kroseberg[23], J. Krstic[14], U. Kruchonak[68], H. Krüger[23], N. Krumnack[67], M. C. Kruse[48], T. Kubota[91], H. Kucuk[81],

S. Kuday[4b], J. T. Kuechler[178], S. Kuehn[32], A. Kugel[60a], F. Kuger[177], T. Kuhl[45], V. Kukhtin[68], R. Kukla[88], Y. Kulchitsky[95], S. Kuleshov[34b], Y. P. Kulinich[169], M. Kuna[11], T. Kunigo[71], A. Kupco[129], T. Kupfer[46], O. Kuprash[155], H. Kurashige[70], L. L. Kurchaninov[163a], Y. A. Kurochkin[95], M. G. Kurth[35a,35d], E. S. Kuwertz[172], M. Kuze[159], J. Kvita[117], T. Kwan[172], D. Kyriazopoulos[141], A. La Rosa[103], J. L. La Rosa Navarro[26d], L. La Rotonda[40a,40b], F. La Ruffa[40a,40b], C. Lacasta[170], F. Lacava[134a,134b], J. Lacey[45], D. P. J. Lack[87], H. Lacker[17], D. Lacour[83], E. Ladygin[68], R. Lafaye[5], B. Laforge[83], S. Lai[57], S. Lammers[64], W. Lampl[7], E. Lançon[27], U. Landgraf[51], M. P. J. Landon[79], M. C. Lanfermann[52], V. S. Lang[45], J. C. Lange[13], R. J. Langenberg[32], A. J. Lankford[166], F. Lanni[27], K. Lantzsch[23], A. Lanza[123a], A. Lapertosa[53a,53b], S. Laplace[83], J. F. Laporte[138], T. Lari[94a], F. Lasagni Manghi[22a,22b], M. Lassnig[32], T. S. Lau[62a], P. Laurelli[50], W. Lavrijsen[16], A. T. Law[139], P. Laycock[77], T. Lazovich[59], M. Lazzaroni[94a,94b], B. Le[91], O. Le Dortz[83], E. Le Guirriec[88], E. P. Le Quilleuc[138], M. LeBlanc[7], T. LeCompte[6], F. Ledroit-Guillon[58], C. A. Lee[27], G. R. Lee[34a], S. C. Lee[153], L. Lee[59], B. Lefebvre[90], G. Lefebvre[83], M. Lefebvre[172], F. Legger[102], C. Leggett[16], G. Lehmann Miotto[32], X. Lei[7], W. A. Leight[45], M. A. L. Leite[26d], R. Leitner[131], D. Lellouch[175], B. Lemmer[57], K. J. C. Leney[81], T. Lenz[23], B. Lenzi[32], R. Leone[7], S. Leone[126a], C. Leonidopoulos[49], G. Lerner[151], C. Leroy[97], R. Les[161], A. A. J. Lesage[138], C. G. Lester[30], M. Levchenko[125], J. Levêque[5], D. Levin[92], L. J. Levinson[175], M. Levy[19], D. Lewis[79], B. Li[36a,w], C.-Q. Li[36a], H. Li[150], L. Li[36c], Q. Li[35a,35d], Q. Li[36a], S. Li[48], X. Li[36c], Y. Li[143], Z. Li[36b], Z. Liang[35a], B. Liberti[135a], A. Liblong[161], K. Lie[62c], W. Liebig[15], A. Limosani[152], C. Y. Lin[30], K. Lin[93], S. C. Lin[182], T. H. Lin[86], R. A. Linck[64], B. E. Lindquist[150], A. E. Lionti[52], E. Lipeles[124], A. Lipniacka[15], M. Lisovyi[60b], T. M. Liss[169,ah], A. Lister[171], A. M. Litke[139], B. Liu[67], H. Liu[92], H. Liu[27], J. K. K. Liu[122], J. Liu[36b], J. B. Liu[36b], K. Liu[88], L. Liu[169], M. Liu[36a], Y. L. Liu[36a], Y. Liu[36a], M. Livan[123a,123b], A. Lleres[58], J. Llorente Merino[35a], S. L. Lloyd[79], C. Y. Lo[62b], F. Lo Sterzo[43], E. M. Lobodzinska[45], P. Loch[7], F. K. Loebinger[87], A. Loesle[51], K. M. Loew[25], T. Lohse[17], K. Lohwasser[141], M. Lokajicek[129], B. A. Long[24], J. D. Long[169], R. E. Long[75], L. Longo[76a,76b], K. A. Looper[113], J. A. Lopez[34b], I. Lopez Paz[13], A. Lopez Solis[83], J. Lorenz[102], N. Lorenzo Martinez[5], M. Losada[21], P. J. Lösel[102], X. Lou[35a], A. Lounis[119], J. Love[6], P. A. Love[75], H. Lu[62a], N. Lu[92], Y. J. Lu[63], H. J. Lubatti[140], C. Luci[134a,134b], A. Lucotte[58], C. Luedtke[51], F. Luehring[64], W. Lukas[65], L. Luminari[134a], B. Lund-Jensen[149], M. S. Lutz[89], P. M. Luzi[83], D. Lynn[27], R. Lysak[129], E. Lytken[84], F. Lyu[35a], V. Lyubushkin[68], H. Ma[27], L. L. Ma[36b], Y. Ma[36b], G. Maccarrone[50], A. Macchiolo[103], C. M. Macdonald[141], B. Maček[78], J. Machado Miguens[124,128b], D. Madaffari[170], R. Madar[37], W. F. Mader[47], A. Madsen[45], N. Madysa[47], J. Maeda[70], S. Maeland[15], T. Maeno[27], A. S. Maevskiy[101], V. Magerl[51], C. Maiani[119], C. Maidantchik[26a], T. Maier[102], A. Maio[128a,128b,128d], O. Majersky[146a], S. Majewski[118], Y. Makida[69], N. Makovec[119], B. Malaescu[83], Pa. Malecki[42], V. P. Maleev[125], F. Malek[58], U. Mallik[66], D. Malon[6], C. Malone[30], S. Maltezos[10], S. Malyukov[32], J. Mamuzic[170], G. Mancini[50], I. Mandić[78], J. Maneira[128a,128b], L. Manhaes de Andrade Filho[26b], J. Manjarres Ramos[47], K. H. Mankinen[84], A. Mann[102], A. Manousos[32], B. Mansoulie[138], J. D. Mansour[35a], R. Mantifel[90], M. Mantoani[57], S. Manzoni[94a,94b], L. Mapelli[32], G. Marceca[29], L. March[52], L. Marchese[122], G. Marchiori[83], M. Marcisovsky[129], C. A. Marin Tobon[32], M. Marjanovic[37], D. E. Marley[92], F. Marroquim[26a], S. P. Marsden[87], Z. Marshall[16], M. U. F Martensson[168], S. Marti-Garcia[170], C. B. Martin[113], T. A. Martin[173], V. J. Martin[49], B. Martin dit Latour[15], M. Martinez[13,v], V. I. Martinez Outschoorn[169], S. Martin-Haugh[133], V. S. Martoiu[28b], A. C. Martyniuk[81], A. Marzin[32], L. Masetti[86], T. Mashimo[157], R. Mashinistov[98], J. Masik[87], A. L. Maslennikov[111,c], L. H. Mason[91], L. Massa[135a,135b], P. Mastrandrea[5], A. Mastroberardino[40a,40b], T. Masubuchi[157], P. Mättig[178], J. Maurer[28b], S. J. Maxfield[77], D. A. Maximov[111,c], R. Mazini[153], I. Maznas[156], S. M. Mazza[94a,94b], N. C. Mc Fadden[107], G. Mc Goldrick[161], S. P. Mc Kee[92], A. McCarn[92], R. L. McCarthy[150], T. G. McCarthy[103], L. I. McClymont[81], E. F. McDonald[91], J. A. Mcfayden[32], G. Mchedlidze[57], S. J. McMahon[133], P. C. McNamara[91], C. J. McNicol[173], R. A. McPherson[172,o], S. Meehan[140], T. J. Megy[51], S. Mehlhase[102], A. Mehta[77], T. Meideck[58], K. Meier[60a], B. Meirose[44], D. Melini[170,ai], B. R. Mellado Garcia[147c], J. D. Mellenthin[57], M. Melo[146a], F. Meloni[18], A. Melzer[23], S. B. Menary[87], L. Meng[77], X. T. Meng[92], A. Mengarelli[22a,22b], S. Menke[103], E. Meoni[40a,40b], S. Mergelmeyer[17], C. Merlassino[18], P. Mermod[52], L. Merola[106a,106b], C. Meroni[94a], F. S. Merritt[33], A. Messina[134a,134b], J. Metcalfe[6], A. S. Mete[166], C. Meyer[124], J-P. Meyer[138], J. Meyer[109], H. Meyer Zu Theenhausen[60a], F. Miano[151], R. P. Middleton[133], S. Miglioranzi[53a,53b], L. Mijović[49], G. Mikenberg[175], M. Mikestikova[129], M. Mikuž[78], M. Milesi[91], A. Milic[161], D. A. Millar[79], D. W. Miller[33], C. Mills[49], A. Milov[175], D. A. Milstead[148a,148b], A. A. Minaenko[132], Y. Minami[157], I. A. Minashvili[54b], A. I. Mincer[112], B. Mindur[41a], M. Mineev[68], Y. Minegishi[157], Y. Ming[176], L. M. Mir[13], A. Mirto[76a,76b], K. P. Mistry[124], T. Mitani[174], J. Mitrevski[102], V. A. Mitsou[170], A. Miucci[18], P. S. Miyagawa[141], A. Mizukami[69], J. U. Mjörnmark[84], T. Mkrtchyan[180], M. Mlynarikova[131], T. Moa[148a,148b], K. Mochizuki[97], P. Mogg[51], S. Mohapatra[38], S. Molander[148a,148b], R. Moles-Valls[23], M. C. Mondragon[93], K. Mönig[45], J. Monk[39], E. Monnier[88], A. Montalbano[150], J. Montejo Berlingen[32], F. Monticelli[74], S. Monzani[94a], R. W. Moore[3], N. Morange[119], D. Moreno[21], M. Moreno Llácer[32], P. Morettini[53a], M. Morgenstern[109], S. Morgenstern[32], D. Mori[144], T. Mori[157], M. Morii[59], M. Morinaga[174], V. Morisbak[121], A. K. Morley[32], G. Mornacchi[32], J. D. Morris[79], L. Morvaj[150], P. Moschovakos[10],

M. Mosidze[54b], H. J. Moss[141], J. Moss[145,aj], K. Motohashi[159], R. Mount[145], E. Mountricha[27], E. J. W. Moyse[89], S. Muanza[88], F. Mueller[103], J. Mueller[127], R. S. P. Mueller[102], D. Muenstermann[75], P. Mullen[56], G. A. Mullier[18], F. J. Munoz Sanchez[87], W. J. Murray[173,133], H. Musheghyan[32], M. Muškinja[78], C. Mwewa[147a], A. G. Myagkov[132,ak], M. Myska[130], B. P. Nachman[16], O. Nackenhorst[52], K. Nagai[122], R. Nagai[69,af], K. Nagano[69], Y. Nagasaka[61], K. Nagata[164], M. Nagel[51], E. Nagy[88], A. M. Nairz[32], Y. Nakahama[105], K. Nakamura[69], T. Nakamura[157], I. Nakano[114], R. F. Naranjo Garcia[45], R. Narayan[11], D. I. Narrias Villar[60a], I. Naryshkin[125], T. Naumann[45], G. Navarro[21], R. Nayyar[7], H. A. Neal[92], P. Yu. Nechaeva[98], T. J. Neep[138], A. Negri[123a,123b], M. Negrini[22a], S. Nektarijevic[108], C. Nellist[57], A. Nelson[166], M. E. Nelson[122], S. Nemecek[129], P. Nemethy[112], M. Nessi[32,al], M. S. Neubauer[169], M. Neumann[178], P. R. Newman[19], T. Y. Ng[62c], Y. S. Ng[17], T. Nguyen Manh[97], R. B. Nickerson[122], R. Nicolaidou[138], J. Nielsen[139], N. Nikiforou[11], V. Nikolaenko[132,ak], I. Nikolic-Audit[83], K. Nikolopoulos[19], P. Nilsson[27], Y. Ninomiya[69], A. Nisati[134a], N. Nishu[36c], R. Nisius[103], I. Nitsche[46], T. Nitta[174], T. Nobe[157], Y. Noguchi[71], M. Nomachi[120], I. Nomidis[31], M. A. Nomura[27], T. Nooney[79], M. Nordberg[32], N. Norjoharuddeen[122], O. Novgorodova[47], M. Nozaki[69], L. Nozka[117], K. Ntekas[166], E. Nurse[81], F. Nuti[91], K. O'connor[25], D. C. O'Neil[144], A. A. O'Rourke[45], V. O'Shea[56], F. G. Oakham[31,d], H. Oberlack[103], T. Obermann[23], J. Ocariz[83], A. Ochi[70], I. Ochoa[38], J. P. Ochoa-Ricoux[34a], S. Oda[73], S. Odaka[69], A. Oh[87], S. H. Oh[48], C. C. Ohm[149], H. Ohman[168], H. Oide[53a,53b], H. Okawa[164], Y. Okumura[157], T. Okuyama[69], A. Olariu[28b], L. F. Oleiro Seabra[128a], S. A. Olivares Pino[34a], D. Oliveira Damazio[27], M. J. R. Olsson[33], A. Olszewski[42], J. Olszowska[42], A. Onofre[128a,128e], K. Onogi[105], P. U. E. Onyisi[11,ab], H. Oppen[121], M. J. Oreglia[33], Y. Oren[155], D. Orestano[136a,136b], N. Orlando[62b], R. S. Orr[161], B. Osculati[53a,53b,*], R. Ospanov[36a], G. Otero y Garzon[29], H. Otono[73], M. Ouchrif[137d], F. Ould-Saada[121], A. Ouraou[138], K. P. Oussoren[109], Q. Ouyang[35a], M. Owen[56], R. E. Owen[19], V. E. Ozcan[20a], N. Ozturk[8], K. Pachal[144], A. Pacheco Pages[13], L. Pacheco Rodriguez[138], C. Padilla Aranda[13], S. Pagan Griso[16], M. Paganini[179], F. Paige[27], G. Palacino[64], S. Palazzo[40a,40b], S. Palestini[32], M. Palka[41b], D. Pallin[37], E. St. Panagiotopoulou[10], I. Panagoulias[10], C. E. Pandini[52], J. G. Panduro Vazquez[80], P. Pani[32], S. Panitkin[27], D. Pantea[28b], L. Paolozzi[52], Th. D. Papadopoulou[10], K. Papageorgiou[9,s], A. Paramonov[6], D. Paredes Hernandez[179], A. J. Parker[75], M. A. Parker[30], K. A. Parker[45], F. Parodi[53a,53b], J. A. Parsons[38], U. Parzefall[51], V. R. Pascuzzi[161], J. M. Pasner[139], E. Pasqualucci[134a], S. Passaggio[53a], Fr. Pastore[80], S. Pataraia[86], J. R. Pater[87], T. Pauly[32], B. Pearson[103], S. Pedraza Lopez[170], R. Pedro[128a,128b], S. V. Peleganchuk[111,c], O. Penc[129], C. Peng[35a,35d], H. Peng[36a], J. Penwell[64], B. S. Peralva[26b], M. M. Perego[138], D. V. Perepelitsa[27], F. Peri[17], L. Perini[94a,94b], H. Pernegger[32], S. Perrella[106a,106b], R. Peschke[45], V. D. Peshekhonov[68,*], K. Peters[45], R. F. Y. Peters[87], B. A. Petersen[32], T. C. Petersen[39], E. Petit[58], A. Petridis[1], C. Petridou[156], P. Petroff[119], E. Petrolo[134a], M. Petrov[122], F. Petrucci[136a,136b], N. E. Pettersson[89], A. Peyaud[138], R. Pezoa[34b], F. H. Phillips[93], P. W. Phillips[133], G. Piacquadio[150], E. Pianori[173], A. Picazio[89], M. A. Pickering[122], R. Piegaia[29], J. E. Pilcher[33], A. D. Pilkington[87], M. Pinamonti[135a,135b], J. L. Pinfold[3], H. Pirumov[45], M. Pitt[175], L. Plazak[146a], M.-A. Pleier[27], V. Pleskot[86], E. Plotnikova[68], D. Pluth[67], P. Podberezko[111], R. Poettgen[84], R. Poggi[123a,123b], L. Poggioli[119], I. Pogrebnyak[93], D. Pohl[23], I. Pokharel[57], G. Polesello[123a], A. Poley[45], A. Policicchio[40a,40b], R. Polifka[32], A. Polini[22a], C. S. Pollard[56], V. Polychronakos[27], K. Pommès[32], D. Ponomarenko[100], L. Pontecorvo[134a], G. A. Popeneciu[28d], D. M. Portillo Quintero[83], S. Pospisil[130], K. Potamianos[45], I. N. Potrap[68], C. J. Potter[30], H. Potti[11], T. Poulsen[84], J. Poveda[32], M. E. Pozo Astigarraga[32], P. Pralavorio[88], A. Pranko[16], S. Prell[67], D. Price[87], M. Primavera[76a], S. Prince[90], N. Proklova[100], K. Prokofiev[62c], F. Prokoshin[34b], S. Protopopescu[27], J. Proudfoot[6], M. Przybycien[41a], A. Puri[169], P. Puzo[119], J. Qian[92], Y. Qin[87], A. Quadt[57], M. Queitsch-Maitland[45], D. Quilty[56], S. Raddum[121], V. Radeka[27], V. Radescu[122], S. K. Radhakrishnan[150], P. Radloff[118], P. Rados[91], F. Ragusa[94a,94b], G. Rahal[181], J. A. Raine[87], S. Rajagopalan[27], C. Rangel-Smith[168], T. Rashid[119], S. Raspopov[5], M. G. Ratti[94a,94b], D. M. Rauch[45], F. Rauscher[102], S. Rave[86], I. Ravinovich[175], J. H. Rawling[87], M. Raymond[32], A. L. Read[121], N. P. Readioff[58], M. Reale[76a,76b], D. M. Rebuzzi[123a,123b], A. Redelbach[177], G. Redlinger[27], R. Reece[139], R. G. Reed[147c], K. Reeves[44], L. Rehnisch[17], J. Reichert[124], A. Reiss[86], C. Rembser[32], H. Ren[35a,35d], M. Rescigno[134a], S. Resconi[94a], E. D. Resseguie[124], S. Rettie[171], E. Reynolds[19], O. L. Rezanova[111,c], P. Reznicek[131], R. Rezvani[97], R. Richter[103], S. Richter[81], E. Richter-Was[41b], O. Ricken[23], M. Ridel[83], P. Rieck[103], C. J. Riegel[178], J. Rieger[57], O. Rifki[115], M. Rijssenbeek[150], A. Rimoldi[123a,123b], M. Rimoldi[18], L. Rinaldi[22a], G. Ripellino[149], B. Ristić[32], E. Ritsch[32], I. Riu[13], F. Rizatdinova[116], E. Rizvi[79], C. Rizzi[13], R. T. Roberts[87], S. H. Robertson[90,o], A. Robichaud-Veronneau[90], D. Robinson[30], J. E. M. Robinson[45], A. Robson[56], E. Rocco[86], C. Roda[126a,126b], Y. Rodina[88,am], S. Rodriguez Bosca[170], A. Rodriguez Perez[13], D. Rodriguez Rodriguez[170], S. Roe[32], C. S. Rogan[59], O. Røhne[121], J. Roloff[59], A. Romaniouk[100], M. Romano[22a,22b], S. M. Romano Saez[37], E. Romero Adam[170], N. Rompotis[77], M. Ronzani[51], L. Roos[83], S. Rosati[134a], K. Rosbach[51], P. Rose[139], N.-A. Rosien[57], E. Rossi[106a,106b], L. P. Rossi[53a], J. H. N. Rosten[30], R. Rosten[140], M. Rotaru[28b], J. Rothberg[140], D. Rousseau[119], D. Roy[147c], A. Rozanov[88], Y. Rozen[154], X. Ruan[147c], F. Rubbo[145], F. Rühr[51], A. Ruiz-Martinez[31], Z. Rurikova[51], N. A. Rusakovich[68], H. L. Russell[90], J. P. Rutherfoord[7], N. Ruthmann[32], E. M. Rüttinger[45], Y. F. Ryabov[125], M. Rybar[169], G. Rybkin[119],

S. Ryu[6], A. Ryzhov[132], G. F. Rzehorz[57], A. F. Saavedra[152], G. Sabato[109], S. Sacerdoti[29], H. F.-W. Sadrozinski[139], R. Sadykov[68], F. Safai Tehrani[134a], P. Saha[110], M. Sahinsoy[60a], M. Saimpert[45], M. Saito[157], T. Saito[157], H. Sakamoto[157], Y. Sakurai[174], G. Salamanna[136a,136b], J. E. Salazar Loyola[34b], D. Salek[109], P. H. Sales De Bruin[168], D. Salihagic[103], A. Salnikov[145], J. Salt[170], D. Salvatore[40a,40b], F. Salvatore[151], A. Salvucci[62a,62b,62c], A. Salzburger[32], D. Sammel[51], D. Sampsonidis[156], D. Sampsonidou[156], J. Sánchez[170], A. Sanchez Pineda[167a,167c], H. Sandaker[121], R. L. Sandbach[79], C. O. Sander[45], M. Sandhoff[178], C. Sandoval[21], D. P. C. Sankey[133], M. Sannino[53a,53b], Y. Sano[105], A. Sansoni[50], C. Santoni[37], H. Santos[128a], I. Santoyo Castillo[151], A. Sapronov[68], J. G. Saraiva[128a,128d], O. Sasaki[69], K. Sato[164], E. Sauvan[5], G. Savage[80], P. Savard[161,d], N. Savic[103], C. Sawyer[133], L. Sawyer[82,u], C. Sbarra[22a], A. Sbrizzi[22a,22b], T. Scanlon[81], D. A. Scannicchio[166], J. Schaarschmidt[140], P. Schacht[103], B. M. Schachtner[102], D. Schaefer[33], L. Schaefer[124], J. Schaeffer[86], S. Schaepe[32], S. Schaetzel[60b], U. Schäfer[86], A. C. Schaffer[119], D. Schaile[102], R. D. Schamberger[150], V. A. Schegelsky[125], D. Scheirich[131], F. Schenck[17], M. Schernau[166], C. Schiavi[53a,53b], S. Schier[139], L. K. Schildgen[23], C. Schillo[51], M. Schioppa[40a,40b], S. Schlenker[32], K. R. Schmidt-Sommerfeld[103], K. Schmieden[32], C. Schmitt[86], S. Schmitt[45], S. Schmitz[86], U. Schnoor[51], L. Schoeffel[138], A. Schoening[60b], B. D. Schoenrock[93], E. Schopf[23], M. Schott[86], J. F. P. Schouwenberg[108], J. Schovancova[32], S. Schramm[52], N. Schuh[86], A. Schulte[86], M. J. Schultens[23], H.-C. Schultz-Coulon[60a], M. Schumacher[51], B. A. Schumm[139], Ph. Schune[138], A. Schwartzman[145], T. A. Schwarz[92], H. Schweiger[87], Ph. Schwemling[138], R. Schwienhorst[93], J. Schwindling[138], A. Sciandra[23], G. Sciolla[25], M. Scornajenghi[40a,40b], F. Scuri[126a], F. Scutti[91], J. Searcy[92], P. Seema[23], S. C. Seidel[107], A. Seiden[139], J. M. Seixas[26a], G. Sekhniaidze[106a], K. Sekhon[92], S. J. Sekula[43], N. Semprini-Cesari[22a,22b], S. Senkin[37], C. Serfon[121], L. Serin[119], L. Serkin[167a,167b], M. Sessa[136a,136b], R. Seuster[172], H. Severini[115], T. Šfiligoj[78], F. Sforza[165], A. Sfyrla[52], E. Shabalina[57], N. W. Shaikh[148a,148b], L. Y. Shan[35a], R. Shang[169], J. T. Shank[24], M. Shapiro[16], P. B. Shatalov[99], K. Shaw[167a,167b], S. M. Shaw[87], A. Shcherbakova[148a,148b], C. Y. Shehu[151], Y. Shen[115], N. Sherafati[31], A. D. Sherman[24], P. Sherwood[81], L. Shi[153,an], S. Shimizu[70], C. O. Shimmin[179], M. Shimojima[104], I. P. J. Shipsey[122], S. Shirabe[73], M. Shiyakova[68,ao], J. Shlomi[175], A. Shmeleva[98], D. Shoaleh Saadi[97], M. J. Shochet[33], S. Shojaii[94a,94b], D. R. Shope[115], S. Shrestha[113], E. Shulga[100], M. A. Shupe[7], P. Sicho[129], A. M. Sickles[169], P. E. Sidebo[149], E. Sideras Haddad[147c], O. Sidiropoulou[177], A. Sidoti[22a,22b], F. Siegert[47], Dj. Sijacki[14], J. Silva[128a,128d], M. Silva Jr.[176], S. B. Silverstein[148a], V. Simak[130], L. Simic[68], S. Simion[119], E. Simioni[86], B. Simmons[81], M. Simon[86], P. Sinervo[161], N. B. Sinev[118], M. Sioli[22a,22b], G. Siragusa[177], I. Siral[92], S. Yu. Sivoklokov[101], J. Sjölin[148a,148b], M. B. Skinner[75], P. Skubic[115], M. Slater[19], T. Slavicek[130], M. Slawinska[42], K. Sliwa[165], R. Slovak[131], V. Smakhtin[175], B. H. Smart[5], J. Smiesko[146a], N. Smirnov[100], S. Yu. Smirnov[100], Y. Smirnov[100], L. N. Smirnova[101,ap], O. Smirnova[84], J. W. Smith[57], M. N. K. Smith[38], R. W. Smith[38], M. Smizanska[75], K. Smolek[130], A. A. Snesarev[98], I. M. Snyder[118], S. Snyder[27], R. Sobie[172,o], F. Socher[47], A. Soffer[155], A. Søgaard[49], D. A. Soh[153], G. Sokhrannyi[78], C. A. Solans Sanchez[32], M. Solar[130], E. Yu. Soldatov[100], U. Soldevila[170], A. A. Solodkov[132], A. Soloshenko[68], O. V. Solovyanov[132], V. Solovyev[125], P. Sommer[141], H. Son[165], W. Song[133], A. Sopczak[130], D. Sosa[60b], C. L. Sotiropoulou[126a,126b], S. Sottocornola[123a,123b], R. Soualah[167a,167c], A. M. Soukharev[111,c], D. South[45], B. C. Sowden[80], S. Spagnolo[76a,76b], M. Spalla[126a,126b], M. Spangenberg[173], F. Spanò[80], D. Sperlich[17], F. Spettel[103], T. M. Spieker[60a], R. Spighi[22a], G. Spigo[32], L. A. Spiller[91], M. Spousta[131], R. D. St. Denis[56,*], A. Stabile[94a,94b], R. Stamen[60a], S. Stamm[17], E. Stanecka[42], R. W. Stanek[6], C. Stanescu[136a], M. M. Stanitzki[45], B. S. Stapf[109], S. Stapnes[121], E. A. Starchenko[132], G. H. Stark[33], J. Stark[58], S. H Stark[39], P. Staroba[129], P. Starovoitov[60a], S. Stärz[32], R. Staszewski[42], M. Stegler[45], P. Steinberg[27], B. Stelzer[144], H. J. Stelzer[32], O. Stelzer-Chilton[163a], H. Stenzel[55], T. J. Stevenson[79], G. A. Stewart[56], M. C. Stockton[118], M. Stoebe[90], G. Stoicea[28b], P. Stolte[57], S. Stonjek[103], A. R. Stradling[8], A. Straessner[47], M. E. Stramaglia[18], J. Strandberg[149], S. Strandberg[148a,148b], M. Strauss[115], P. Strizenec[146b], R. Ströhmer[177], D. M. Strom[118], R. Stroynowski[43], A. Strubig[49], S. A. Stucci[27], B. Stugu[15], N. A. Styles[45], D. Su[145], J. Su[127], S. Suchek[60a], Y. Sugaya[120], M. Suk[130], V. V. Sulin[98], DMS Sultan[162a,162b], S. Sultansoy[4c], T. Sumida[71], S. Sun[59], X. Sun[3], K. Suruliz[151], C. J. E. Suster[152], M. R. Sutton[151], S. Suzuki[69], M. Svatos[129], M. Swiatlowski[33], S. P. Swift[2], I. Sykora[146a], T. Sykora[131], D. Ta[51], K. Tackmann[45], J. Taenzer[155], A. Taffard[166], R. Tafirout[163a], E. Tahirovic[79], N. Taiblum[155], H. Takai[27], R. Takashima[72], E. H. Takasugi[103], K. Takeda[70], T. Takeshita[142], Y. Takubo[69], M. Talby[88], A. A. Talyshev[111,c], J. Tanaka[157], M. Tanaka[159], R. Tanaka[119], R. Tanioka[70], B. B. Tannenwald[113], S. Tapia Araya[34b], S. Tapprogge[86], S. Tarem[154], G. F. Tartarelli[94a], P. Tas[131], M. Tasevsky[129], T. Tashiro[71], E. Tassi[40a,40b], A. Tavares Delgado[128a,128b], Y. Tayalati[137e], A. C. Taylor[107], A. J. Taylor[49], G. N. Taylor[91], P. T. E. Taylor[91], W. Taylor[163b], P. Teixeira-Dias[80], D. Temple[144], H. Ten Kate[32], P. K. Teng[153], J. J. Teoh[120], F. Tepel[178], S. Terada[69], K. Terashi[157], J. Terron[85], S. Terzo[13], M. Testa[50], R. J. Teuscher[161,o], S. J. Thais[179], T. Theveneaux-Pelzer[88], F. Thiele[39], J. P. Thomas[19], J. Thomas-Wilsker[80], P. D. Thompson[19], A. S. Thompson[56], L. A. Thomsen[179], E. Thomson[124], Y. Tian[38], M. J. Tibbetts[16], R. E. Ticse Torres[57], V. O. Tikhomirov[98,aq], Yu. A. Tikhonov[111,c], S. Timoshenko[100], P. Tipton[179], S. Tisserant[88], K. Todome[159], S. Todorova-Nova[5], S. Todt[47], J. Tojo[73], S. Tokár[146a], K. Tokushuku[69],

E. Tolley[113], L. Tomlinson[87], M. Tomoto[105], L. Tompkins[145,ar], K. Toms[107], B. Tong[59], P. Tornambe[51], E. Torrence[118], H. Torres[47], E. Torró Pastor[140], J. Toth[88,as], F. Touchard[88], D. R. Tovey[141], C. J. Treado[112], T. Trefzger[177], F. Tresoldi[151], A. Tricoli[27], I. M. Trigger[163a], S. Trincaz-Duvoid[83], M. F. Tripiana[13], W. Trischuk[161], B. Trocmé[58], A. Trofymov[45], C. Troncon[94a], M. Trovatelli[172], L. Truong[147b], M. Trzebinski[42], A. Trzupek[42], K. W. Tsang[62a], J. C.-L. Tseng[122], P. V. Tsiareshka[95], N. Tsirintanis[9], S. Tsiskaridze[13], V. Tsiskaridze[51], E. G. Tskhadadze[54a], I. I. Tsukerman[99], V. Tsulaia[16], S. Tsuno[69], D. Tsybychev[150], Y. Tu[62b], A. Tudorache[28b], V. Tudorache[28b], T. T. Tulbure[28a], A. N. Tuna[59], S. Turchikhin[68], D. Turgeman[175], I. Turk Cakir[4b,at], R. Turra[94a], P. M. Tuts[38], G. Ucchielli[22a,22b], I. Ueda[69], M. Ughetto[148a,148b], F. Ukegawa[164], G. Unal[32], A. Undrus[27], G. Unel[166], F. C. Ungaro[91], Y. Unno[69], K. Uno[157], J. Urban[146b], P. Urquijo[91], P. Urrejola[86], G. Usai[8], J. Usui[69], L. Vacavant[88], V. Vacek[130], B. Vachon[90], K. O. H. Vadla[121], A. Vaidya[81], C. Valderanis[102], E. Valdes Santurio[148a,148b], M. Valente[52], S. Valentinetti[22a,22b], A. Valero[170], L. Valéry[13], A. Vallier[5], J. A. Valls Ferrer[170], W. Van Den Wollenberg[109], H. van der Graaf[109], P. van Gemmeren[6], J. Van Nieuwkoop[144], I. van Vulpen[109], M. C. van Woerden[109], M. Vanadia[135a,135b], W. Vandelli[32], A. Vaniachine[160], P. Vankov[109], G. Vardanyan[180], R. Vari[134a], E. W. Varnes[7], C. Varni[53a,53b], T. Varol[43], D. Varouchas[119], A. Vartapetian[8], K. E. Varvell[152], J. G. Vasquez[179], G. A. Vasquez[34b], F. Vazeille[37], D. Vazquez Furelos[13], T. Vazquez Schroeder[90], J. Veatch[57], V. Veeraraghavan[7], L. M. Veloce[161], F. Veloso[128a,128c], S. Veneziano[134a], A. Ventura[76a,76b], M. Venturi[172], N. Venturi[32], V. Vercesi[123a], M. Verducci[136a,136b], W. Verkerke[109], A. T. Vermeulen[109], J. C. Vermeulen[109], M. C. Vetterli[144,d], N. Viaux Maira[34b], O. Viazlo[84], I. Vichou[169,*], T. Vickey[141], O. E. Vickey Boeriu[141], G. H. A. Viehhauser[122], S. Viel[16], L. Vigani[122], M. Villa[22a,22b], M. Villaplana Perez[94a,94b], E. Vilucchi[50], M. G. Vincter[31], V. B. Vinogradov[68], A. Vishwakarma[45], C. Vittori[22a,22b], I. Vivarelli[151], S. Vlachos[10], M. Vogel[178], P. Vokac[130], G. Volpi[13], H. von der Schmitt[103], E. von Toerne[23], V. Vorobel[131], K. Vorobev[100], M. Vos[170], R. Voss[32], J. H. Vossebeld[77], N. Vranjes[14], M. Vranjes Milosavljevic[14], V. Vrba[130], M. Vreeswijk[109], R. Vuillermet[32], I. Vukotic[33], P. Wagner[23], W. Wagner[178], J. Wagner-Kuhr[102], H. Wahlberg[74], S. Wahrmund[47], K. Wakamiya[70], J. Walder[75], R. Walker[102], W. Walkowiak[143], V. Wallangen[148a,148b], C. Wang[35b], C. Wang[36b,au], F. Wang[176], H. Wang[16], H. Wang[3], J. Wang[45], J. Wang[152], Q. Wang[115], R.-J. Wang[83], R. Wang[6], S. M. Wang[153], T. Wang[38], W. Wang[153,av], W. Wang[36a,aw], Z. Wang[36c], C. Wanotayaroj[45], A. Warburton[90], C. P. Ward[30], D. R. Wardrope[81], A. Washbrook[49], P. M. Watkins[19], A. T. Watson[19], M. F. Watson[19], G. Watts[140], S. Watts[87], B. M. Waugh[81], A. F. Webb[11], S. Webb[86], M. S. Weber[18], S. M. Weber[60a], S. W. Weber[177], S. A. Weber[31], J. S. Webster[6], A. R. Weidberg[122], B. Weinert[64], J. Weingarten[57], M. Weirich[86], C. Weiser[51], P. S. Wells[32], T. Wenaus[27], T. Wengler[32], S. Wenig[32], N. Wermes[23], M. D. Werner[67], P. Werner[32], M. Wessels[60a], T. D. Weston[18], K. Whalen[118], N. L. Whallon[140], A. M. Wharton[75], A. S. White[92], A. White[8], M. J. White[1], R. White[34b], D. Whiteson[166], B. W. Whitmore[75], F. J. Wickens[133], W. Wiedenmann[176], M. Wielers[133], C. Wiglesworth[39], L. A. M. Wiik-Fuchs[51], A. Wildauer[103], F. Wilk[87], H. G. Wilkens[32], H. H. Williams[124], S. Williams[109], C. Willis[93], S. Willocq[89], J. A. Wilson[19], I. Wingerter-Seez[5], E. Winkels[151], F. Winklmeier[118], O. J. Winston[151], B. T. Winter[23], M. Wittgen[145], M. Wobisch[82,u], A. Wolf[86], T. M. H. Wolf[109], R. Wolff[88], M. W. Wolter[42], H. Wolters[128a,128c], V. W. S. Wong[171], N. L. Woods[139], S. D. Worm[19], B. K. Wosiek[42], J. Wotschack[32], K. W. Wozniak[42], M. Wu[33], S. L. Wu[176], X. Wu[52], Y. Wu[92], T. R. Wyatt[87], B. M. Wynne[49], S. Xella[39], Z. Xi[92], L. Xia[35c], D. Xu[35a], L. Xu[27], T. Xu[138], W. Xu[92], B. Yabsley[152], S. Yacoob[147a], D. Yamaguchi[159], Y. Yamaguchi[159], A. Yamamoto[69], S. Yamamoto[157], T. Yamanaka[157], F. Yamane[70], M. Yamatani[157], T. Yamazaki[157], Y. Yamazaki[70], Z. Yan[24], H. Yang[36c], H. Yang[16], Y. Yang[153], Z. Yang[15], W-M. Yao[16], Y. C. Yap[45], Y. Yasu[69], E. Yatsenko[5], K. H. Yau Wong[23], J. Ye[43], S. Ye[27], I. Yeletskikh[68], E. Yigitbasi[24], E. Yildirim[86], K. Yorita[174], K. Yoshihara[124], C. Young[145], C. J. S. Young[32], J. Yu[8], J. Yu[67], S. P. Y. Yuen[23], I. Yusuff[30,ax], B. Zabinski[42], G. Zacharis[10], R. Zaidan[13], A. M. Zaitsev[132,ak], N. Zakharchuk[45], J. Zalieckas[15], A. Zaman[150], S. Zambito[59], D. Zanzi[91], C. Zeitnitz[178], G. Zemaityte[122], A. Zemla[41a], J. C. Zeng[169], Q. Zeng[145], O. Zenin[132], T. Ženiš[146a], D. Zerwas[119], D. Zhang[36b], D. Zhang[92], F. Zhang[176], G. Zhang[36a,aw], H. Zhang[119], J. Zhang[6], L. Zhang[51], L. Zhang[36a], M. Zhang[169], P. Zhang[35b], R. Zhang[23], R. Zhang[36a,au], X. Zhang[36b], Y. Zhang[35a,35d], Z. Zhang[119], X. Zhao[43], Y. Zhao[36b,x], Z. Zhao[36a], A. Zhemchugov[68], B. Zhou[92], C. Zhou[176], L. Zhou[43], M. Zhou[35a,35d], M. Zhou[150], N. Zhou[36c], Y. Zhou[7], C. G. Zhu[36b], H. Zhu[35a], J. Zhu[92], Y. Zhu[36a], X. Zhuang[35a], K. Zhukov[98], A. Zibell[177], D. Zieminska[64], N. I. Zimine[68], C. Zimmermann[86], S. Zimmermann[51], Z. Zinonos[103], M. Zinser[86], M. Ziolkowski[143], L. Živković[14], G. Zobernig[176], A. Zoccoli[22a,22b], R. Zou[33], M. zur Nedden[17], L. Zwalinski[32].

[1] Department of Physics, University of Adelaide, Adelaide, Australia
[2] Physics Department, SUNY Albany, Albany, NY, USA
[3] Department of Physics, University of Alberta, Edmonton, AB, Canada
[4] (a)Department of Physics, Ankara University, Ankara, Turkey; (b)Istanbul Aydin University, Istanbul, Turkey; (c)Division of Physics, TOBB University of Economics and Technology, Ankara, Turkey

[5] LAPP, CNRS/IN2P3 and Université Savoie Mont Blanc, Annecy-le-Vieux, France

[6] High Energy Physics Division, Argonne National Laboratory, Argonne, IL, USA

[7] Department of Physics, University of Arizona, Tucson, AZ, USA

[8] Department of Physics, The University of Texas at Arlington, Arlington, TX, USA

[9] Physics Department, National and Kapodistrian University of Athens, Athens, Greece

[10] Physics Department, National Technical University of Athens, Zografou, Greece

[11] Department of Physics, The University of Texas at Austin, Austin, TX, USA

[12] Institute of Physics, Azerbaijan Academy of Sciences, Baku, Azerbaijan

[13] Institut de Física d'Altes Energies (IFAE), The Barcelona Institute of Science and Technology, Barcelona, Spain

[14] Institute of Physics, University of Belgrade, Belgrade, Serbia

[15] Department for Physics and Technology, University of Bergen, Bergen, Norway

[16] Physics Division, Lawrence Berkeley National Laboratory, University of California, Berkeley, CA, USA

[17] Department of Physics, Humboldt University, Berlin, Germany

[18] Albert Einstein Center for Fundamental Physics, Laboratory for High Energy Physics, University of Bern, Bern, Switzerland

[19] School of Physics and Astronomy, University of Birmingham, Birmingham, UK

[20] [a]Department of Physics, Bogazici University, Istanbul, Turkey; [b]Department of Physics Engineering, Gaziantep University, Gaziantep, Turkey; [c]Faculty of Engineering and Natural Sciences, Istanbul Bilgi University, Istanbul, Turkey; [d]Faculty of Engineering and Natural Sciences, Bahcesehir University, Istanbul, Turkey

[21] Centro de Investigaciones, Universidad Antonio Narino, Bogotá, Colombia

[22] [a]INFN Sezione di Bologna, Bologna, Italy; [b]Dipartimento di Fisica e Astronomia, Università di Bologna, Bologna, Italy

[23] Physikalisches Institut, University of Bonn, Bonn, Germany

[24] Department of Physics, Boston University, Boston, MA, USA

[25] Department of Physics, Brandeis University, Waltham, MA, USA

[26] [a]Universidade Federal do Rio De Janeiro COPPE/EE/IF, Rio de Janeiro, Brazil; [b]Electrical Circuits Department, Federal University of Juiz de Fora (UFJF), Juiz de Fora, Brazil; [c]Federal University of Sao Joao del Rei (UFSJ), Sao Joao del Rei, Brazil; [d]Instituto de Fisica, Universidade de Sao Paulo, São Paulo, Brazil

[27] Physics Department, Brookhaven National Laboratory, Upton, NY, USA

[28] [a]Transilvania University of Brasov, Brasov, Romania; [b]Horia Hulubei National Institute of Physics and Nuclear Engineering, Bucharest, Romania; [c]Department of Physics, Alexandru Ioan Cuza University of Iasi, Iasi, Romania; [d]Physics Department, National Institute for Research and Development of Isotopic and Molecular Technologies, Cluj Napoca, Romania; [e]University Politehnica Bucharest, Bucharest, Romania; [f]West University in Timisoara, Timisoara, Romania

[29] Departamento de Física, Universidad de Buenos Aires, Buenos Aires, Argentina

[30] Cavendish Laboratory, University of Cambridge, Cambridge, UK

[31] Department of Physics, Carleton University, Ottawa, ON, Canada

[32] CERN, Geneva, Switzerland

[33] Enrico Fermi Institute, University of Chicago, Chicago, IL, USA

[34] [a]Departamento de Física, Pontificia Universidad Católica de Chile, Santiago, Chile; [b]Departamento de Física, Universidad Técnica Federico Santa María, Valparaiso, Chile

[35] [a]Institute of High Energy Physics, Chinese Academy of Sciences, Beijing, China; [b]Department of Physics, Nanjing University, Nanjing, Jiangsu, China; [c]Physics Department, Tsinghua University, Beijing 100084, China; [d]University of Chinese Academy of Science (UCAS), Beijing, China

[36] [a]Department of Modern Physics and State Key Laboratory of Particle Detection and Electronics, University of Science and Technology of China, Anhui, China; [b]School of Physics, Shandong University, Shandong, China; [c]School of Physics and Astronomy, Key Laboratory for Particle Physics, Astrophysics and Cosmology, Ministry of Education, Shanghai Key Laboratory for Particle Physics and Cosmology, Tsung-Dao Lee Institute, Shanghai Jiao Tong University, Shanghai, China

[37] Université Clermont Auvergne, CNRS/IN2P3, LPC, Clermont-Ferrand, France

[38] Nevis Laboratory, Columbia University, Irvington, NY, USA

[39] Niels Bohr Institute, University of Copenhagen, Copenhagen, Denmark

40 (a)INFN Gruppo Collegato di Cosenza, Laboratori Nazionali di Frascati, Frascati, Italy; (b)Dipartimento di Fisica, Università della Calabria, Rende, Italy

41 (a)Faculty of Physics and Applied Computer Science, AGH University of Science and Technology, Kraków, Poland; (b)Marian Smoluchowski Institute of Physics, Jagiellonian University, Kraków, Poland

42 Institute of Nuclear Physics, Polish Academy of Sciences, Kraków, Poland

43 Physics Department, Southern Methodist University, Dallas, TX, USA

44 Physics Department, University of Texas at Dallas, Richardson, TX, USA

45 DESY, Hamburg and Zeuthen, Germany

46 Lehrstuhl für Experimentelle Physik IV, Technische Universität Dortmund, Dortmund, Germany

47 Institut für Kern- und Teilchenphysik, Technische Universität Dresden, Dresden, Germany

48 Department of Physics, Duke University, Durham, NC, USA

49 SUPA-School of Physics and Astronomy, University of Edinburgh, Edinburgh, UK

50 INFN e Laboratori Nazionali di Frascati, Frascati, Italy

51 Fakultät für Mathematik und Physik, Albert-Ludwigs-Universität, Freiburg, Germany

52 Departement de Physique Nucleaire et Corpusculaire, Université de Genève, Geneva, Switzerland

53 (a)INFN Sezione di Genova, Genoa, Italy; (b)Dipartimento di Fisica, Università di Genova, Genoa, Italy

54 (a)E. Andronikashvili Institute of Physics, Iv. Javakhishvili Tbilisi State University, Tbilisi, Georgia; (b)High Energy Physics Institute, Tbilisi State University, Tbilisi, Georgia

55 II Physikalisches Institut, Justus-Liebig-Universität Giessen, Giessen, Germany

56 SUPA-School of Physics and Astronomy, University of Glasgow, Glasgow, UK

57 II Physikalisches Institut, Georg-August-Universität, Göttingen, Germany

58 Laboratoire de Physique Subatomique et de Cosmologie, Université Grenoble-Alpes, CNRS/IN2P3, Grenoble, France

59 Laboratory for Particle Physics and Cosmology, Harvard University, Cambridge, MA, USA

60 (a)Kirchhoff-Institut für Physik, Ruprecht-Karls-Universität Heidelberg, Heidelberg, Germany; (b)Physikalisches Institut, Ruprecht-Karls-Universität Heidelberg, Heidelberg, Germany

61 Faculty of Applied Information Science, Hiroshima Institute of Technology, Hiroshima, Japan

62 (a)Department of Physics, The Chinese University of Hong Kong, Shatin, N.T., Hong Kong; (b)Department of Physics, The University of Hong Kong, Hong Kong, China; (c)Department of Physics, Institute for Advanced Study, The Hong Kong University of Science and Technology, Clear Water Bay, Kowloon, Hong Kong, China

63 Department of Physics, National Tsing Hua University, Taiwan, Taiwan

64 Department of Physics, Indiana University, Bloomington, IN, USA

65 Institut für Astro- und Teilchenphysik, Leopold-Franzens-Universität, Innsbruck, Austria

66 University of Iowa, Iowa City, IA, USA

67 Department of Physics and Astronomy, Iowa State University, Ames, IA, USA

68 Joint Institute for Nuclear Research, JINR Dubna, Dubna, Russia

69 KEK, High Energy Accelerator Research Organization, Tsukuba, Japan

70 Graduate School of Science, Kobe University, Kobe, Japan

71 Faculty of Science, Kyoto University, Kyoto, Japan

72 Kyoto University of Education, Kyoto, Japan

73 Research Center for Advanced Particle Physics and Department of Physics, Kyushu University, Fukuoka, Japan

74 Instituto de Física La Plata, Universidad Nacional de La Plata and CONICET, La Plata, Argentina

75 Physics Department, Lancaster University, Lancaster, UK

76 (a)INFN Sezione di Lecce, Lecce, Italy; (b)Dipartimento di Matematica e Fisica, Università del Salento, Lecce, Italy

77 Oliver Lodge Laboratory, University of Liverpool, Liverpool, UK

78 Department of Experimental Particle Physics, Jožef Stefan Institute and Department of Physics, University of Ljubljana, Ljubljana, Slovenia

79 School of Physics and Astronomy, Queen Mary University of London, London, UK

80 Department of Physics, Royal Holloway University of London, Surrey, UK

81 Department of Physics and Astronomy, University College London, London, UK

82 Louisiana Tech University, Ruston, LA, USA

83 Laboratoire de Physique Nucléaire et de Hautes Energies, UPMC and Université Paris-Diderot and CNRS/IN2P3, Paris, France

84 Fysiska institutionen, Lunds universitet, Lund, Sweden

[85] Departamento de Fisica Teorica C-15, Universidad Autonoma de Madrid, Madrid, Spain

[86] Institut für Physik, Universität Mainz, Mainz, Germany

[87] School of Physics and Astronomy, University of Manchester, Manchester, UK

[88] CPPM, Aix-Marseille Université and CNRS/IN2P3, Marseille, France

[89] Department of Physics, University of Massachusetts, Amherst, MA, USA

[90] Department of Physics, McGill University, Montreal, QC, Canada

[91] School of Physics, University of Melbourne, Victoria, Australia

[92] Department of Physics, The University of Michigan, Ann Arbor, MI, USA

[93] Department of Physics and Astronomy, Michigan State University, East Lansing, MI, USA

[94] [a]INFN Sezione di Milano, Milan, Italy; [b]Dipartimento di Fisica, Università di Milano, Milan, Italy

[95] B.I. Stepanov Institute of Physics, National Academy of Sciences of Belarus, Minsk, Republic of Belarus

[96] Research Institute for Nuclear Problems of Byelorussian State University, Minsk, Republic of Belarus

[97] Group of Particle Physics, University of Montreal, Montreal, QC, Canada

[98] P.N. Lebedev Physical Institute of the Russian Academy of Sciences, Moscow, Russia

[99] Institute for Theoretical and Experimental Physics (ITEP), Moscow, Russia

[100] National Research Nuclear University MEPhI, Moscow, Russia

[101] D.V. Skobeltsyn Institute of Nuclear Physics, M.V. Lomonosov Moscow State University, Moscow, Russia

[102] Fakultät für Physik, Ludwig-Maximilians-Universität München, Munich, Germany

[103] Max-Planck-Institut für Physik (Werner-Heisenberg-Institut), Munich, Germany

[104] Nagasaki Institute of Applied Science, Nagasaki, Japan

[105] Graduate School of Science and Kobayashi-Maskawa Institute, Nagoya University, Nagoya, Japan

[106] [a]INFN Sezione di Napoli, Naples, Italy; [b]Dipartimento di Fisica, Università di Napoli, Naples, Italy

[107] Department of Physics and Astronomy, University of New Mexico, Albuquerque, NM, USA

[108] Institute for Mathematics, Astrophysics and Particle Physics, Radboud University Nijmegen/Nikhef, Nijmegen, The Netherlands

[109] Nikhef National Institute for Subatomic Physics, University of Amsterdam, Amsterdam, The Netherlands

[110] Department of Physics, Northern Illinois University, DeKalb, IL, USA

[111] Budker Institute of Nuclear Physics, SB RAS, Novosibirsk, Russia

[112] Department of Physics, New York University, New York, NY, USA

[113] Ohio State University, Columbus, OH, USA

[114] Faculty of Science, Okayama University, Okayama, Japan

[115] Homer L. Dodge Department of Physics and Astronomy, University of Oklahoma, Norman, OK, USA

[116] Department of Physics, Oklahoma State University, Stillwater, OK, USA

[117] Palacký University, RCPTM, Olomouc, Czech Republic

[118] Center for High Energy Physics, University of Oregon, Eugene, OR, USA

[119] LAL, Univ. Paris-Sud, CNRS/IN2P3, Université Paris-Saclay, Orsay, France

[120] Graduate School of Science, Osaka University, Osaka, Japan

[121] Department of Physics, University of Oslo, Oslo, Norway

[122] Department of Physics, Oxford University, Oxford, UK

[123] [a]INFN Sezione di Pavia, Pavia, Italy; [b]Dipartimento di Fisica, Università di Pavia, Pavia, Italy

[124] Department of Physics, University of Pennsylvania, Philadelphia, PA, USA

[125] National Research Centre "Kurchatov Institute" B.P. Konstantinov Petersburg Nuclear Physics Institute, St. Petersburg, Russia

[126] [a]INFN Sezione di Pisa, Pisa, Italy; [b]Dipartimento di Fisica E. Fermi, Università di Pisa, Pisa, Italy

[127] Department of Physics and Astronomy, University of Pittsburgh, Pittsburgh, PA, USA

[128] [a]Laboratório de Instrumentação e Física Experimental de Partículas-LIP, Lisbon, Portugal; [b]Faculdade de Ciências, Universidade de Lisboa, Lisbon, Portugal; [c]Department of Physics, University of Coimbra, Coimbra, Portugal; [d]Centro de Física Nuclear da Universidade de Lisboa, Lisbon, Portugal; [e]Departamento de Fisica, Universidade do Minho, Braga, Portugal; [f]Departamento de Fisica Teorica y del Cosmos, Universidad de Granada, Granada, Spain; [g]Dep Fisica and CEFITEC of Faculdade de Ciencias e Tecnologia, Universidade Nova de Lisboa, Caparica, Portugal

[129] Institute of Physics, Academy of Sciences of the Czech Republic, Prague, Czech Republic

[130] Czech Technical University in Prague, Prague, Czech Republic

[131] Faculty of Mathematics and Physics, Charles University, Prague, Czech Republic

[132] State Research Center Institute for High Energy Physics (Protvino), NRC KI, Protvino, Russia

[133] Particle Physics Department, Rutherford Appleton Laboratory, Didcot, UK

[134] [a]INFN Sezione di Roma, Rome, Italy; [b]Dipartimento di Fisica, Sapienza Università di Roma, Rome, Italy

[135] [a]INFN Sezione di Roma Tor Vergata, Rome, Italy; [b]Dipartimento di Fisica, Università di Roma Tor Vergata, Rome, Italy

[136] [a]INFN Sezione di Roma Tre, Rome, Italy; [b]Dipartimento di Matematica e Fisica, Università Roma Tre, Rome, Italy

[137] [a]Faculté des Sciences Ain Chock, Réseau Universitaire de Physique des Hautes Energies-Université Hassan II, Casablanca, Morocco; [b]Centre National de l'Energie des Sciences Techniques Nucleaires, Rabat, Morocco; [c]Faculté des Sciences Semlalia, Université Cadi Ayyad, LPHEA-Marrakech, Marrakech, Morocco; [d]Faculté des Sciences, Université Mohamed Premier and LPTPM, Oujda, Morocco; [e]Faculté des Sciences, Université Mohammed V, Rabat, Morocco

[138] DSM/IRFU (Institut de Recherches sur les Lois Fondamentales de l'Univers), CEA Saclay (Commissariat à l'Energie Atomique et aux Energies Alternatives), Gif-sur-Yvette, France

[139] Santa Cruz Institute for Particle Physics, University of California Santa Cruz, Santa Cruz, CA, USA

[140] Department of Physics, University of Washington, Seattle, WA, USA

[141] Department of Physics and Astronomy, University of Sheffield, Sheffield, UK

[142] Department of Physics, Shinshu University, Nagano, Japan

[143] Department Physik, Universität Siegen, Siegen, Germany

[144] Department of Physics, Simon Fraser University, Burnaby, BC, Canada

[145] SLAC National Accelerator Laboratory, Stanford, CA, USA

[146] [a]Faculty of Mathematics, Physics and Informatics, Comenius University, Bratislava, Slovak Republic; [b]Department of Subnuclear Physics, Institute of Experimental Physics of the Slovak Academy of Sciences, Kosice, Slovak Republic

[147] [a]Department of Physics, University of Cape Town, Cape Town, South Africa; [b]Department of Physics, University of Johannesburg, Johannesburg, South Africa; [c]School of Physics, University of the Witwatersrand, Johannesburg, South Africa

[148] [a]Department of Physics, Stockholm University, Stockholm, Sweden; [b]The Oskar Klein Centre, Stockholm, Sweden

[149] Physics Department, Royal Institute of Technology, Stockholm, Sweden

[150] Departments of Physics and Astronomy and Chemistry, Stony Brook University, Stony Brook, NY, USA

[151] Department of Physics and Astronomy, University of Sussex, Brighton, UK

[152] School of Physics, University of Sydney, Sydney, Australia

[153] Institute of Physics, Academia Sinica, Taipei, Taiwan

[154] Department of Physics, Technion: Israel Institute of Technology, Haifa, Israel

[155] Raymond and Beverly Sackler School of Physics and Astronomy, Tel Aviv University, Tel Aviv, Israel

[156] Department of Physics, Aristotle University of Thessaloniki, Thessaloniki, Greece

[157] International Center for Elementary Particle Physics and Department of Physics, The University of Tokyo, Tokyo, Japan

[158] Graduate School of Science and Technology, Tokyo Metropolitan University, Tokyo, Japan

[159] Department of Physics, Tokyo Institute of Technology, Tokyo, Japan

[160] Tomsk State University, Tomsk, Russia

[161] Department of Physics, University of Toronto, Toronto, ON, Canada

[162] [a]INFN-TIFPA, Trento, Italy; [b]University of Trento, Trento, Italy

[163] [a]TRIUMF, Vancouver, BC, Canada; [b]Department of Physics and Astronomy, York University, Toronto, ON, Canada

[164] Faculty of Pure and Applied Sciences, and Center for Integrated Research in Fundamental Science and Engineering, University of Tsukuba, Tsukuba, Japan

[165] Department of Physics and Astronomy, Tufts University, Medford, MA, USA

[166] Department of Physics and Astronomy, University of California Irvine, Irvine, CA, USA

[167] [a]INFN Gruppo Collegato di Udine, Sezione di Trieste, Udine, Italy; [b]ICTP, Trieste, Italy; [c]Dipartimento di Chimica, Fisica e Ambiente, Università di Udine, Udine, Italy

[168] Department of Physics and Astronomy, University of Uppsala, Uppsala, Sweden

[169] Department of Physics, University of Illinois, Urbana, IL, USA

[170] Instituto de Fisica Corpuscular (IFIC), Centro Mixto Universidad de Valencia-CSIC, Valencia, Spain

[171] Department of Physics, University of British Columbia, Vancouver, BC, Canada

[172] Department of Physics and Astronomy, University of Victoria, Victoria, BC, Canada

[173] Department of Physics, University of Warwick, Coventry, UK

[174] Waseda University, Tokyo, Japan

[175] Department of Particle Physics, The Weizmann Institute of Science, Rehovot, Israel

[176] Department of Physics, University of Wisconsin, Madison, WI, USA

[177] Fakultät für Physik und Astronomie, Julius-Maximilians-Universität, Würzburg, Germany

[178] Fakultät für Mathematik und Naturwissenschaften, Fachgruppe Physik, Bergische Universität Wuppertal, Wuppertal, Germany

[179] Department of Physics, Yale University, New Haven, CT, USA

[180] Yerevan Physics Institute, Yerevan, Armenia

[181] Centre de Calcul de l'Institut National de Physique Nucléaire et de Physique des Particules (IN2P3), Villeurbanne, France

[182] Academia Sinica Grid Computing, Institute of Physics, Academia Sinica, Taipei, Taiwan

[a] Also at Department of Physics, King's College London, London, UK

[b] Also at Institute of Physics, Azerbaijan Academy of Sciences, Baku, Azerbaijan

[c] Also at Novosibirsk State University, Novosibirsk, Russia

[d] Also at TRIUMF, Vancouver, BC, Canada

[e] Also at Department of Physics and Astronomy, University of Louisville, Louisville, KY, USA

[f] Also at Physics Department, An-Najah National University, Nablus, Palestine

[g] Also at Department of Physics, California State University, Fresno, CA, USA

[h] Also at Department of Physics, University of Fribourg, Fribourg, Switzerland

[i] Also at II Physikalisches Institut, Georg-August-Universität, Göttingen, Germany

[j] Also at Departament de Fisica de la Universitat Autonoma de Barcelona, Barcelona, Spain

[k] Also at Departamento de Fisica e Astronomia, Faculdade de Ciencias, Universidade do Porto, Porto, Portugal

[l] Also at Tomsk State University, Tomsk, and Moscow Institute of Physics and Technology State University, Dolgoprudny, Russia

[m] Also at The Collaborative Innovation Center of Quantum Matter (CICQM), Beijing, China

[n] Also at Universita di Napoli Parthenope, Naples, Italy

[o] Also at Institute of Particle Physics (IPP), Canada

[p] Also at Horia Hulubei National Institute of Physics and Nuclear Engineering, Bucharest, Romania

[q] Also at Department of Physics, St. Petersburg State Polytechnical University, St. Petersburg, Russia

[r] Also at Borough of Manhattan Community College, City University of New York, New York, USA

[s] Also at Department of Financial and Management Engineering, University of the Aegean, Chios, Greece

[t] Also at Centre for High Performance Computing, CSIR Campus, Rosebank, Cape Town, South Africa

[u] Also at Louisiana Tech University, Ruston, LA, USA

[v] Also at Institucio Catalana de Recerca i Estudis Avancats, ICREA, Barcelona, Spain

[w] Also at Department of Physics, The University of Michigan, Ann Arbor MI, USA

[x] Also at LAL, Univ. Paris-Sud, CNRS/IN2P3, Université Paris-Saclay, Orsay, France

[y] Also at Graduate School of Science, Osaka University, Osaka, Japan

[z] Also at Fakultät für Mathematik und Physik, Albert-Ludwigs-Universität, Freiburg, Germany

[aa] Also at Institute for Mathematics, Astrophysics and Particle Physics, Radboud University Nijmegen/Nikhef, Nijmegen, The Netherlands

[ab] Also at Department of Physics, The University of Texas at Austin, Austin, TX, USA

[ac] Also at Institute of Theoretical Physics, Ilia State University, Tbilisi, Georgia

[ad] Also at CERN, Geneva, Switzerland

[ae] Also at Georgian Technical University (GTU), Tbilisi, Georgia

[af] Also at Ochadai Academic Production, Ochanomizu University, Tokyo, Japan

[ag] Also at Manhattan College, New York, NY, USA

[ah] Also at The City College of New York, New York NY, USA

[ai] Also at Departamento de Fisica Teorica y del Cosmos, Universidad de Granada, Granada, Portugal

[aj] Also at Department of Physics, California State University, Sacramento, CA, USA

[ak] Also at Moscow Institute of Physics and Technology State University, Dolgoprudny, Russia

[al] Also at Departement de Physique Nucleaire et Corpusculaire, Université de Genève, Geneva, Switzerland

[am] Also at Institut de Física d'Altes Energies (IFAE), The Barcelona Institute of Science and Technology, Barcelona, Spain

[an] Also at School of Physics, Sun Yat-sen University, Guangzhou, China

[ao] Also at Institute for Nuclear Research and Nuclear Energy (INRNE) of the Bulgarian Academy of Sciences, Sofia, Bulgaria

[ap] Also at Faculty of Physics, M.V. Lomonosov Moscow State University, Moscow, Russia

[aq] Also at National Research Nuclear University MEPhI, Moscow, Russia

[ar] Also at Department of Physics, Stanford University, Stanford, CA, USA

[as] Also at Institute for Particle and Nuclear Physics, Wigner Research Centre for Physics, Budapest, Hungary

[at] Also at Faculty of Engineering, Giresun University, Giresun, Turkey

[au] Also at CPPM, Aix-Marseille Université and CNRS/IN2P3, Marseille, France

[av] Also at Department of Physics, Nanjing University, Jiangsu, China

[aw] Also at Institute of Physics, Academia Sinica, Taipei, Taiwan

[ax] Also at University of Malaya, Department of Physics, Kuala Lumpur, Malaysia

*Deceased